British Journal of Cancer (1999) 81(2), 194–202

Article no. bjoc.1999.0677

主論文

Prostaglandin production in mouse mammary tumour cells confers invasive growth potential by inducing hepatocyte growth factor in stromal fibroblasts

N Matsumoto-Taniura, K Matsumoto and T Nakamura

Division of Biochemistry, Department of Oncology, Biomedical Research Centre, Osaka University Medical School, Suita, Osaka 565-0871, Japan

Summary Interactions between stromal and mammary tumour cells play a crucial role in determining the malignant behaviour of tumour cells. Although MMT mouse mammary tumour cells do not produce hepatocyte growth factor (HGF), addition of conditioned medium (CM) from MMT cells to cultures of human fibroblasts derived from skin and breast tissues stimulated the production of HGF, thereby indicating that MMT cells secrete an inducing factor for HGF. This HGF-inducing factor, purified from MMT-derived CM, proved to be prostaglandin E_2 (PGE_2). Consistently, treatment of MMT cells with indomethacin, an inhibitor of cyclooxygenase, abolished this HGF-inducing activity in MMT-derived CM, while treatment of MMT cells with HGF stimulated cell growth and cell motility. Likewise, HGF strongly enhanced urokinase-type plasminogen activator activity and invasion of MMT cells through Matrigel: a 15-fold stimulation in the invasion of MMT cells was seen by HGF. Finally, MMT cells in the upper compartment were co-cultivated with fibroblasts in the lower compartment of the Matrigel chamber, HGF levels in the co-culture system exceeded the level in fibroblasts alone and suppression occurred with exposure to indomethacin. Together with increase in the HGF level, the invasion of MMT cells was enhanced by co-cultivation with fibroblasts, whereas the increased invasion of MMT cells was significantly inhibited by an anti-HGF antibody and by indomethacin. These results indicate mutual interactions between MMT cells and fibroblasts: MMT-derived PGE_2 plays a role in up-regulating HGF production in fibroblasts, while fibroblast-derived HGF leads to invasive growth in MMT cells. The mutual interactions mediated by HGF and prostaglandins may possibly be a mechanism regulating malignant behaviour of mammary tumour cells, through tumour–stromal interactions.

Keywords: HGF; prostaglandin E_2; tumour invasion; tumour–stromal interaction, mammary tumour

Interactions between epithelium and mesenchyme (or stroma) mediate crucial aspects of normal development, tissue morphogenesis and neoplasia. In tissue recombination, growth, differentiation and morphogenesis of developing epithelia are regulated either inductively or permissively by neighbouring mesenchyme, including pancreas, salivary gland, kidney, mammary gland, etc. (Grobstein, 1967; Sakakura, 1991; Birchmeier and Birchmeier, 1993). Host stromal influence on epithelial neoplasia and malignant progression of carcinoma cells have also been noted in various tumours, including cancers in prostate, stomach, skin, oral cavity, mammary gland, etc. (van den Hoof, 1988). In vivo growth of certain carcinoma cells was markedly accelerated by a broad spectrum of fibroblasts, and in vitro invasiveness of several carcinoma cells was induced by co-cultivation with stromal fibroblasts (Picard et al, 1986; Grey et al, 1989; Camps et al, 1990; Matsumoto et al, 1994). Although matrix metalloproteinases, growth factors and cell motility factors are implicated in tumour–stromal interactions, less is known of molecular mechanisms which confer invasive growth of cancer cells through interactions with surrounding stroma.

Hepatocyte growth factor (HGF), originally identified as a potent mitogen for hepatocytes (Nakamura et al, 1984), is a kringle-containing growth factor which has mitogenic, motogenic and morphogenic activities in a wide variety of cells (Nakamura et al, 1989; Montesano et al, 1991; Zarnegar and Michalopoulos, 1995; Matsumoto and Nakamura, 1997). HGF specifically activates the Met/HGF receptor of heterodimeric tyrosine kinase, which is expressed on a wide variety of epithelial cells, endothelial cells and several mesenchymal cells. During normal development, HGF supports growth, migration and morphogenesis of organs and tissues, including the liver, kidney, tooth, limb muscle, lung and mammary gland, as a mesenchymal-derived paracrine factor (Santos et al, 1994; Bladt et al, 1995; Niranjan et al, 1995; Soriano et al, 1995; Yang et al, 1995; Tabata et al, 1996; Ohmichi et al, 1998). Likewise, HGF plays a 'trophic' role to enhance regeneration of organs, including the liver, kidney and lung, as a stromal-derived factor (see review, Matsumoto and Nakamura, 1997). Thus, HGF seems to be a mediator in epithelial–mesenchymal (or –stromal) interactions during tissue formation and repair.

Accumulating evidence shows that HGF is likely to play a role in tumour progression through tumour and host stromal interactions (Seslar et al, 1993; Rosen et al, 1994; Matsumoto et al, 1996; Nakamura et al, 1997). As scatter factor, originally identified as fibroblast-derived cell motility factor for epithelial cells (Stoker et al, 1987), proved to be identical with HGF (Furlong et al, 1991; Konishi et al, 1991; Weidner et al, 1991), HGF potently stimulates migration and invasion of various types of cells, including carcinoma cells (Weidner et al, 1990; Jiang et al, 1993; Matsumoto et al, 1994, 1996; Nakamura et al, 1997), and autocrine activation of Met results in increased tumourigenicity and metastasis

Received 10 November 1998
Revised 9 March 1999
Accepted 11 March 1999

Correspondence to: T Nakamura

(Bellusci et al, 1994; Jeffers et al, 1996). HGF is an angiogenic factor and plays a role in tumour angiogenesis (Bussolino et al, 1992; Grant et al, 1993; Lamszus et al, 1997). Fibroblast-derived factor, which induces in vitro invasion of carcinoma cells, proved to be HGF (Matsumoto et al, 1994). On the other hand, various types of carcinoma cells secrete soluble factors that regulate the production of HGF in stromal fibroblasts (Seslar et al, 1993; Matsumoto et al, 1996; Nakamura et al, 1997). These results suggest the presence of the mutual interaction between carcinoma cells and fibroblasts, as mediated by tumour-derived regulator for expression of HGF, and fibroblast-derived HGF, which affects invasive growth of tumour cells.

During a search for tumour-derived inducers for expression of HGF in fibroblasts, we found that the murine mammary carcinoma cell line, MMT cells, secreted a distinct type of HGF-inducer for fibroblasts. We now report that the MMT-derived HGF-inducer is prostaglandin E_2 (PGE_2), and the biological significance of PGE_2 in invasive growth of MMT cells was investigated.

MATERIALS AND METHODS

Cell culture

MMT mouse mammary carcinoma cells were obtained from the Human Science Research Resources Bank, Japan. MMT cell line was originally established from a spontaneous mammary tumour which arose in a (C57BL × Af)F_1 female mouse (Sykes et al, 1968). MMT cells are epithelial in appearance and produce mouse mammary tumour virus, implicating that MMT cells were originally transformed by mammary tumour virus infection (Sykes et al, 1968). MMT cells were cultured in modified Eagle's medium (MEM) supplemented with 10% calf serum. Normal or tumour associated human fibroblasts were, respectively, proliferated outward from the skin and breast cancer tissues obtained during surgery and the cells were cultured in Dulbecco's modified Eagle's medium (DMEM) supplemented with 10% fetal calf serum (FCS).

Growth factors and antibodies

Human recombinant HGF was purified from culture medium of Chinese hamster ovary cells transfected with expression plasmid for human HGF cDNA (Nakamura et al, 1989; Seki et al, 1990). The purity of HGF exceeded 98%, as determined by sodium dodecyl sulphate polyacrylamide gel electrophoresis (SDS-PAGE) and protein staining. Human recombinant platelet-derived growth factor (PDGF) and bovine recombinant basic fibroblast growth factor (bFGF) were obtained from Toyobo Co. (Osaka, Japan). Human recombinant interleukin-1α (IL-1α) and IL-1β were obtained from Genzyme Co. (Boston, MA, USA). A recombinant IL-1 receptor antagonist was obtained from R&D systems Co. (Minneapolis, MN, USA) and monoclonal anti-human epidermal growth factor (EGF) receptor antibody were obtained from Genzyme Co. (Boston, MA, USA). Polyclonal anti-PDGF antibody was obtained from Promega (Madison, WI, USA) and monoclonal anti-bFGF (Matsuzaki et al, 1989) was a kind gift from Dr K Nishikawa (Kanazawa Medical College). Polyclonal antibody against human HGF was prepared from the serum of a rabbit immunized with human recombinant HGF. IgG was purified using protein A-Sepharose (Pharmacia, Uppsala, Sweden) and anti-human HGF IgG (1 μg ml^{-1}) completely neutralized biological activities of 1 ng ml^{-1} human HGF.

Measurement of cell growth and scattering

To measure cell growth, MMT cells were seeded on 12-well plates (Costar, Cambridge, MA, USA) at a density of 1.1×10^3 cells cm^{-2} and cultured for 24 h. After washing with MEM, the cells were cultured for 4.5 days in serum-free MEM in the absence or presence of HGF. The medium was changed on day 3.

For the measurement of cell scattering, MMT cells were seeded on 24-well plates (Costar, Cambridge, MA, USA) at a density of 2.8×10^3 cells cm^{-2} and cultured for 48 h. After medium was changed, HGF was added and the cells were cultured for 18 h.

In-vitro invasion assay

In-vitro invasion of MMT cells was measured using a Matrigel invasion chamber (Collaborative Biomedical Products, Bedford, MA, USA). MMT cells were seeded onto the upper compartment of a Matrigel chamber at a density of 6.7×10^4 cells cm^{-2} and cultured in MEM containing 10% FCS. HGF was added to the lower compartment and cells were cultured for 15 h. Invasive cells penetrating through Matrigel components and pores to the underside of the membrane were stained with haematoxylin and eosin, viewed microscopically and counted.

For co-cultivation of MMT cells and fibroblasts, human dermal fibroblasts were initially plated onto the lower compartment of a Matrigel invasion chamber, at a density of 5×10^4 cells cm^{-2} and cultured for 24 h. The medium was changed to fresh medium composed of MEM/DMEM (1/1) containing 5% FCS and 5% calf serum. The MMT cells were seeded onto the upper compartment at a density of 6.7×10^4 cells cm^{-2}. The cells were cultured for 48 h in the absence or presence of preimmune IgG, anti-human HGF IgG (10 μg ml^{-1}), 10^{-7} M indomethacin or 10^{-7} M indomethacin plus 10^{-6} M PGE_2.

Measurement of HGF production in fibroblasts

Human fibroblasts were seeded on a 48-well plate (Costar, Cambridge, MA, USA) at a density of 5×10^4 cells cm^{-2} and cultured for 24 h. After replacing the medium with DMEM supplemented with 1% FCS and 2 μg ml^{-1} heparin, test samples were added to each well. Following a 24 h culture, the concentration of HGF in the medium was measured using enzyme-linked immunosorbent assay (ELISA), as described elsewhere (Matsumoto et al, 1996).

Measurement of PGE_2 production in MMT cells

Subconfluent MMT cells were washed twice with serum-free MEM, cultured in serum-free MEM, with or without indomethacin for 24 h and the conditioned medium (CM) was collected. The concentration of PGE_2 in the medium was determined using an ELISA kit obtained from Cayman Co. (Ann Arbor, MI, USA). This ELISA specifically detects PGE_2, not other prostaglandins.

Zymographies for gelatinase and urokinase-type plasminogen activator

Subconfluent MMT cells were cultured in serum-free MEM, with or without HGF for 24 h, and the CM was collected. For the measurement of gelatinase activity, samples were subjected to SDS-PAGE, using a 10% polyacrylamide gel containing 1 mg ml^{-1}

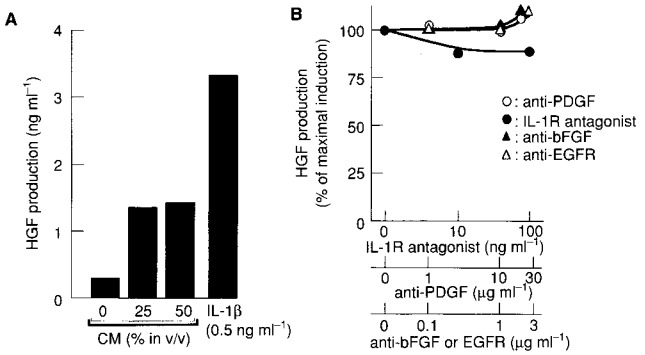

Figure 1 Stimulatory effect of conditioned medium (CM) from MMT cells on HGF production in human skin fibroblasts. (**A**) Stimulation of HGF production by MMT-derived CM. (**B**) Effects of antibodies and an antagonist against polypeptide HGF-inducers. Fibroblasts were seeded on 48-well plates and cultured for 24 h. After replacing the medium with fresh DMEM supplemented with 1% FCS and 2 μg ml^{-1} heparin, CM from MMT cells was added in the absence or presence of antibodies and an antagonist. The cells were cultured for 24 h and the concentration of HGF in the medium was measured by ELISA. Values represent the mean of triplicate measurements

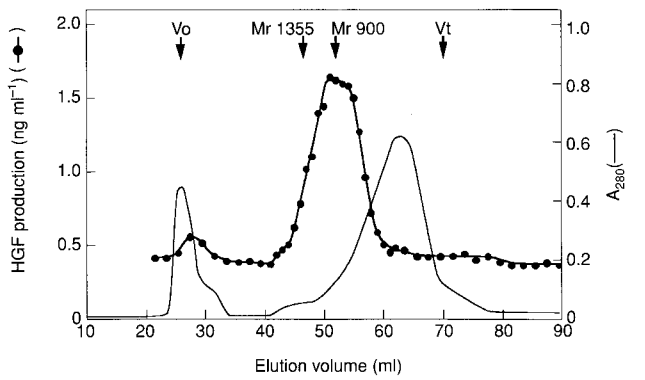

Figure 2 Elution profile of HGF-inducing activity from MMT-derived CM in molecular sieve chromatography with a Sephadex G-25 column. The CM was concentrated by lyophilization and applied to a Sephadex G-25 column equilibrated with 15 mM phosphate buffer (pH 7.2), 0.15 M sodium chloride. Eluted fractions were subjected to assay for HGF-inducing activity, using human skin fibroblasts

gelatin. After electrophoresis, the gel was washed in 2.5% Triton X-100, and incubated in 50 mM Tris–HCl buffer (pH 8.0) containing 0.5 mM calcium chloride and 1 mM zinc chloride for 24 h at 37°C. The gel was stained with Coomassie brilliant blue and photographed. For the measurement of urokinase-type plasminogen activator (u-PA), culture supernatants were prepared and analysed as described elsewhere (Vassalli et al, 1984).

Purification of MMT-derived HGF-inducer

After MMT cells grew to confluency, the culture medium was changed to serum-free medium and the cells were cultured for a further 48 h. CM was concentrated by lyophilization and subjected to molecular sieve chromatography, using a Sephadex G-25 column (Pharmacia Biotech, Uppsala, Sweden), equilibrated with 15 mM phosphate buffer (pH 7.2), 0.15 M sodium chloride. Active fractions were pooled, concentrated by lyophilization, and applied to reverse phase high-performance liquid chromatography (RP-HPLC) with a C_{18} column. Absorbed materials were eluted by a concentration gradient of acetonitrile. The eluate was concentrated by vacuum centrifugation and dissolved in H_2O.

RESULTS

Characterization of MMT-derived HGF-inducer

HGF-inducing activity was determined by measuring HGF production in cultures of human skin fibroblasts after addition of CM from MMT mouse mammary tumour cells. The addition of MMT-derived CM stimulated HGF production in cultures of fibroblasts (Figure 1A): a four- to fivefold increase in HGF level in fibroblast cultures occurred when CM was added at 50% (v/v), whereas its potential to stimulate HGF-production was less than that of 0.5 ng ml^{-1} IL-1β. Since the MMT-derived CM itself did not contain a detectable level of HGF (not shown), our observations indicated that MMT cells secrete a factor which stimulates the production of HGF in normal human fibroblasts.

Our previous studies demonstrated that several types of tumour cells secrete inducing factors for HGF production in fibroblasts, and these factors were identified to be IL-1α, IL-1β, PDGF and bFGF (Matsumoto et al, 1996; Nakamura et al, 1997). We therefore asked whether the MMT-derived HGF-inducer is identical to one of these factors. MMT-derived CM was added to fibroblast cultures and the cells were cultured in the absence or presence of an IL-1 receptor (IL-1R) antagonist or an antibody against PDGF, bFGF or EGF-R. IL-1R antagonist and these antibodies almost completely inhibited the respective activities of IL-1α, IL-1β, PDGF, bFGF and TGF-α to stimulate HGF production (not shown). The stimulatory effect of MMT-derived CM on HGF production was slightly inhibited by the IL-1R antagonist but was hardly inhibited by any of the antibodies (Figure 1B). This indicates that the HGF-inducer derived from MMT cells is distinct from these cytokines and growth factors.

MMT-derived CM was concentrated by lyophilization, subjected to molecular sieve chromatography, using a Sephadex G-25 column, and the eluted fractions were tested to determine if they would stimulate HGF production in fibroblast cultures (Figure 2). HGF-inducing activity was eluted as two distinct peaks: the major peak eluted at positions of M_r around 900 and the minor peak eluted near V_0 position.

Identification of MMT-derived HGF inducer

We repeated molecular sieve chromatography and active fractions from CM were pooled and lyophilized. The pooled material was dissolved in H_2O, dialysed against H_2O, and subjected to RP-HPLC with a C_{18} column (Figure 3A). The adsorbed materials were eluted with a concentration gradient of acetonitrile and the eluted fractions were subjected to assay. When the pooled material from CM of MMT cells was applied to RP-HPLC, HGF-inducing activity was seen as a single peak of fraction 55. It is worth noting that the HGF-inducing activity eluted after RP-HPLC was comparable to that seen with 0.5 ng ml^{-1} IL-1β (a dose which gives the maximal activity of IL-1β) and it was approximately twofold higher than that of the maximal activity seen in the pooled materials subjected to RP-HPLC. The potentiation of HGF-inducing activity after RP-HPLC means that an inhibitory factor which suppresses HGF-inducing factor in MMT-derived CM was dissociated during RP-HPLC.

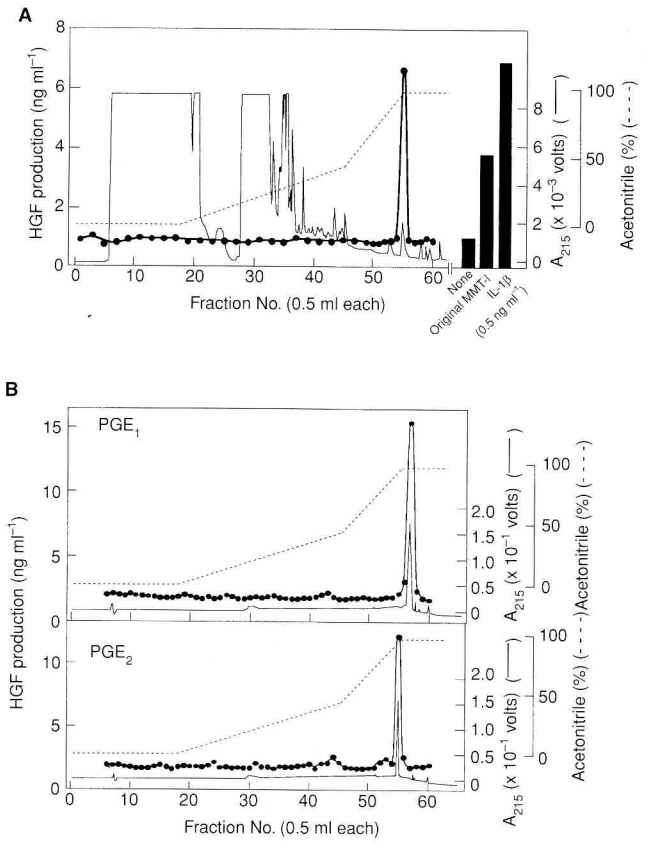

Figure 3 Elution profile of HGF-inducing activity from MMT-derived CM (**A**) and PGE_1 and PGE_2 (**B**) in C_{18} RP-HPLC. Pooled active fractions after molecular sieve chromatography were concentrated and subjected to C_{18} RP-HPLC. The absorbed materials were eluted with a concentration gradient of acetonitrile and eluted fractions were subjected to assay for HGF-inducing activity

The above results indicated that the MMT-derived HGF-inducer was a lipophilic molecule with a relatively low M_r, and we speculated it might be prostaglandins. We therefore tested whether various prostaglandins might stimulate HGF production in the fibroblasts. Among prostaglandins tested, including prostaglandin D_2 (PGD_2), PGE_1, PGE_2, $PGF_{2\alpha}$, PGI_2, staurosporin A_2 and thromboxan B_2, PGE_1 and PGE_2 patently stimulated HGF production in the fibroblasts (not shown). We therefore applied authentic PGE_1 and PGE_2, respectively, to a C_{18} RP-HPLC column followed by elution under the same conditions as used for MMT-derived HGF-inducer (Figure 3B). PGE_1 eluted as a major single peak at fraction 57 and HGF-inducing activity in the elute coincided with the peak, while PGE_2 eluted at fraction 55, thus, coinciding with its biological activity to stimulate HGF production. Taken together, these results strongly suggest that the HGF-inducer secreted from MMT cells is PGE_2.

To obtain further evidence that the HGF-inducer derived from MMT cells is PGE_2, MMT cells were cultured in the presence of indomethacin, a specific inhibitor for cyclooxygenase, and HGF-inducing activity in the CM was measured. HGF-inducing activity in CM from MMT cells was almost completely inhibited by exposure to indomethacin, in a dose-dependent manner (Figure 4A). Likewise, HGF-inducing activity in CM of MMT cells treated

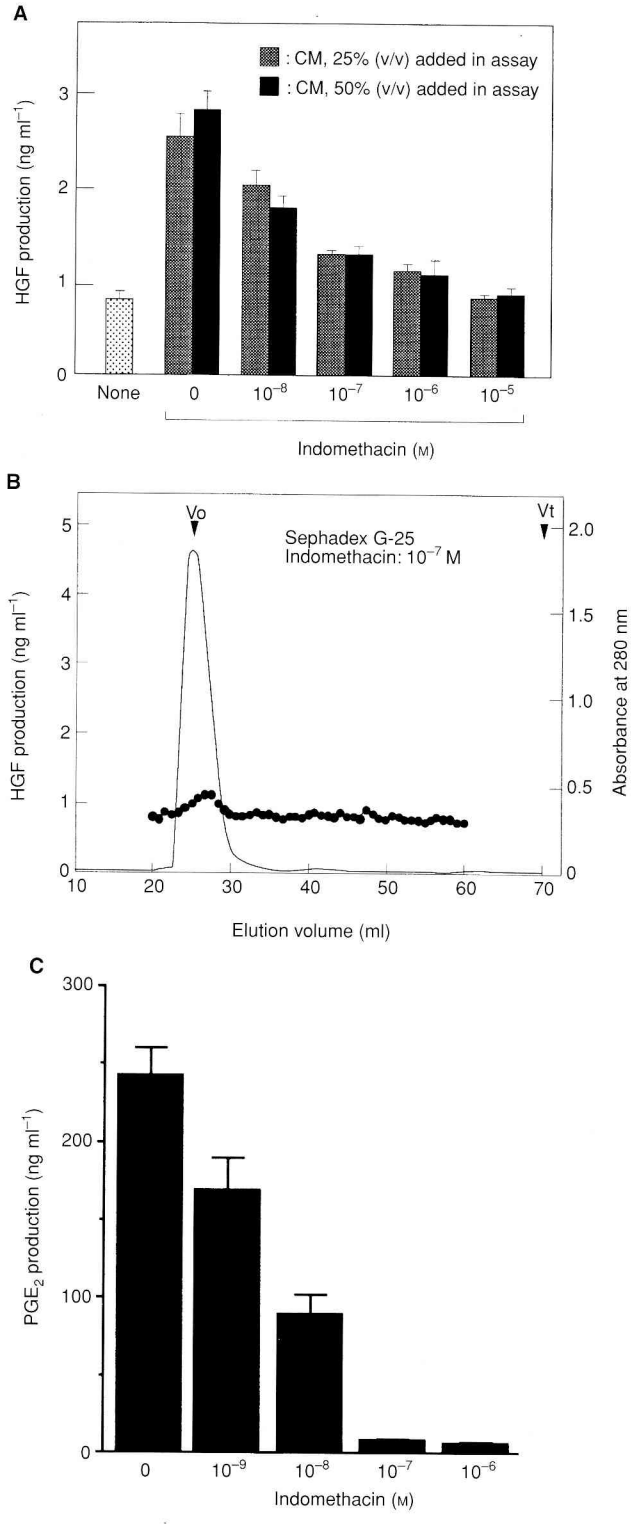

Figure 4 Inhibition of HGF-inducing activity in CM from MMT cells exposed to indomethacin (**A, B**) and PGE_2 production in MMT cells (**C**). (**A**) Concentration-dependent inhibition of HGF-inducing activity in MMT-derived CM by indomethacin. (**B**) Elution profile of HGF-inducing activity in CM of MMT cells exposed or not exposed to 10^{-7} M indomethacin. Subconfluent MMT cells were cultured in the absence or presence of indomethacin for 48 h and CM from indomethacin-exposed MMT cells were subjected to assay for HGF-inducing activity (**A**) or molecular sieve chromatography with Sephadex G-25 column (**B**). (**C**) PGE_2 production in MMT cells cultured with or without indomethacin for 24 h. PGE_2 production in CM of MMT cells was measured using ELISA

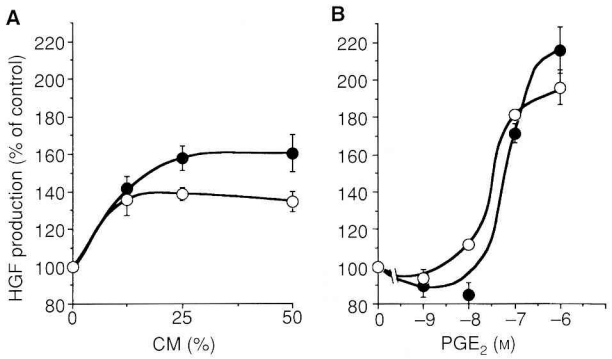

Figure 5 Stimulatory effects of MMT-derived CM (**A**) and PGE_2 (**B**) on HGF production in human fibroblasts derived from normal breast and breast carcinoma tissues. Values represent the mean ± s.d. of triplicate measurements

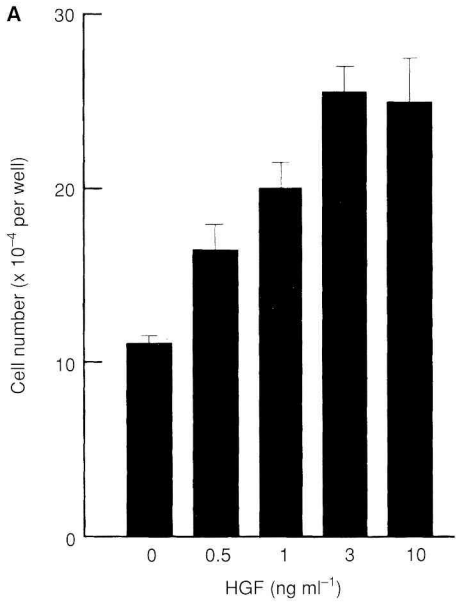

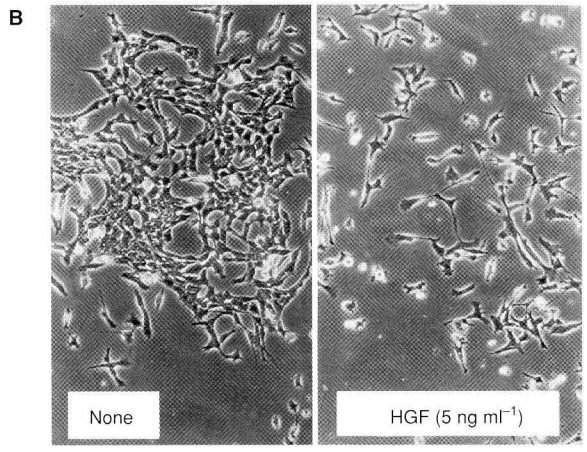

Figure 6 Enhancement of cell growth (**A**) and cell scattering (**B**) of MMT cells by HGF. For measurement of cell growth, MMT cells were cultured for 4.5 days in serum-free MEM in the absence or presence of HGF. For the measurement of cell scattering, MMT cells were cultured in the absence or presence of HGF for 18 h

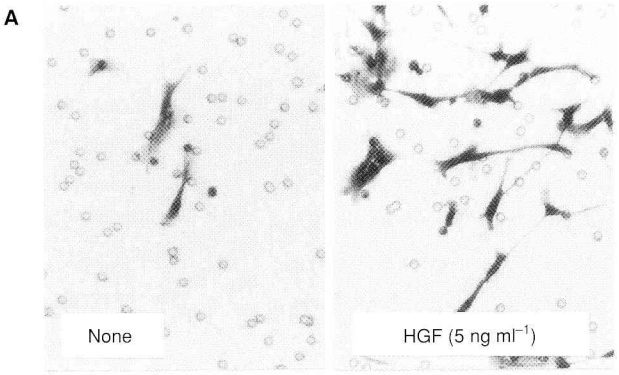

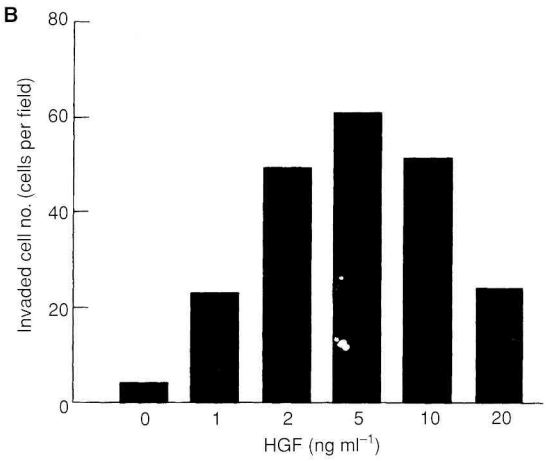

Figure 7 Stimulatory effect of HGF on in vitro invasion of MMT cells. (**A**) Appearance of invasive cells migrating under the membrane. (**B**) Dose-dependent enhancement of invasion of MMT cells by HGF. MMT cells were seeded on Matrigel basement membrane components for 2 days in the absence or presence of HGF. Invasive cells invading through Matrigel and 8-μm pores of the filter membrane to the underside of the membrane were stained with haematoxylin and counted, as viewed microscopically

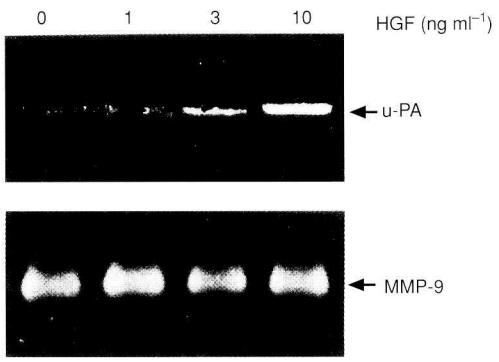

Figure 8 Regulation of u-PA and gelatinase activities in MMT cells by HGF. u-PA activity (**A**) and gelatinase activity (**B**) were measured in CM from MMT cells. MMT cells were cultured for 24 h in the absence or presence of HGF, and CM was subjected to SDS-PAGE. u-PA and gelatinase activities were respectively measured using zymographical methods

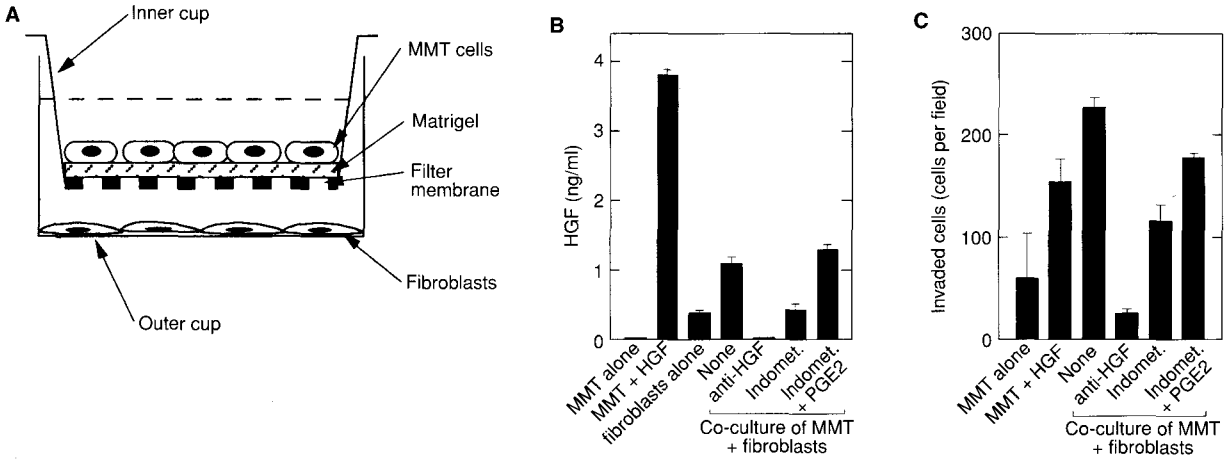

Figure 9 In vitro invasion of MMT cells cocultured with fibroblasts. (**A**) Diagram showing method we used to co-culture MMT cells and fibroblasts. (**B**) HGF concentration in co-culture system of MMT cells and fibroblasts. (**C**) Number of invasive MMT cells in the co-culture of MMT cells and fibroblasts. Human fibroblasts were initially seeded on 24-well plates, and MMT cells were seeded in the upper compartment of a 24-well Matrigel invasion chamber. Cells were cultured for 48 h in the absence or presence of 5 ng ml^{-1} HGF, 10 μg ml^{-1} anti-HGF IgG, 10^{-7} M indomethacin, or 10^{-7} M indomethacin plus 10^{-6} M PGE_2, and the number of invasive cells was enumerated

with 10^{-7} M indomethacin was measured after molecular sieve chromatography with Sephadex G-25 (Figure 4B). The elution profile clearly indicated that the HGF-inducing activity in the major peak corresponding to M_r around 900 Da was almost completely diminished, whereas the HGF-inducing activity in the minor peak which eluted near V_0 position was not inhibited. We next measured PGE_2 production by MMT cells, using a specific ELISA (Figure 4C). During 24-h culture, PGE_2 level in the CM of MMT cells reached 242 ng ml^{-1} (6.9×10^{-7} M). Furthermore, the addition of indomethacin dose-dependently inhibited PGE_2 production in MMT cells and PGE_2 production in the cells treated with 10^{-7} M indomethacin was only 1/30 of that seen in control culture. Together with these results, we concluded that the HGF-inducer from MMT cells was PGE_2.

Since the MMT cells originated from mammary tissue, we asked if HGF production in human fibroblasts derived from normal breast and breast carcinoma tissues in a patient with breast carcinoma was regulated by MMT-derived CM and PGE_2 (Figure 5). The basal HGF production in fibroblasts from normal and breast carcinoma tissues was 3.74 ± 0.12 ng ml^{-1} and 5.27 ± 0.14 ng ml^{-1} respectively. Although HGF production in fibroblasts from breast carcinoma tissue was higher than that in normal breast fibroblasts, HGF production in fibroblasts from breast carcinoma tissue was not consistently higher than that in normal breast fibroblasts to some extent, it was not consistent (not shown). HGF production in breast fibroblasts from both normal and tumour tissues was dose-dependently stimulated by both MMT-derived CM (Figure 5A) and PGE_2 (Figure 5B). Similar stimulatory effects were seen in other human breast fibroblasts derived from other patients with breast cancer (not shown).

Biological effects of HGF on MMT cells

On the basis of our data that MMT cells secrete PGE_2 as a potent HGF inducer for fibroblasts, we assume that MMT cells might stimulate HGF production in fibroblasts and fibroblast-derived HGF might affect growth, migration and invasion of MMT cells. Interactions of tumour cells with stromal fibroblasts have a significant effect on the malignant behaviour of carcinoma cells (Lippman and Dickson, 1990; Sakakura, 1991; Wernert, 1997). When HGF was added to cultures of MMT cells, HGF stimulated proliferation of the cells, in a dose-dependent manner (Figure 6A). The maximal activity with a 2.5-fold increase in cell number was seen with 3–10 ng ml^{-1} HGF. In addition to cell growth stimulation, HGF stimulated migration of the cells. Addition of HGF in MMT cells in monolayer culture induced scattering of the cells (Figure 6B), thereby indicating that HGF stimulates motility of MMT cells.

To determine if HGF would affect invasion of MMT cells, the cells were cultured in a Matrigel invasion chamber in the absence or presence of HGF (Figure 7A). Although some cells invaded through the Matrigel basement membrane components and migrated under the filter membrane in the absence of HGF, the addition of HGF strongly enhanced invasion of these cells. The maximal effect by 15-fold stimulation was seen with 5 ng ml^{-1} HGF, while at a higher concentration, the number of invading cells decreased (Figure 7B). Therefore, HGF may stimulate the invasion of MMT cells through the basement membrane.

Since the process of invasion requires increased activities in both cell migration and extracellular proteolysis, we investigated the effects of HGF on extracellular protease activities in MMT cells. HGF-treatment strongly increased u-PA activity, in a dose-dependent manner (Figure 8). On the other hand, although MMT cells secreted 92 kDa gelatinase (MMP-9), this secretion remained unchanged with HGF-treatment (Figure 8).

In vitro invasion through tumour–stromal interaction

Based on findings that MMT cells secrete PGE_2 as an inducer for HGF production in fibroblasts, while HGF strongly stimulates invasion of MMT cells, we set up a co-culture method, using a Matrigel invasion chamber in which fibroblasts were cultured in the lower compartment and MMT cells were cultured in the upper compartment (Figure 9A). This co-culture system mimics the

tumour–stromal interaction through basement membrane components. Without co-cultured MMT cells, basal HGF production in fibroblasts was 0.4 ng ml^{-1} during 48-h culture, but the production of HGF was stimulated to 1.1 ng ml^{-1} by co-cultivation with MMT cells (Figure 9B). HGF was undetectable when anti-HGF IgG was added to this culture. The addition of 10^{-7} M indomethacin decreased the HGF to near basal levels seen in the culture of fibroblasts alone, indicating that the increase in HGF level under this co-culture condition was probably due to PGE_2 secreted from MMT cells. Simultaneous addition of 10^{-6} M PGE_2 and 10^{-7} M indomethacin to this culture again increased HGF levels 3.1-fold higher than seen in the culture with 10^{-7} M indomethacin alone.

When MMT cells were cultured alone, the addition of 5 ng ml^{-1} HGF stimulated the invasion of MMT cells to a 2.6-fold higher level than seen without HGF (Figure 9C). The addition of 10 μg ml^{-1} anti-HGF IgG almost completely neutralized the invasion of MMT cells stimulated by 5 ng ml^{-1} HGF, while anti-HGF IgG alone had no effect on invasion of MMT cells (not shown). Co-cultivation of MMT cells with fibroblasts increased the number of invading cells by a 3.9-fold higher level than that seen without fibroblasts. The number of invading cells in the co-culture was higher than that seen with MMT cells alone in the presence of 5 ng ml^{-1}, even though the HGF level in the co-culture was only 1.1 ng ml^{-1} (Figure 9B). This finding suggests that fibroblasts might secrete a factor(s) distinct from HGF and such a factor(s) might stimulate invasion of the cells, in this co-culture system (see below). Importantly, the addition of anti-HGF strongly inhibited invasion of the cells to the level seen in the culture of MMT cells alone. Likewise, the addition of 10^{-7} M indomethacin inhibited invasion of MMT cells, but this inhibitory effect was less than that seen with anti-HGF antibody, because the basal HGF production in fibroblasts was retained, even in the presence of indomethacin. Moreover, the addition of 10^{-6} M PGE_2 to this co-culture in the presence of 10^{-7} M indomethacin again stimulated invasion of MMT cells, consistent with the increase in HGF level in this culture condition. Therefore, in this co-culture system, the mutual interaction between MMT cells and fibroblasts was evident: HGF production in fibroblasts is stimulated by PGE_2 secreted from MMT cells, while fibroblast-derived HGF in turn strongly stimulates invasion of MMT cells.

Since the enhanced invasion of MMT cells in the co-culture with fibroblasts was inhibited to the basal level by anti-HGF antibody, the above fibroblast-derived factor(s) distinct from HGF is likely to depend on the co-existence of HGF, in stimulating invasion of MMT cells. Although we have yet to specify such a fibroblast-derived factor(s), one possible explanation is that fibroblasts might produce pro-matrix metalloproteinases (pro-MMPs), and the activation of pro-MMPs might depend on tumour-derived proteinase such as u-PA. HGF strongly stimulated u-PA activity in MMT cells (Figure 8).

DISCUSSION

HGF is a mesenchymal- or stromal-derived factor which elicits mitogenic, motogenic and morphogenic responses in a wide variety of cells (Zarnegar and Michalopoulos, 1995; Matsumoto and Nakamura, 1997). During development of the mammary gland, HGF is involved in branching duct formation in mammary gland epithelial cells (Niranjan et al, 1995; Soriano et al, 1995; Yang et al, 1995). A fibroblast-derived mitogen for mammary gland epithelial cells was identified to be HGF (Sasaki et al, 1994), indicating that HGF affects growth of mammary epithelial cells as a stromal-derived paracrine factor. It is therefore conceivable that HGF functions as a mediator in tumour–stromal interactions in breast cancer, leading to the acquisition of malignant phenotypes in breast cancer cells. In the present study, we found that HGF potently stimulates migration and invasion of MMT mouse mammary carcinoma cells, as well as stimulating their growth. Of importance in our study is the finding that there is a mutual interaction between MMT carcinoma cells and fibroblasts, as mediated by MMT-derived PGE_2 and fibroblast-derived HGF. MMT-derived PGE_2 up-regulates HGF production in fibroblasts, while fibroblast-derived HGF stimulates growth and invasion of MMT cells. There have been reports that PGE_2 levels are elevated in malignant human breast tumours and murine mammary tumours (Rolland et al, 1980; Karmali et al, 1983; Bennett et al, 1989). In-vitro studies using tissue explants or human breast tumour cells in primary culture also revealed higher PGE_2 production by tumour cells from malignant tissue than that seen in cells from benign tumour and normal tissues (Watson and Chuah, 1992). Together with these results, one possible mechanism is that breast carcinoma cells secrete PGE_2, the elevated PGE_2 stimulates HGF production in stromal fibroblasts, and fibroblast-derived HGF induces invasive growth of breast carcinoma cells. We also found that HGF strongly increased u-PA activity in MMT cells. Since involvement of u-PA-induction in tumour invasion has been demonstrated in various cancer cells (Vassalli and Pepper, 1994) and induction of u-PA by HGF correlates with in vitro invasiveness and in vivo metastatic potential (Jeffers et al, 1996), increase in u-PA activity by HGF could possibly be one critical event, leading to increased invasive potential in MMT cells.

Previous studies noted that various types of cancer cells secrete stimulatory factors for production of HGF in distinct types of fibroblasts and such tumour-derived HGF-inducers were identified to be polypeptide cytokines and growth factors such as IL-1α, IL-1β, bFGF and PDGF (Matsumoto et al, 1996; Nakamura et al, 1997). It should be emphasized that we here have newly identified PGE_2 to be a non-polypeptide HGF-inducer derived from tumour cells. Previous studies indicated that some prostaglandins (PGE_1, PGE_2 and PGI_2 analogue) stimulate HGF production by activating gene expression of HGF rather than by regulating post-transcriptional processes (Matsumoto et al, 1995). On the other hand expression of HGF gene is up-regulated by at least two distinct signalling pathways: A-kinase-mediated and C-kinase-mediated pathways (Matsunaga et al, 1994; Matsumoto et al, 1995). Although we did not investigate the pathway through which PGE_2 exhibits HGF-inducing activity, the A-kinase-mediated pathway is likely to be responsible, for the following reasons: (1) PGE_2 stimulates both cAMP levels and HGF production through the EP2/EP4 prostaglandin receptor which stimulates adenylate cyclase (Takahashi et al, 1996); (2) stimulatory effect on HGF production in fibroblasts is additive/synergistic between PGE_2 and an activator of C-kinase, but not additive between PGE_2 and a cAMP analogue which activates A-kinase (Matsumoto et al, 1995).

Most mammary carcinoma cells and many types of other carcinoma cells do not produce HGF in vitro (Jiang et al, 1993; Byers et al, 1994; Rosen et al, 1994; Nakamura et al, 1997; our unpublished data), whereas many different types of fibroblasts, including mammary fibroblasts produce moderate to high levels of HGF (Stoker et al, 1987; Seslar et al, 1993; Rosen et al, 1994). Thus, stromal cells seem to be a major source of HGF within tumour tissues. On the other hand, there are data that HGF protein and mRNA are expressed in mammary carcinoma cells (Wang et al,

1994; Rahimi et al, 1996; Tuck et al, 1996; Jin et al, 1997*a*), as well as in stromal cells. The expression of HGF is elevated in mammary carcinomas, in comparison with findings in benign hyperplasia (Jin et al, 1997*a*; Tuck et al, 1996), and HGF levels in breast cancer tissue are a strong predictor of a recurrence in breast cancer patients (Yamashita et al, 1994; Nagy et al, 1996; Yao et al, 1996). The lack of potential of cultured mammary carcinoma cells to produce HGF may possibly reflect the absence of a stimulatory cofactor required for HGF production in tumour tissues, or a characteristic change of the cells due to consequences of serial cultivation. Although this issue remains to be addressed, the source of HGF in malignant mammary carcinomas may be extended to tumour components, as well as stromal components in more progressed breast cancers. It seems likely that increased PGE_2 production in malignant breast cancer cells leads to an increased HGF production in the tumour microenvironment, at least in stromal cells in close proximity to tumour cells.

A number of studies indicate that compounds known as non-steroidal anti-inflammatory drugs (NSAIDs) reduce the incidence of cancers, including colon, bladder, lung and breast cancers (Marnett, 1995; Rosenberg, 1995). Although NSAIDs inhibit cyclooxygenase which catalyses the biosynthesis of PGH_2, precursors for prostanoids such as prostaglandins, the mechanisms by which inhibition of PG synthesis contribute to decreased carcinogenesis in colon and some other tissues have yet to be defined. In addition to breast cancer, studies have shown that colon cancer tissues produce a large amount of PGE_2 (Narisawa et al, 1990). Moreover, our very recent study showed that a potent stimulatory effect of IL-1 on HGF production in fibroblasts was mediated via PGE_2 production and was almost completely abrogated by indomethacin (unpublished data). IL-1 (IL-1α and IL-1β) are HGF-inducers derived from various tumour cell lines (Matsumoto et al, 1996; Nakamura et al, 1997), and the elevated expression of IL-1 in various tumour tissues has been noted (Colasante et al, 1997; Jin et al, 1997*b*). These results provide insight into one possible mechanism of how the inhibition of PG synthesis by NSAIDs is involved in reduced carcinogenesis. Active PG production in stromal cells as well as in tumour cells in a tumour microenvironment stimulates HGF production, an event which may lead to acquisition of invasive growth potential in cancer cells, and to an increased likelihood of development of a malignant tumour. This hypothesis is now being tested using colon cancer cells.

The neoplastic cells of breast carcinomas are often embedded in stromal tissues, an event which may be important to control their growth, invasion and metastasis. Indeed, stromal cells influence the growth of normal mammary epithelial cells as well as epithelial carcinogenesis in the mammary gland (Tremblay, 1979; van den Hoof, 1988; Lippman and Dickson, 1990; Sakakura, 1991). Our results, at least in part, explain the pathological significance of elevated levels of PGE_2 and HGF in malignant cancer tissues, and a possible mechanism for tumour–stromal interaction, as mediated by PGE_2 and HGF, which would confer invasive growth potential in breast cancer. If our thesis is tenable, the disruption of such mutual interactions between carcinoma cells and stromal fibroblasts, as mediated by PGE_2 and HGF, may possibly be a unique therapeutic strategy toward prevention of invasion and metastasis of breast cancer.

ACKNOWLEDGEMENTS

We are grateful to M Ohara for useful comments and language assistance and to Dr K Nishikawa (Kanazawa Medical College) for kindly providing a monoclonal antibody against bFGF. This study was supported by a Research Grant for Science and Cancer from the Ministry of Education, Science, Sports, and Culture of Japan, a Research Grant from the Ministry of Welfare of Japan, and grants from Sagawa Cancer Research Foundation, the Ryoichi Naito Foundation for Medical Research, Haraguchi Memorial Foundation for Cancer Research and Tanabe Medical Science Foundation.

REFERENCES

Bellusci S, Moens G, Gaudino G, Comoglio PM, Nakamura T, Thiery JP and Jouanneau J (1994) Creation of hepatocyte growth factor/scatter factor autocrine loop in carcinoma cells induces invasive properties associated with increased tumorigenicity. *Oncogene* **9**: 1091–1099

Bennett A, Stamford IF, Berstock DA, Dische F, Singh L and A'Hern RP (1989) Breast cancer, prostaglandins and patient survival. *Br J Cancer* **59**: 268–275

Birchmeier C and Birchmeier W (1993) Molecular aspects of mesenchymal–epithelial interactions. *Annu Rev Cell Biol* **9**: 511–540

Bladt F, Riethmacher D, Isenmann S, Aguzzi A and Birchmeier C (1995) Essential role for the c-met receptor in the migration of myogenic precursor cells into the limb bud. *Nature* **376**: 768–771

Bussolino F, Di Renzo MF, Ziche M, Bocchietto E, Olivero M, Naldini L, Gaudino G, Tamagnone L, Coffer A and Comoglio PM (1992) Hepatocyte growth factor is a potent angiogenic factor which stimulates endothelial cell motility and growth. *J Cell Biol* **119**: 629–641

Byers S, Park M, Sommers C and Seslar S (1994) Breast carcinoma: a collective disorder. *Breast Cancer Res Treat* **31**: 203–215

Camps JL, Chang S, Hsu TC, Freeman MR, Hong S, Zhau HE, von Eschenbach AC and Chung LW (1990) Fibroblast-mediated acceleration of human epithelial tumor growth in vivo. *Proc Natl Acad Sci USA* **87**: 75–79

Colasante A, Mascetra N, Brunetti M, Lattanzio G, Diodoro M, Caltagirone S, Musiani P and Aiello FB (1997) Transforming growth factor β1, interleukin-8 and interleukin-1, in non-small-cell lung tumors. *Am J Respir Crit Care Med* **156**: 968–973

Furlong RA, Takehara T, Taylor WG, Nakamura T and Rubin JS (1991) Comparison of biological and immunochemical properties indicates that scatter factor and hepatocyte growth factor are indistinguishable. *J Cell Sci* **100**: 173–177

Grant DS, Kleinman HK, Goldberg ID, Bhargava MM, Nickoloff BJ, Kinsella JL, Polverini P and Rosen EM (1993) Scatter factor induces blood vessel formation in vivo. *Proc Natl Acad Sci USA* **90**: 1937–1941

Grey AM, Schor AM, Rushton G, Ellis I and Schor SL (1989) Purification of the migration stimulating factor produced by fetal and breast cancer patient fibroblasts. *Proc Natl Acad Sci USA* **86**: 2438–2442

Grobstein C (1967) Mechanisms of organogenetic tissue interactions. *Natl Cancer Inst Monogr* **26**: 279–299

Jeffers M, Rong S and Vande Woude GF (1996) Enhanced tumorigenicity and invasion-metastasis by hepatocyte growth factor/scatter factor-met signalling in human cells concomitant with induction of the urokinase proteolysis network. *Mol Cell Biol* **16**: 1115–1125

Jiang WG, Lloyds D, Puntis MC, Nakamura T and Hallett MB (1993) Regulation of spreading and growth of colon cancer cells by hepatocyte growth factor. *Clin Exp Metastasis* **11**: 235–242

Jin L, Fuchs A, Schnitt SJ, Yao Y, Joseph A, Lamszus K, Park M, Goldberg ID and Rosen EM (1997*a*) Expression of scatter factor and c-met receptor in benign and malignant breast tissue. *Cancer* **79**: 749–760

Jin L, Yuan RQ, Fuchs A, Yao Y, Joseph A, Schwall R, Schnitt SJ, Guida A, Hastings HM, Andres J, Turkel G, Polverini PJ, Goldberg D, Rosen EM (1997*b*) Expression of interleukin-1β in human breast carcinoma. *Cancer* **80**: 421–434

Karmali RA, Welt S, Thaler HT and Lefevre F (1983) Prostaglandins in breast cancer: relationship to disease stage and hormone status. *Br J Cancer* **48**: 689–696

Konishi T, Takehara T, Tsuji T, Ohsato K, Matsumoto K and Nakamura T (1991) Scatter factor from human embryonic lung fibroblasts is probably identical to hepatocyte growth factor. *Biochem Biophys Res Commun* **180**: 765–773

Lamszus K, Jin L, Fuchs A, Shi E, Chowdhury S, Yao Y, Polverni PJ, Laterra J, Goldberg ID and Rosen EM (1997) Scatter factor stimulates tumor growth and angiogenesis in human breast cancers in the mammary fat pads of nude mice. *Lab Invest* **76**: 339–353

Lippman ME and Dickson RB (1990) Growth control of normal and malignant breast epithelium. *Prog Clin Biol Res* **354A**: 147–178

Marnett LJ (1995) Aspirin and related nonsteroidal anti-inflammatory drugs as chemopreventive agents against colon cancer. *Prevent Med* **24**: 103–106

Matsumoto K, Matsumoto K, Nakamura T and Kramer RH (1994) Hepatocyte growth factor/scatter factor induces tyrosine phosphorylation of focal adhesion kinase (p125 FAK) and promotes migration and invasion by oral squamous cell carcinoma cells. *J Biol Chem* **269**: 31807–31813

Matsumoto K, Okazaki H and Nakamura T (1995) Novel function of prostaglandins as inducers of gene expression of HGF and putative mediators of tissue regeneration. *J Biochem (Tokyo)* **117**: 458–464

Matsumoto K, Date K, Shimura H and Nakamura T (1996) Acquisition of invasive phenotype in gallbladder cancer cells via mutual interaction of stromal fibroblasts and cancer cells as mediated by hepatocyte growth factor. *Jpn J Cancer Res* **87**: 702–710

Matsumoto K and Nakamura T (1997) Hepatocyte growth factor (HGF) as a tissue organizer for organogenesis and regeneration. *Biochem Biophys Res Commun* **239**: 639–644

Matsunaga T, Gohda E, Takebe T, Wu YL, Iwao M, Kataoka H and Yamamoto I (1994) Expression of hepatocyte growth factor is up-regulated through activation of a cAMP-mediated pathway. *Exp Cell Res* **210**: 326–335

Matsuzaki K, Yoshitake Y, Matuo Y, Sasaki H and Nishikawa K (1989) Monoclonal antibodies against heparin-binding growth factor II/basic fibroblast growth factor that block its biological activity: invalidity of the antibodies for tumor angiogenesis. *Proc Natl Acad Sci USA* **86**: 9911–9915

Montesano R, Matsumoto K, Nakamura T and Orci L (1991) Identification of a fibroblast-derived epithelial morphogen as hepatocyte growth factor. *Cell* **67**: 901–908

Nagy J, Curry GW, Hillan KJ, McKay IC, Mallon E, Purushotham AD and George WD (1996) Hepatocyte growth factor/scatter factor expression and c-met in primary breast cancer. *Surg Oncol* **5**: 15–21

Nakamura T, Nawa K and Ichihara A (1984) Partial purification and characterization of hepatocyte growth factor from serum of hepatectomized rats. *Biochem Biophys Res Commun* **122**: 1450–1459

Nakamura T, Nishizawa T, Hagiya M, Seki T, Shimonishi M, Sugimura A, Tashiro K and Shimizu S (1989) Molecular cloning and expression of human hepatocyte growth factor. *Nature* **342**: 440–443

Nakamura T, Matsumoto K, Kiritoshi A, Tano Y and Nakamura T (1997) Induction of hepatocyte growth factor in fibroblasts by tumor–derived factors affects invasive growth of tumour cells: in vitro analysis of tumor-stromal interactions. *Cancer Res* **57**: 3305–3313

Narisawa T, Kusaka H, Yamazaki Y, Takahashi M, Koyama H, Koyama K, Fukuda Y and Wakizaka A (1990) Relationship between blood plasma prostaglandin E_2 and liver and lung metastases in colorectal cancer. *Dis Colon Rectum* **33**: 840–845

Niranjan B, Buluwela L, Yant J, Perusinghe N, Atherton-A, Phippard D, Dale T, Gusterson B and Kamalati T (1995) HGF/SF: a potent cytokine for mammary growth, morphogenesis and development. *Development* **121**: 2897–2908

Ohmichi H, Koshimizu U, Matsumoto K and Nakamura T (1998) Hepatocyte growth factor (HGF) acts as a mesenchyme-derived morphogenic factor during fetal lung development. *Development* **125**: 1315–1324

Picard O, Rolland Y and Poupon MF (1986) Fibroblast-dependent tumorigenicity of cells in nude mice: implication for implantation of metastases. *Cancer Res* **46**: 3290–3294

Rahimi N, Tremblay E, McAdam L, Park M, Schwall R and Elliott B (1996) Identification of a hepatocyte growth factor autocrine loop in a murine mammary carcinoma. *Cell Growth Differ* **7**: 263–270

Rolland PH, Martin PM, Jacquemier J, Rolland AM and Toga M (1980) Prostaglandin in human breast cancer: evidence suggesting that an elevated prostaglandin production is a marker of high metastatic potential for neoplastic cells. *J Natl Cancer Inst* **64**: 1061–1070

Rosen EM, Joseph A, Jin L, Rockwell S, Elias JA, Knesel J, Wines J, McClellan J, Kluger MJ, Goldberg ID and Zitnik R (1994) Regulation of scatter factor production via a soluble inducing factor. *J Cell Biol* **127**: 225–234

Rosenberg L (1995) Nonsteroidal anti-inflammatory drugs and cancer. *Prev Med* **24**: 107–109

Sakakura T (1991) New aspects of stroma-parenchyma relations in mammary gland differentiation. *Int Rev Cytol* **125**: 165–202

Santos OF, Barros EJ, Yang XM, Matsumoto K, Nakamura T, Park M and Nigam SK (1994) Involvement of hepatocyte growth factor in kidney development. *Dev Biol* **163**: 525–529

Sasaki M, Nishio M, Sasaki T and Enami J (1994) Identification of mouse mammary fibroblast-derived mammary growth factor as hepatocyte growth factor. *Biochem Biophys Res Commun* **199**: 772–779

Seki T, Ihara I, Sugimura A, Shimonishi M, Nishizawa T, Asami O, Hagiya M, Nakamura T and Shimizu S (1990) Isolation and expression of cDNA for different forms of hepatocyte growth factor from human leukocyte. *Biochem Biophys Res Commun* **172**: 321–327

Seslar S, Nakamura T and Byers S (1993) Regulation of fibroblast hepatocyte growth factor/scatter factor expression by human breast carcinoma cell lines and peptide growth factors. *Cancer Res* **53**: 1233–1238

Soriano JV, Pepper MS, Nakamura T, Orci L and Montesano R (1995) Hepatocyte growth factor stimulates extensive development of branching duct-like structures by cloned mammary gland epithelial cells. *J Cell Sci* **108**: 413–430

Stoker M, Gherardi E, Perryman M and Gray J (1987) Scatter factor is a fibroblast-derived modulator of epithelial cell mobility. *Nature* **327**: 239–242

Sykes JA, Whitescarver J and Briggs L (1968) Observations on a cell line producing mammary tumor virus. *J Natl Cancer Inst* **41**: 1315–1327

Tabata MJ, Kim K, Liu J, Yamashita K, Matsumura T, Kato J, Iwamoto M, Wakisaka S, Matsumoto K, Nakamura T, Kumegawa M and Kurisu K (1996) Hepatocyte growth factor is involved in the morphogenesis of tooth germ in murine molars. *Development* **122**: 1243–1251

Takahashi M, Ota S, Hata Y, Mikami Y, Azuma N, Nakamura T, Terano A and Omata M (1996) Hepatocyte growth factor as a key to modulate anti-ulcer action of prostaglandins in stomach. *J Clin Invest* **98**: 2604–2611

Tremblay G (1979) Stromal aspects of breast carcinoma. *Exp Mol Pathol* **31**: 248–260

Tuck AB, Park M, Sterns EE, Boag A and Elliott BE (1996) Coexpression of hepatocyte growth factor and receptor (Met) in human breast carcinoma. *Am J Pathol* **148**: 225–232

van den Hooff A (1988) Stromal involvement in malignant growth. *Adv Cancer Res* **50**: 159–196

Vassalli JD, Dayer JM, Wohlwend A and Belin D (1984) Concomitant secretion of prourokinase and of a plasminogen activator-specific inhibitor by cultured human monocytes-macrophages. *J Exp Med* **159**: 1653–1668

Vassalli JD and Pepper MS (1994) Tumour biology. Membrane proteases in focus. *Nature* **370**: 14–15

Wang Y, Selden AC, Morgan N, Stamp GWH and Hodgson HJF (1994) Hepatocyte growth factor/scatter factor expression in human mammary epithelium. *Am J Pathol* **144**: 675–682

Watson J and Chuah SY (1992) Technique for the primary culture of human breast cancer cells and measurement of their prostaglandin secretion. *Clin Sci (Colch)* **83**: 347–352

Weidner KM, Behrens J, Vandekerckhove J and Birchmeier W (1990) Scatter factor: molecular characteristics and effect on the invasiveness of epithelial cells. *J Cell Biol* **111**: 2097–2108

Weidner KM, Arakaki N, Hartmann G, Vandekerckhove J, Weingart S, Rieder H, Fonatsch C, Tsubouchi H, Hishida T, Daikuhara Y and Birchmeier W (1991) Evidence for the identity of human scatter factor and human hepatocyte growth factor. *Proc Natl Acad Sci USA* **88**: 7001–7005

Wernert N (1997) The multiple roles of tumour stroma. *Virchows Arch* **430**: 433–443

Yamashita J, Ogawa M, Yamashita S, Nomura K, Kuramoto M, Saishoji T and Shin S (1994) Immunoreactive hepatocyte growth factor is a strong and independent predictor of recurrence and survival in human breast cancer. *Cancer Res* **54**: 1630–1633

Yang Y, Spitzer E, Meyer D, Sachs M, Niemann C, Hartmann G, Weidner KM ,Birchmeier C and Birchmeier W (1995) Sequential requirement of hepatocyte growth factor and neuregulin in the morphogenesis and differentiation of the mammary gland. *J Cell Biol* **131**: 215–226

Yao Y, Jin L, Fuchs A, Joseph A, Hastings HM, Goldberg ID and Rosen EM (1996) Scatter factor protein levels in human breast cancers: clinicopathological and biological correlations. *Am J Pathol* **149**: 1707–1717

Zarnegar R and Michalopoulos GK (1995) The many faces of hepatocyte growth factor: from hepatopoiesis to hematopoiesis. *J Cell Biol* **129**: 1177–1180

British Journal of Cancer (1999) 80(11), 1708–1717

Article no. bjoc.1999.0587

参考論文

Autocrine and paracrine motility factors and their involvement in invasiveness in a human oral carcinoma cell line

R Hasina[1,2], K Matsumoto[1], N Matsumoto-Taniura[1], I Kato[2], M Sakuda[2] and T Nakamura[1]

[1]Division of Biochemistry, Biomedical Research Center, Osaka University Medical School, Suita, Osaka 565-0871, Japan; [2]Second Department of Oral and Maxillofacial Surgery, Osaka University Faculty of Dentistry, Suita, Osaka 565-0871, Japan

Summary Invasive potentials of malignant cancer cells are regulated by cell motility factors. To examine the regulation of motility and invasiveness in oral squamous carcinoma, we investigated autocrine- and/or paracrine-acting cell motility factors, using a newly established human cell line (IF cells) from oral squamous cell carcinoma, which has highly invasive and metastatic characteristics. Conditioned medium derived from IF cells stimulated cell scattering and migration of GB-d1 gallbladder carcinoma cells, indicating that IF cells secreted cell motility factors. Using antibodies, IF-derived cell motility factors proved to be transforming growth factor (TGF)-α and TGF-β1. Antibodies against TGF-α and TGF-β1 inhibited autonomous migration of the IF cells. On the other hand, in vitro invasion of IF cells was strongly enhanced by hepatocyte growth factor (HGF) but only slightly by TGF-α and TGF-β1. The conditioned medium from fibroblasts enhanced in vitro invasion of IF cells, an event abrogated by anti-HGF antibody, but not by antibodies against TGF-α and TGF-β1. Importantly, IF cells secreted a factor inducing HGF production in fibroblasts and the factor was identified as interleukin-1, which means that a mutual interaction exists between tumour cells and fibroblasts, as mediated by the HGF/HGF-inducer loop. These results indicate that IF cells utilize TGF-α and TGF-β1 as autocrine-acting motility factors and HGF as a paracrine-acting motility factor, and that invasiveness of IF cells is particularly stimulated by HGF derived from stromal fibroblasts. Utilization of multiple cell motility/invasion factors that act in distinct pathways may confer highly invasive and metastatic potentials in IF oral squamous carcinoma cells.

Keywords: cell motility factor; HGF; TGF-α; TGF-β; tumour invasion; tumour–stromal interaction

The transition from in situ tumour growth to invasive and metastatic disease is initially characterized by the potential of the tumour cells at the primary site to cross tissue barriers and to invade local tissues. In case of malignant tumours originating from epithelial tissue, cells in the primary tumour lose adherent cell–cell interaction, create a pathway through basement membrane and surrounding stroma, and migrate through the pathway it has created. Thus, degradation of local extracellular matrix components and accompanying cellular movement are particular characteristics associated with invasive tumours.

Studies done in the past decade revealed a unique group of cell motility factors and that many growth factors and ligands for receptor tyrosine kinases share motogenic activity (enhancement of cell motility) (reviewed in Stoker and Gherardi, 1991; Wright et al, 1993; Levine et al, 1995; Chicoine and Silbergeld, 1997). Scatter factor was originally identified as fibroblast-derived motility factor for epithelial cells (Stoker and Perryman, 1985), while subsequent purification and characterization revealed this factor to be identical to hepatocyte growth factor (HGF) (Gherardi et al, 1989; Weidner et al, 1990, 1991; Furlong et al, 1991; Konishi et al, 1991; Naldini et al, 1991). HGF was originally identified and cloned as a mitogenic polypeptide for hepatocytes (Nakamura et al, 1984, 1989; Russell et al, 1984; Miyazawa et al, 1989).

Received 19 October 1998
Revised 16 February 1999
Accepted 17 February 1999

Correspondence to: T Nakamura

Several growth factors, initially identified as mitogenic polypeptides, also affect motility of a wide variety of cells, including platelet-derived growth factor (PDGF), insulin-like growth factor-I (IGF-I), IGF-II, basic fibroblast growth factor (bFGF), transforming growth factor (TGF)-α and TGF-β1 (also see above reviews). These cell motility factors play important roles in regulating cell movement in physiological and pathological processes, including embryogenesis, tissue repair, inflammation as well as tumour invasion (reviewed in Levine et al, 1995; Chicoine and Silbergeld, 1997; Wehrle-Haller and Weston, 1997; Birchmeier and Gherardi, 1998).

Migration and invasion of cancer cells are particularly regulated by cell motility factors which act in autocrine- and/or paracrine-related manner. Establishment of an autocrine loop of growth factors is involved in tumorigenic transformation and progression to malignant cancer cells (Sporn and Roberts, 1985; Ullrich and Schlessinger, 1990; Wright et al, 1993; Levine et al, 1995; Silletti and Raz, 1996; Chicoine and Silbergeld, 1997). In addition to these factors, participation of paracrine factors have been implicated in tumour invasion and malignant progression, as based on the notion that growth and invasive potentials of carcinoma cells are influenced through interactions with host stromal cells (van den Hooff, 1988; Matsumoto et al, 1989; Camps et al, 1990; Wernert, 1997). HGF is a mesenchymal- (or stromal-)derived paracrine factor which affects cell growth, cell motility and morphogenesis of a wide variety of cells, including malignant ones (Jiang et al, 1993; Matsumoto and Nakamura, 1997; Birchmeier and Gherardi, 1998). In vitro, HGF stimulates migration or

invasion of various types of carcinoma cells (Weidner et al, 1990; Matsumoto et al, 1994; Shibamoto et al, 1994; Jeffers et al, 1996; Bennett et al, 1997; Inoue et al, 1997; Nakamura et al, 1997; also reviewed in Jiang et al, 1998) and autonomous activation of cMet/HGF receptor through the autocrine loop of HGF confers invasive and metastatic potential of tumour cells (Jeffers et al, 1996).

Oral squamous cell carcinomas are generally malignant tumours, with invasive and metastatic potentials. We established a distinct tumour cell line (IF cells) from a patient with oral squamous cell carcinoma. These IF cells are highly invasive and metastatic when implanted into athymic mice and thus IF cells retain invasive and metastatic potential (manuscript in preparation). We hypothesized that cell motility and invasiveness of IF cells might be regulated by cell motility factors which act in an autocrine or paracrine manner. In the present study, we identified paracrine and autocrine cell motility factors in this tumour cell line. Therefore, IF oral squamous cell carcinoma cells utilize both autocrine- and paracrine-acting cell motility factors and utilization of these multiple factors presumably confers invasive and metastatic potential in this malignant oral squamous carcinoma cell line.

MATERIALS AND METHODS

Materials

Mouse monoclonal antibodies against human TGF-α and TGF-β1 were obtained from Calbiochem, Calbiochem-Novabiochem Int. (Cambridge, MA, USA) and TAGO Products (Burlingame, CA, USA) respectively. Polyclonal antibody against HGF was prepared from the serum of a rabbit immunized with human recombinant HGF and 1 μg ml^{-1} anti-human HGF IgG completely neutralized the biological activities of 1 ng ml^{-1} of human HGF (Matsumoto et al, 1996). Human recombinant TGF-α was kindly provided by Genentec (San Francisco, CA, USA) and TGF-β1 was purified from human platelets (Okada et al, 1989). HGF was purified from the culture media of Chinese hamster ovary cells transfected with an expression plasmid containing human HGF cDNA (Nakamura et al, 1989). Human recombinant interleukin-1 receptor antagonist (IL-1 RA) was obtained from R & D Systems Inc. (Minneapolis, MN, USA). Antibody against human PDGF was obtained from Promega (Madison, WI, USA).

Cell culture

IF cells were originally established from a patient with squamous cell carcinoma of gingiva of the lower jaw. The cells were cultured in α-modified Eagle's medium (α-MEM) supplemented with 10% fetal bovine serum (FBS). MDCK clone 3B (Madin-Darby Canine Kidney) epithelial cells and GB-d1 human gallbladder carcinoma cells were kind gifts from Dr R Montesano (University of Geneva) and Dr H Shimura (Fukuoka University) respectively. MDCK and GB-d1 cells were cultured in Dulbecco's modified Eagle's medium (DMEM) supplemented with 10% FBS. Human dermal and oral fibroblasts were initially allowed to proliferate outward from tissue obtained during surgery and the cells were cultured in DMEM supplemented with 10% FBS.

Assay for cell growth and scattering

IF cells were plated at 500 cells cm^{-2} in 12-well plates in α-MEM supplemented with 10% FBS and cultured for 24 h. The culture media was replaced by α-MEM containing 1% FBS and the cells were cultured in the absence or presence of 10 ng ml^{-1} HGF, TGF-α or TGF-β1 for 72 h. The number of cells was counted using a Coulter counter after dissociation by trypsin.

For cell scattering assay, MDCK or GB-d1 cells were plated at 2.5×10^3 cells cm^{-2} in DMEM containing 10% FBS and cultured for 24 h. The conditioned medium from IF cells or growth factors were added, cells were further cultured for 24 h, placed under a microscope and photographed.

Measurement of HGF production

Human skin or oral fibroblasts were seeded on 48-well plates at a density of 5×10^4 cells cm^{-2} and cultured for 24 h. After replacing the media with fresh DMEM supplemented with 1% FBS and 2 μg ml^{-1} heparin, appropriate amounts of cytokines or the conditioned medium from IF cells was added and the cells were cultured for 24 h. The concentration of HGF in culture media was measured by enzyme-linked immunoabsorbent assay (ELISA), using a kit (Institute of Immunology Co. Ltd, Tokyo, Japan).

In vitro migration assay

Migration of tumour cells was carried out using Transwell chamber equipped with a filter membrane with 8-μm pores (Corning Costar Co., Cambridge, MA, USA). Tumour cells were plated at 5×10^4 cells cm^{-2} in the upper compartment of the chamber, and cultured for 24 h, fixed in 70% ethanol and stained with haematoxylin and eosin. The number of cells migrating to the undersurface of the membrane through the pores was counted, as viewed microscopically. Six microscopic fields were randomly selected for cell counting. To examine the inhibitory effects of specific antibodies on migration of tumour cells, antibodies against TGF-α, TGF-β and HGF were added at 10 μg ml^{-1}.

In vitro invasion assay

In vitro invasion of tumour cells was measured using the Biocoat Matrigel Invasion Chamber (Becton Dickinson Labware, Bedford, MA, USA). In this apparatus, Matrigel basement membrane components are reconstituted on a filter membrane with 8-μm pores. The cells were plated at a density of 10^5 cells cm^{-2} on the Matrigel in the upper compartment of the chamber and cultured for 48 h. The number of cells that invaded the undersurface of the membrane was counted, as described above. To examine the extent of invasion of IF cells into collagen gel matrix, the tumour cells were embedded in collagen gel (Type I Collagen, Nitta gelatin, Osaka, Japan) at 5×10^3 cells ml^{-1}, and cultured for 7 days. The culture medium was changed every second day.

RESULTS

Production and identification of motility factors from IF cells

IF cells were established from a lymph node metastasis of poorly differentiated squamous cell carcinoma which had primarily developed in the lower jaw. Histologically the tumour was highly infiltrative and invaded the capsular sheath of metastasized lymph nodes. When IF cell were subcutaneously implanted in the

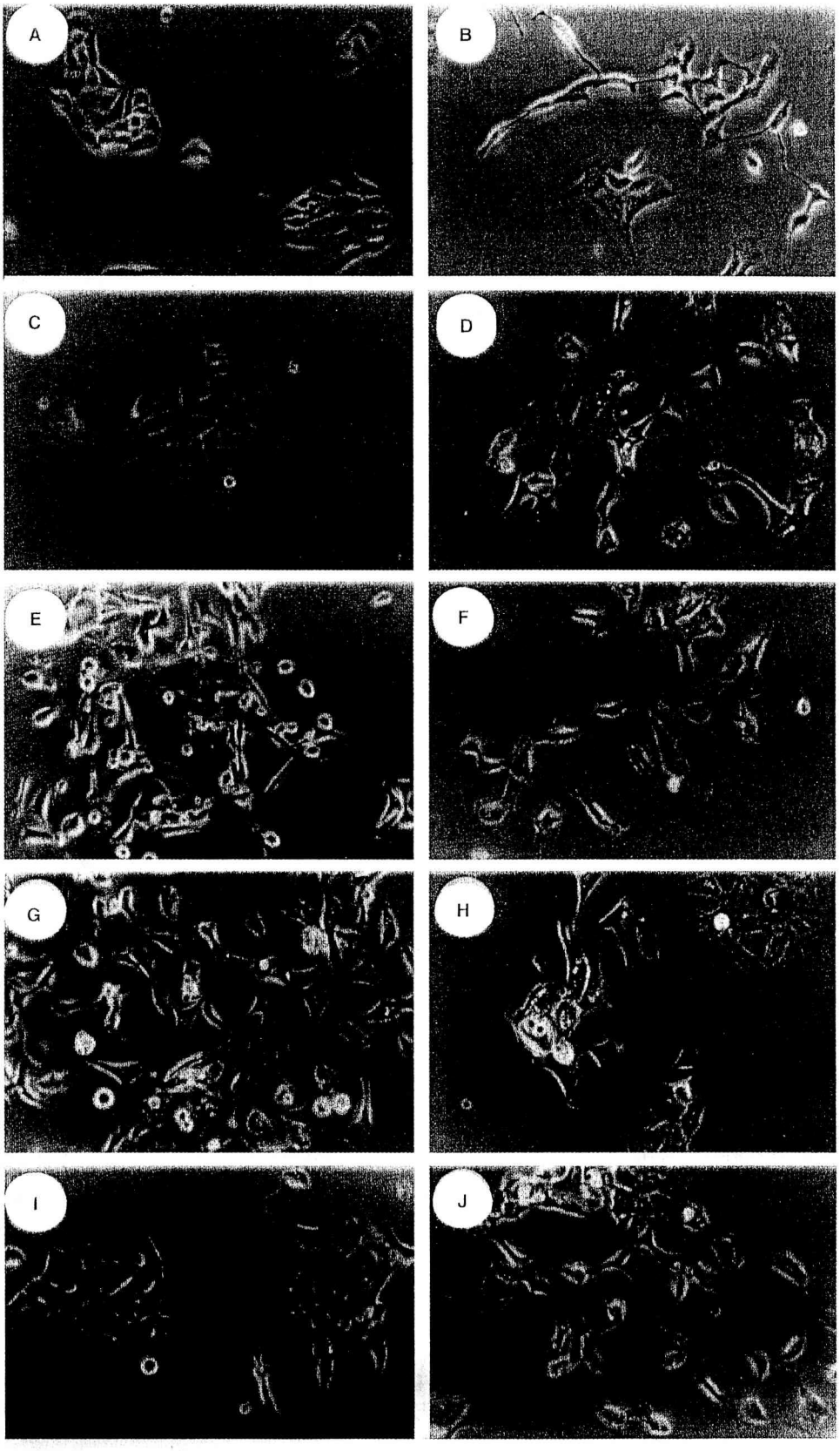

Figure 1 Cell scattering induced by conditioned medium from IF cells and growth factors. Cell scattering was examined using MDCK renal epithelial cells (**A**, **B**) and GB-d1 gallbladder carcinoma cells (**C**–**J**). These cells were cultured in the absence (**A**, **C**) or presence of IF-derived conditioned medium (IF-CM) (**B**, **D**), TGF-α (**E**), TGF-β1 (**F**), HGF (**G**), IF-CM + anti-TGF-α IgG (**H**), IF-CM + anti-TGF-β IgG (**I**), or IF-CM + anti-HGF IgG (**J**). IF-CM was added at 50% (v/v) to these cultures, growth factors were at 10 ng ml^{-1} and IgGs were at 10 μg ml^{-1}. These antibodies respectively neutralized cell scattering activity of 10 ng ml^{-1} TGF-α, TGF-β1 and HGF and normal IgG had no effect on cell scattering activity of IF-CM (not shown)

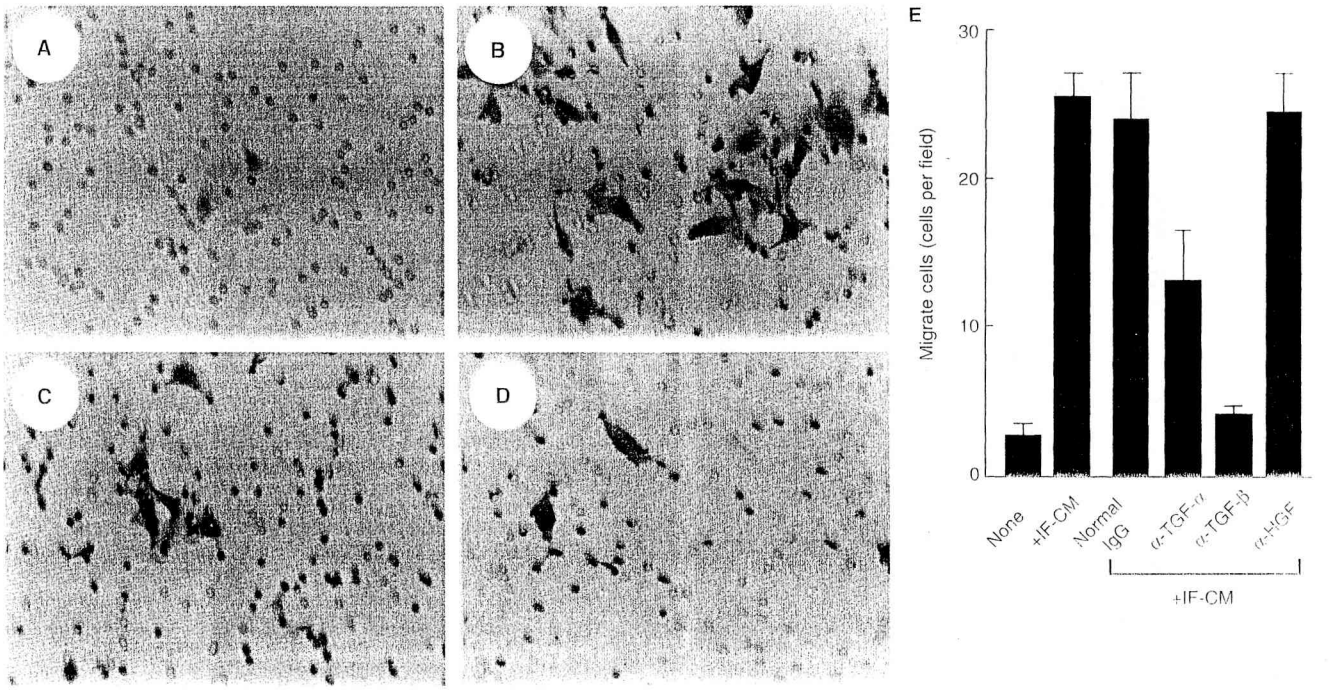

Figure 2 Inhibitory effect of antibodies on stimulatory effect of IF-derived conditioned medium on migration of GB-d1 cells. Migration of GB-d1 cells was measured using Transwell chamber. (**A–D**) Appearance of cells which migrated through the membrane with pores. GB-d1 cells were cultured in the absence (**A**) or presence of IF-derived conditioned medium (IF-CM) (**B**), IF-CM + anti-TGF-α IgG (**C**), IF-CM + anti-TGF-β1 IgG (**D**). (**E**) The number of migrated cells. IF-CM was added at 50% (v/v) to cultures of GB-d1 cells and antibodies (IgGs) against TGF-α, TGF-β1 and HGF (α-TGF-α, α-TGF-β1, α-HGF) were added at 10 μg ml^{-1}. These antibodies neutralized migration of GB-d1 cells stimulated by 10 ng ml^{-1} TGF-α, TGF-β1 and HGF (not shown)

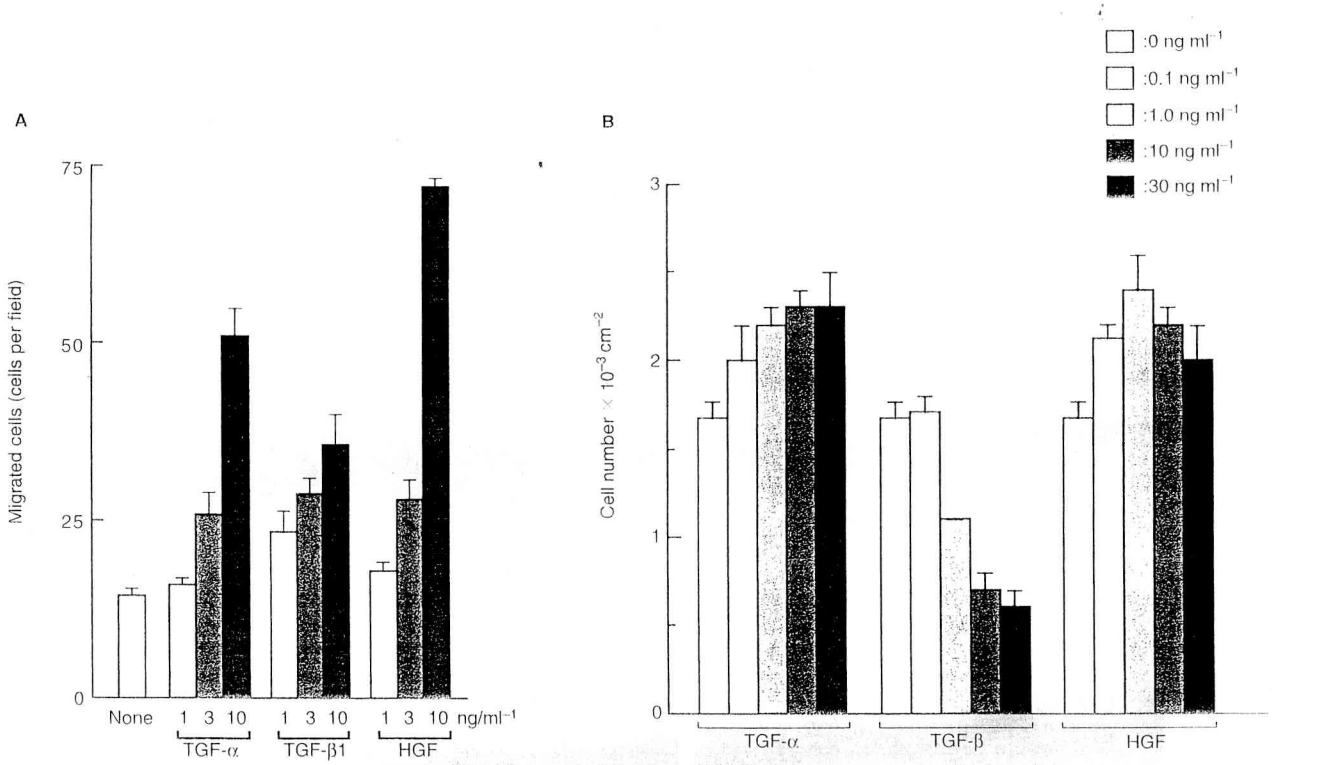

Figure 3 Effects of TGF-α, TGF-β1 and HGF on migration (**A**) and growth (**B**) of IF cells. Migration of IF cells was measured using Transwell chamber. For cell growth assay, IF cells were cultured in the absence or presence of TGF-α, TGF-β1, or HGF for 72 h

athymic mouse, the tumour cells invaded inguinal and axillary lymph nodes, and visible metastatic nodules were present on lungs within 4–6 weeks (manuscript in preparation). To determine if IF human oral squamous cell carcinoma cells produce cell motility factors, conditioned medium derived from IF cells was added to monolayer cultures of MDCK cells and GB-d1 gallbladder carcinoma cells respectively (Figure 1). Addition of conditioned medium from IF cells induced scattering of both MDCK and GB-d1 cells (Figure 1 A–D), indicating that IF cells secrete motility factor(s) bioactive for both MDCK and GB-d1 cells.

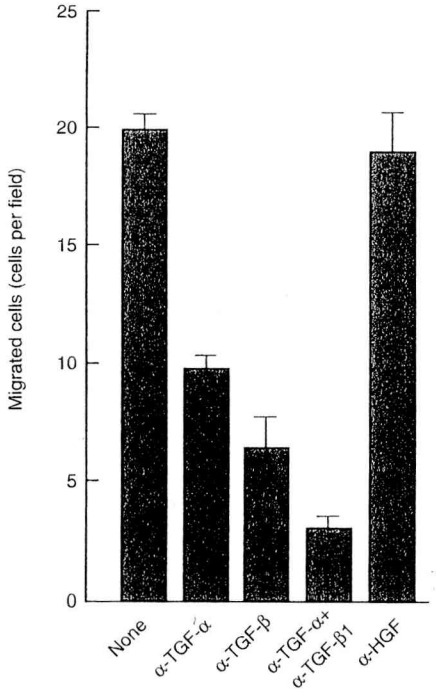

Figure 4 Effects of antibodies on autonomous migration of IF cells. Migration of IF cells was measured using Transwell chamber and antibodies (IgGs) against TGF-α, TGF-β1 and HGF (α-TGF-α, α-TGF-β1, α-HGF) were added at 10 μg ml^{-1}

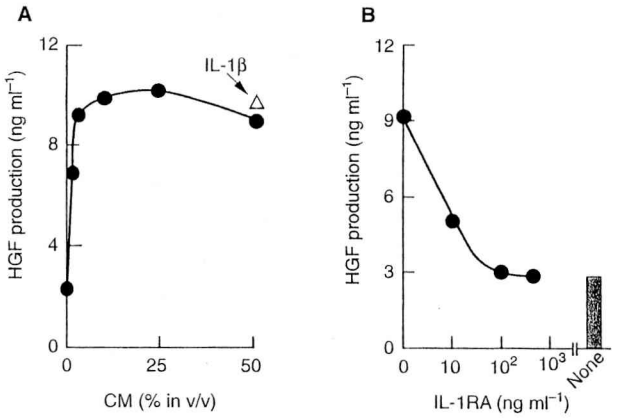

Figure 5 Enhancement of HGF production in human skin fibroblasts by IF-derived conditioned medium (**A**) and its inhibition by IL-1 receptor antagonist (**B**). Human skin fibroblasts were cultured in the absence or presence of IF-derived conditioned medium or 1 ng ml^{-1} IL-1β and HGF production during 24-h culture of the fibroblasts was measured (**A**). IF-derived conditioned medium was added at 10% (v/v) to cultures of fibroblasts and various concentrations of IL-1 receptor antagonist (IL-1RA) were added (**B**)

To identify motility factor(s) derived from IF cells, we asked if known growth factors and cytokines would induce scattering of GB-d1 cells (Figure 1). Among various growth factors and cytokines tested, TGF-α, TGF-β1 and HGF showed scattering effects on GB-d1 cells (Figure 1 E–G), while PDGF, bFGF, vascular endothelial cell growth factor, IL-1β, IL-2, IL-6 and tumour necrosis factor-α did not induce cell scattering (not shown). We therefore examined effects of antibodies against TGF-α, TGF-β1 and HGF on cell scattering activity in IF-derived conditioned medium. When an antibody against TGF-α or TGF-β1 was added to the conditioned medium of IF cells, cell scattering activity in the medium was significantly inhibited (Figure 1 H, I), whereas anti-HGF antibody had no inhibitory effect on the cell scattering induced by IF-derived medium (Figure 1, J). This finding meant that IF-derived cell motility factors might be TGF-α and TGF-β1.

For further evidence that IF-derived motility factors are TGF-α and TGF-β1, migration of GB-d1 cells was quantitatively analysed using a Transwell apparatus (Figure 2). GB-d1 gallbladder carcinoma cells were seeded on Transwell filter membrane and the number of cells migrating to the undersurface of the membrane through 8-μm pores was counted. When IF-derived conditioned medium was added, the number of migrated cells greatly increased. However, the addition of anti-TGF-α and anti-TGF-β1 antibodies inhibited migration of GB-d1 cells: the inhibitory effect of anti-TGF-β1 antibody was more potent than that of anti-TGF-α (Figure 2E). These results indicate that IF cells do secrete cell motility factors, which proved to be TGF-α and TGF-β1.

Autocrine regulation of IF cell motility by TGF-β1 and TGF-α

Based on the finding that IF cells secreted TGF-α and TGF-β1 as cell motility factors, we analysed the regulation of IF cell motility by TGF-α, TGF-β1 and HGF, using Transwell assay. When TGF-α, TGF-β1 and HGF were individually added to culture of IF cells the migration of IF cells was dose-dependently stimulated by these growth factors (Figure 3A). Although a significant number of IF cells migrated through the membrane in control culture, migration of IF cells was further stimulated by these growth factors, in a dose-dependent manner. The potential to stimulate migration of IF cells was HGF > TGF-α > TGF-β1. HGF was most potent in stimulating IF cell motility and fivefold enhancement was seen with 10 ng ml^{-1} HGF. We also examined effects of these growth factors on proliferation of IF cells (Figure 3B). When the cells were cultured in the absence or presence of growth factors for 72 h, both TGF-α and HGF weakly stimulated the proliferation of IF cells, whereas TGF-β1 inhibited IF cell proliferation; therefore HGF and TGF-α are weak mitogens while TGF-β1 inhibits growth of IF cells.

To observe if the motility of IF cells was regulated by these factors in an autocrine manner, effects of antibodies on autonomous migration of IF cells were tested, using Transwell assay (Figure 4). When antibodies against TGF-α and TGF-β1 were added, migration of IF cells was inhibited to 49% and 33% of the control culture respectively. Simultaneous addition of these antibodies inhibited migration of IF cells to lower levels than seen in cases of anti-TGF-β1 or anti-TGF-α antibody alone. However, anti-HGF antibody had no significant effect on the autonomous migration of IF cells. Consistent with this, HGF was not detected in conditioned medium of IF cells by ELISA (not shown). Therefore, although TGF-α, TGF-β1 and HGF stimulate migration of IF cells, TGF-α and TGF-β, but not HGF, act as autocrine cell motility factors which regulate their own cell motility.

Induction of fibroblast production of HGF by IF-derived factor

Although IF cells do not produce HGF and HGF does not act as an autocrine motility factor in IF cells, we speculated that stromal fibroblasts-derived HGF might affect migration of IF cells in a paracrine manner. We previously showed that several types of

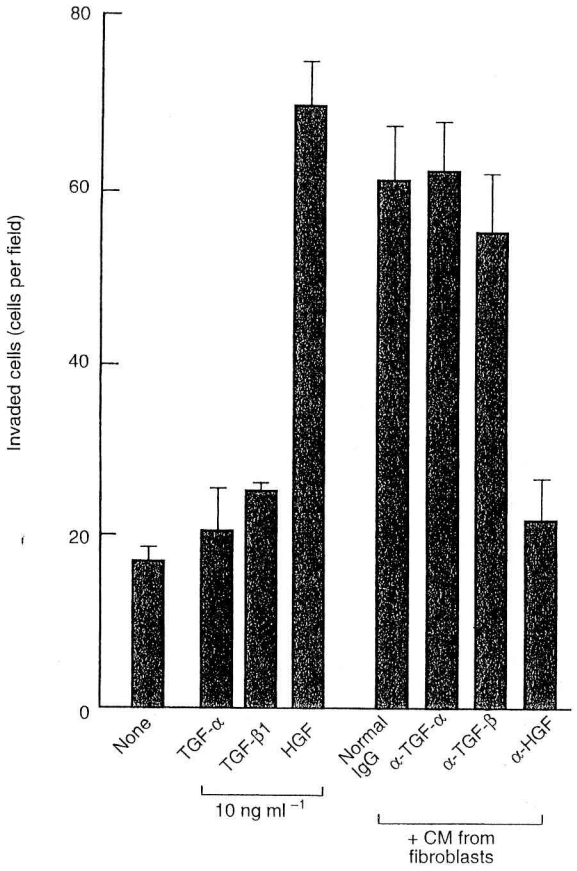

Figure 6 Effects of TGF-α, TGF-β1, HGF and fibroblast-derived conditioned medium (CM) on invasion of IF cells and inhibition of IF cell invasion induced by fibroblast-derived CM by antibodies. Invasion of IF cells was measured using Matrigel invasion chamber. Growth factors were added at 10 ng ml^{-1}, CM from human oral stromal fibroblasts at 50% (v/v) and antibodies (α-TGF-α, α-TGF-β1, α-HGF) were at 10 μg ml^{-1}

carcinoma cells secrete inducing factors for HGF production in normal human fibroblasts (Matsumoto et al, 1996; Nakamura et al, 1997). We therefore examined if IF cells would produce an inducing factor for HGF production in normal human fibroblasts derived from dermal tissue. When IF-derived conditioned medium was added to culture of human fibroblasts, HGF production by fibroblasts was dose-dependently stimulated and the maximal stimulatory effect by 4.4-fold was comparable to that seen with 1 ng ml^{-1} IL-1β (Figure 5A). Therefore, IF cells secrete a potent inducing factor for HGF production in fibroblasts.

To identify the IF-derived inducing factor for HGF production, we tested effects of antibodies and antagonistic molecules for inducers of HGF production in fibroblasts, including anti-bFGF, anti-PDGF and an IL-1 receptor antagonist. Addition of an IL-1 receptor antagonist suppressed the inducing activity in IF-derived conditioned medium to close to basal level (Figure 5B), whereas anti-bFGF and anti-PDGF antibodies had no significant effect on HGF-inducing activity in IF-derived conditioned medium (not shown). This finding indicates that IF cells secrete IL-1 (IL-1α, IL-1β1 or both) as an HGF inducer for stromal fibroblast. Similar results were obtained when fibroblasts derived from oral stromal tissue were used, while IL-1β was less potent in stimulating HGF production than that seen with skin fibroblasts (not shown).

Regulation of IF tumour invasiveness

Our findings indicate that motility of IF cells is regulated by at least three distinct growth factors: TGF-α and TGF-β1 act as autocrine motility factors, while HGF may act as a paracrine motility factor derived from stromal fibroblasts. We then asked whether the invasiveness of IF cells is regulated by these autocrine and paracrine motility factors. IF tumour cells were seeded on Matrigel invasion chamber and cultured for 48 h in the absence or presence of TGF-α, TGF-β1 or HGF (Figure 6). In this apparatus, invasive cells degrade Matrigel extracellular matrix components and then migrate to the undersurface of the membrane. During 48-h culture, a few cells invaded through Matrigel components and a filter membrane in the absence of growth factors. When IF cells were cultured in the presence of HGF, the number of invaded cells greatly increased: fourfold enhancement by HGF. However, both TGF-α and TGF-β1 weakly stimulated invasion of IF cells and their potency in stimulating invasion of IF cells was much less than that of HGF. On the other hand, addition of conditioned medium from human oral stromal fibroblasts also stimulated the invasion of IF cells. The stimulatory effect by this medium was little inhibited by antibodies against TGF-α and TGF-β1 but was greatly suppressed by anti-HGF antibody.

We next analysed invasiveness of IF tumour cells cultured in collagen gel matrix (Figure 7). When IF cells were grown in collagen gel matrix for 6 days in the absence of growth factors, they grew in a cystic structure with no invasive characteristics (Figure 7A, G). In contrast, when the cells were grown in the presence of HGF, they showed invasive and some characteristics of scattering (Figure 7D). Transverse section of these cells showed that IF cells lost cell–cell contact and several cells invaded the collagen gel matrix (Figure 7H). Similarly, the addition of conditioned medium from human oral stromal fibroblasts to cultures of IF cells induced significant invasive characteristics (Figure 7E). In contrast, addition of TGF-α or TGF-β1 did not induce invasive characteristics in IF cells grown in collagen gels (Figure 7B, C). Importantly, the invasive phenotype induced by fibroblast-derived conditioned medium was almost completely prevented by anti-HGF antibody (Figure 7F), but not by anti-TGF-α and anti-TGF-β1 antibodies (not shown). These observations mean that the invasiveness of IF cells is potently stimulated by HGF, but only marginally so by TGF-α and TGF-β1.

DISCUSSION

Malignant tumours are characterized by unrestrained growth and invasion into surrounding host tissue. Tumour invasion involves the active locomotion of tumour cells into and through host tissue barriers. Various polypeptide growth factors such as epidermal growth factor, PDGF, TGF-α, TGF-β1 and HGF stimulate not only cell proliferation but also chemotactic migration of various types of tumour cells. Likewise, a few classes of proteins which predominantly stimulate the motility of cells have been identified, using assay systems that measure cell motility (Stoker and Gherardi, 1991; Levine et al, 1995; Silletti and Raz, 1996). It is reasonable to consider that these motility factors are responsible for the highly motile behaviour in invasive tumour cells. Using human oral squamous carcinoma cell line, we analysed the regulation of cellular motility and invasiveness by extracellularly acting proteins produced by tumour cells themselves and stromal

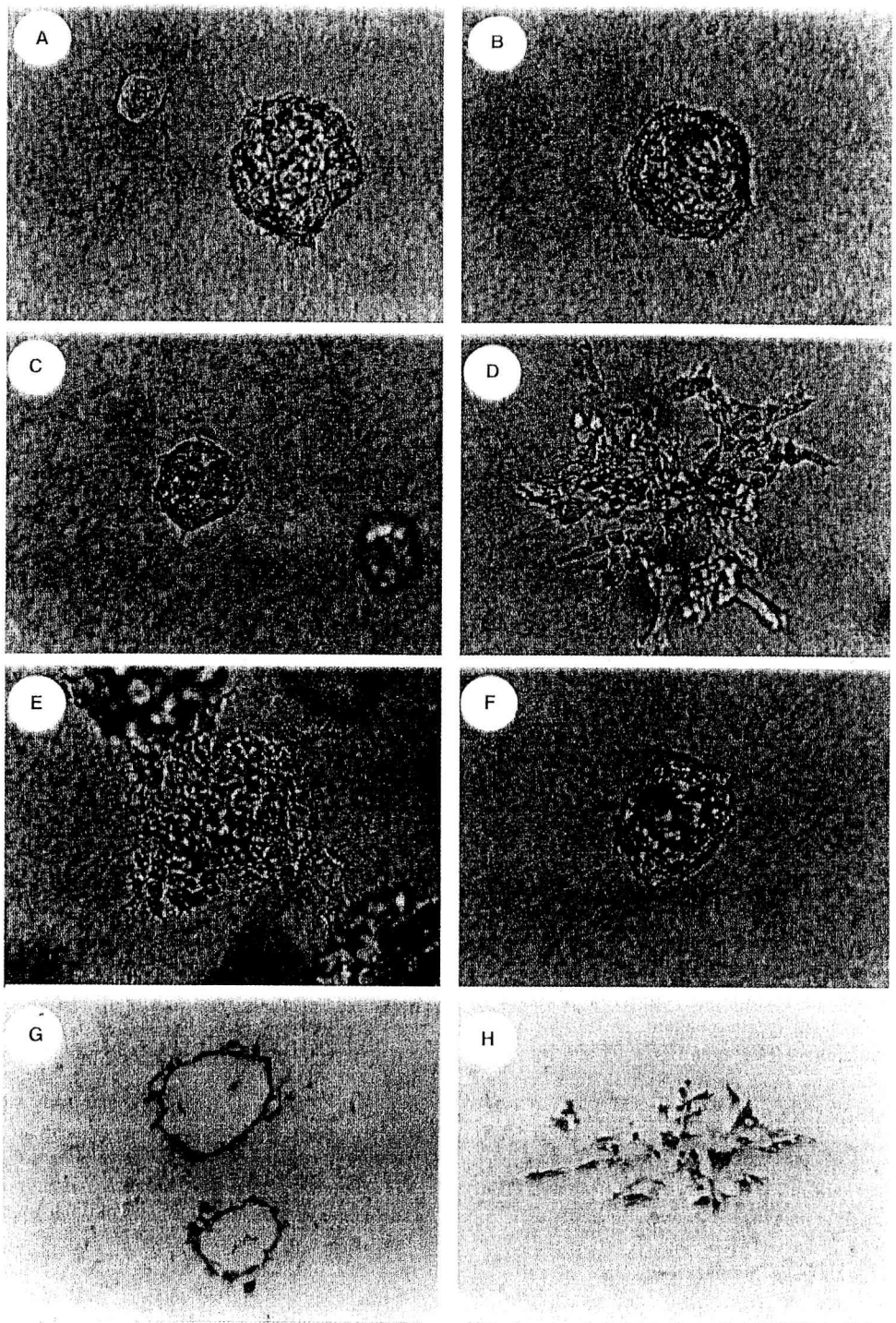

Figure 7 Invasive growth of IF cells in collagen gel matrix. IF cells were cultured for 7 days in the absence (**A, G**) or presence of TGF-α (**B**), TGF-β1 (**C**), HGF (**D, H**), conditioned medium (CM) from oral stromal fibroblasts (**E**), or fibroblast-derived CM + anti-HGF IgG (**F**). Anti-HGF IgG was added at 10 μg ml^{-1}. Appearances of IF cells (**A–F**) and transverse sections (**G, H**) were shown

fibroblasts. We identified TGF-α and TGF-β1 to be autocrine-acting motility factors, and HGF to be a stromal-derived paracrine motility factor in IF oral squamous carcinoma cells (Figure 8). Importantly, the invasiveness of IF cells was potently stimulated by HGF, but not by TGF-α and TGF-β1.

TGF-α and TGF-β1 were originally identified as tumour-derived factors which confer anchorage-independent tumour growth, while subsequent studies showed that TGF-α and TGF-β1 are produced in a wide variety of tumour cells and regulate their own growth and motility (Derynck et al, 1987; Sporn et al, 1987; Wright et al, 1993; Wright and Huang, 1996). Several investigators noted that TGF-β1 stimulates migration and invasion of distinct types of tumour cells, through an autocrine or a paracrine manner (Welch et al, 1990; Mooradian et al, 1992; Wright et al, 1993;

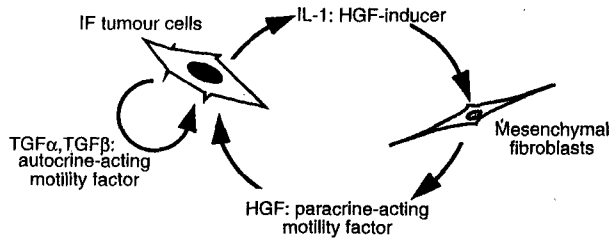

Figure 8 A schematic representation of the regulation of the IF tumour invasion by autocrine- and paracrine-acting factors. TGF-α and TGF-β1 act as autocrine-acting motility factors, while HGF acts as fibroblast-derived paracrine-acting motility factor. IF cells secrete IL-1 as an inducer for HGF production in fibroblasts

Wright and Huang, 1996; Chicoine and Silbergeld, 1997; Inoue et al, 1997). Likewise, TGF-α stimulates migration and invasion of certain types of tumour cells such as endometrial adenocarcinoma, glioma and uterine cervical carcinoma cells (Ueda et al, 1996, 1997; El Obeid et al, 1997). We identified motility factors derived from IF oral squamous cell carcinoma cells as TGF-α and TGF-β1. Since autonomous migration of IF cells was significantly inhibited by antibodies against TGF-α and TGF-β1, these growth factors may play a role as autocrine-acting cell motility factors which stimulate self migration in IF oral carcinoma cells. On the other hand, HGF stimulates the motility of a diversity of cells, including normal epithelial cells, endothelial cells and a wide variety of tumour cells (reviewed in Jiang et al, 1993, 1998; Zarnegar and Michalopoulas, 1995; Matsumoto et al, 1997). It is noteworthy that, although the motility of IF cells is enhanced by TGF-α, TGF-β1 and HGF, invasion of IF cells is particularly regulated by HGF rather than by TGF-α and TGF-β1. Similarly, we previously noted that the invasiveness of GB-d1 gallbladder cancer cells is potently stimulated by HGF but not TGF-α and TGF-β1, while TGF-α and TGF-β1 both stimulate migration of the cells (Matsumoto et al, 1996). Therefore, cellular responsiveness to stimulatory effects of TGF-α and TGF-β1 on invasion of cancer cells seems to be cell type-dependent. Nevertheless, we speculate that the production of TGF-α and TGF-β1 and autocrine activation of their receptors may be involved in invasive and metastatic behaviour in IF cells. Coexistence of TGF-α and TGF-β1 supports anchorage-independent growth in cancer cells (Derynck et al, 1987; Sporn et al, 1987), which is likely to increase metastatic potential. Enhancement of tumour migration by TGF-α and TGF-β1 may possibly increase invasiveness in IF cells, in collaboration with stromal-derived HGF.

Invasiveness of tumour cells involves disruption of cell–cell adhesion, enhanced cycle of detachment and attachment of cell–substrate interaction, breakdown of extracellular matrix components and enhanced cell motility. HGF induces tyrosine phosphorylation of β-catenin (Watabe et al, 1993; Shibamoto et al, 1994; Hiscox and Jiang, 1999) and focal adhesion kinase (Matsumoto et al, 1994). HGF activates Rho small GTP-binding protein (Takaishi et al, 1994; Ridly et al, 1995), by which intracellular cytoskeletal rearrangement occurs. These events are likely to lead to increased cell motility, dissociation of cell–cell interaction and remodelling of cell–substrate interactions. In addition to these events, HGF induces urokinase-type plasminogen activator (uPA) expression (Pepper et al, 1992; Jeffers et al, 1996; Bennett et al, 1997; Date et al, 1998) and stimulates the production of matrix metalloproteinases (MMPs) (Dunsmore et al, 1996; Bennett et al, 1997; Date et al, 1998). Jeffers et al (1996) demonstrated that induction of the uPA proteolysis network by HGF is coupled to enhanced tumorigenicity and invasive and metastatic properties in certain tumour cell lines. Since the induction and/or activation of proteinases that break down extracellular matrix components seem to be, at the least, critical for induction of invasive potential also in IF tumour cells, we analysed changes in activities of uPA and gelatinases (MMP-2 and MMP-9) in IF cells treated with TGF-α, TGF-β1 or HGF. However, we could not find specific changes in these proteinase activities that correlate to distinct potentials of TGF-α, TGF-β1 and HGF to stimulate invasiveness of IF tumour cells. Identification of extracellular matrix proteinases responsible for the induction of invasiveness by HGF remains to be addressed. Nevertheless, cooperative activation of multiple events driven by cMet/HGF receptor activation seems to be a cause for particular potency of HGF to stimulate the invasion of IF oral carcinoma cells, as well as other tumour cells.

Several lines of studies indicate that the growth and invasive potential of carcinoma cells are influenced through interaction with host stromal cells (van den Hooff, 1988; Matsumoto et al, 1989; Camps et al, 1990; Wernert, 1997). Indeed, the in vitro invasion of various human oral squamous carcinoma cells into collagen gel matrix was specifically induced by co-cultivation with stromal fibroblasts (Matsumoto et al, 1989) and the fibroblast-derived factor responsible for invasion of oral carcinoma cells proved to be HGF (Matsumoto et al, 1994). Thus these earlier findings apparently coincide with our present results: invasion of IF oral squamous carcinoma cells is particularly stimulated by stroma-derived HGF. Moreover, of interest in this study is that IF cells secrete IL-1 as a potent inducer for production of HGF in stromal fibroblasts. We reported that several types of carcinoma cells secrete inducers for HGF production in fibroblasts and fibroblast-derived HGF stimulates invasion of carcinoma cells. IL-1, bFGF and PDGF were identified as tumour-derived HGF-inducers (Matsumoto et al, 1996; Nakamura et al, 1997). There may be mutual paracrine interactions between IF tumour cells and fibroblasts: IL-1 derived from IF tumour cells activates neighbouring fibroblasts to up-regulate HGF production, while fibroblast-derived HGF in turn affects invasion of IF cells (Figure 8). Moreover, HGF has angiogenic activity (Bussolino et al, 1992; Grant et al, 1993) and breast carcinoma cells capable of producing HGF induced more extensive angiogenesis in vivo than that seen in parental cells incapable of producing HGF (Lamszus et al, 1997). Taken together, HGF seems to increase invasive and angiogenic characteristics in IF tumours through a paracrine interaction.

We used a newly established IF human oral squamous carcinoma cell line which possesses highly invasive and metastatic potentials, and identified distinct cells that affect motility and invasiveness of tumour cells in an autocrine or paracrine fashion. The utilization of multiple cell motility/invasion factors that act in distinct pathways in IF oral squamous carcinoma cells may confer highly invasive and metastatic potentials in microenvironments of tumour. Finally, based on the finding that local interaction between IF cells and fibroblasts, as mediated by HGF, is a mechanism leading to even more invasive events, we propose that disruption of this mutual interaction may be one strategy for prevention of tumour invasion and metastasis. In this context, the application of a newly identified four kringle containing antagonist for HGF (Date et al, 1997, 1998) can be tested for potential therapeutic value in suppressing invasion and metastasis of malignant oral squamous carcinoma cells.

ACKNOWLEDGEMENTS

We are very grateful to M Ohara for helpful comments. This study was supported by a Research Grant for Science and Cancer from the Ministry of Education, Science, Sports and Culture of Japan, a Research Grant for Cancer Research from the Ministry of Welfare of Japan and Research Grants from Haraguchi Memorial Foundation for Cancer Research, the Ryoichi Naito Foundation for Medical Research, Suzuken Memorial Foundation and Nissan Science Foundation.

REFERENCES

Bennett JH, Furness J, Atkin P and Speight PM (1997) Scatter factor (SF) regulation of matrix metalloproteinase production by oral carcinoma cells. *J Dental Res* **76**: 2140

Birchmeier C and Gherardi E (1998) Developmental role of HGF/SF and its receptor, the Met tyrosine kinase. *Trends Cell Biol* **8**: 404–410

Bussolino F, DiRenzo MF, Ziche M, Bochietto E, Olivero M, Naldini L, Goudino G, Tamagnone L, Coffer A and Comoglio PM (1992) Hepatocyte growth factor is a potent angiogenic factor which stimulates endothelial cell motility and growth. *J Cell Biol* **119**: 629–641

Camps JL, Chang S, Hsu TC, Freeman MR, Hong S, Zhau HE, von Eschenbach AC and Chung LWK (1990) Fibroblast-mediated acceleration of human epithelial tumour growth in vivo. *Proc Natl Acad Sci USA* **87**: 75–79

Chicoine MR and Silbergeld DL (1997) Mitogens as motogens. *J Neurooncol* **35**: 249–257

Date K, Matsumoto K, Shimura H, Tanaka M and Nakamura T (1997) HGF/NK4 is a specific antagonist for pleiotrophic actions of hepatocyte growth factor. *FEBS Lett* **420**: 1–6

Date K, Matsumoto K, Shimura H, Tanaka M and Nakamura T (1998) Inhibition of tumour growth and invasion by a four-kringle antagonist (HGF/NK4) for hepatocyte growth factor. *Oncogene* **17**: 3045–3054

Derynck R, Goeddel DV, Ullrich A, Gutterman JV, Williams RD, Bringman TS and Berger WH (1987) Synthesis of messenger RNAs for transforming growth factor-α and β and the epidermal growth factor receptor by human tumours. *Cancer Res* **47**: 707–712

Dunsmore SE, Rubin JS, Kovacs SO, Chedid M, Parks WC and Welgus HG (1996) Mechanisms of hepatocyte growth factor-stimulation of keratinocyte metalloproteinase production. *J Biol Chem* **271**: 24567–24582

El Obeid A, Bongcan-Rudloff E, Sorby M, Ostman A, Nister M and Westermark B (1997) Cell scattering and invasion induced by autocrine transforming growth factor-α in human glioma cells in vitro. *Cancer Res* **57**: 5598–5604

Furlong RA, Takehara T, Taylor WG, Nakamura T and Rubin JS (1991) Comparison of biological and immunochemical properties indicate that scatter factor and hepatocyte growth factor are indistinguishable. *J Cell Sci* **100**: 173–177

Gherardi E, Gray J, Stoker M, Perryman M and Furlong R (1989) Purification of scatter factor, a fibroblast-derived basic protein that modulates epithelial interaction and movement. *Proc Natl Acad Sci USA* **86**: 5844–5848

Grant DS, Kleinman HK, Goldberg ID, Bhargava MM, Nickoloff BJ, Kinsella JI, Polverini P and Rosen EM (1993) Scatter factor induces blood vessel formation in vivo. *Proc Natl Acad Sci USA* **90**: 1937–1941

Hiscox S and Jiang WG (1999) HGF/SF regulates the phosphorylation of β-catenin and cell–cell adhesion in cancer cells. *Proc Am Assoc Cancer Res*, in press

Inoue T, Chung YS, Yashiro M, Nishimura S, Hasuma T, Otani S and Sowa M (1997) Transforming growth factor-β and hepatocyte growth factor produced by gastric fibroblasts stimulate the invasiveness of scirrhous gastric cancer cells. *Jpn J Cancer Res* **88**: 152–159

Jeffers M, Rong S and Vande Woude GF (1996) Enhanced tumorigenicity and invasion-metastasis by hepatocyte growth factor/scatter factor met signalling in human cells concomitant with induction of the urokinase proteolysis network. *Mol Cell Biol* **16**: 1115–1125

Jiang WG, Hallett MB and Puntis MC (1993) Hepatocyte growth factor/scatter factor, liver regeneration and cancer metastasis. *Br J Surg* **80**: 1368–1373

Jiang WG, Hiscox S, Matsumoto K and Nakamura T (1999) Hepatocyte growth factor/scatter factor, its molecular, cellular and clinical implications in cancer. *Crit Rev Oncol Hematol* **29**: 209–248

Konishi T, Takehara T, Tsuji T, Ohsato K, Matsumoto K and Nakamura T (1991) Scatter factor from human embryonic lung fibroblasts is probably identical to hepatocyte growth factor. *Biochem Biophys Res Commun* **180**: 765–773

Lamszus K, Jin L, Fuchs A, Shi E, Chowdhury S, Yao Y, Polverini PJ, Laterra J, Goldberg ID and Rosen EM (1997) Scatter factor stimulates tumour growth and angiogenesis in human breast cancers in the mammary fat pads of nude mice. *Lab Invest* **76**: 339–353

Levine MD, Liotta LA and Stracke ML (1995) Stimulation and regulation of tumour cell motility in invasion and metastasis. In: *Epithelial–Mesenchymal Interactions in Cancer EXS* **74**: 157–179

Matsumoto K and Nakamura T (1997) Hepatocyte growth factor (HGF) as a tissue organizer for organogenesis and regeneration. *Biochem Biophys Res Commun* **239**: 639–644

Matsumoto K, Horikoshi M, Rikimaru K and Enomoto S (1989) A study of an in vitro model for invasion of oral squamous cell carcinoma. *J Oral Pathol Med* **18**: 498–501

Matsumoto K, Matsumoto K, Nakamura T and Kramer RH (1994) Hepatocyte growth factor/scatter factor induces tyrosine phosphorylation of focal adhesion kinase ($p125^{FAK}$) and promotes migration and invasion by oral squamous cell carcinoma cells. *J Biol Chem* **269**: 31807–31813

Matsumoto K, Date K, Shimura H and Nakamura T (1996) Acquisition of invasive phenotype in gallbladder cancer cells via mutual interaction of stromal fibroblasts and cancer cells as mediated by hepatocyte growth factor. *Jpn J Cancer Res* **87**: 702–710

Miyazawa K, Tsubouchi H, Naka D, Takahashi K, Okigaki M, Gohda E, Daikuhara Y and Kitamura N (1989) Molecular cloning and sequence analysis of cDNA for human hepatocyte growth factor. *Biochem Biophys Res Commun* **163**: 967–973

Mooradian DL, McCarthy JB, Kommanduri KV and Furcht LT (1992) Effect of transforming growth factor-β1 on human pulmonary adenocarcinoma cell adhesion, motility and invasion in vitro. *J Natl Cancer Inst* **84**: 523–527

Nakamura T, Nawa K and Ichihara A (1984) Partial purification and characterization of hepatocyte growth factor from serum of hepatectomized rats. *Biochem Biophys Res Commun* **122**: 1450–1459

Nakamura T, Nishizawa T, Hagiya M, Seki T, Shimonishi M, Sugimura A, Tashiro K and Shimizu S (1989) Molecular cloning and expression of human hepatocyte growth factor. *Nature* **342**: 440–443

Nakamura T, Matsumoto K, Kiritoshi A, Tano Y and Nakamura T (1997) Induction of hepatocyte growth factor in fibroblasts by tumour-derived factors affects invasive growth of tumour cells: in vitro analysis of tumour-stromal interactions. *Cancer Res* **57**: 3305–3313

Naldini L, Weidner KM, Vigna E, Gaudino G, Bardelli A, Ponzetto C, Narsimhan RP, Hartmann G, Zarnegar R and Michalopoulos GK (1991) Hepatocyte growth factor and scatter factor are indistinguishable ligands for the Met receptor. *EMBO* **10**: 2867–2878.

Okada F, Yamaguchi K, Ichihara A and Nakamura T (1989) Purification and structural analysis of a latent transforming growth factor-β from rat platelets. *J Biochem* **106**: 304–310

Pepper MS, Matsumoto K, Nakamura T, Orci L and Montesano R (1992) Hepatocyte growth factor increases urokinase-type plasminogen activator (u-PA) and u-PA receptor expression in Madin-Darby canine kidney epithelial cells. *J Biol Chem* **267**: 20493–20496

Ridly AJ, Comoglio PM and Hall A (1995) Regulation of scatter factor/hepatocyte growth factor responses by Ras, Rac and Rho in MDCK cells. *Mol Cell Biol* **15**: 1110–1122

Russell WE, McGowan JA and Bucher NLR (1984) Partial characterization of hepatocyte growth factor from rat platelets. *J Cell Physiol* **119**: 183–192

Shibamoto S, Hayakawa M, Takeuchi K, Hori T, Oku N, Miyazawa K, Kitamura N, Takeichi M and Ito F (1994) Tyrosine phosphorylation of β-catenin and plakoglobin enhanced by hepatocyte growth factor and epidermal growth factor in human carcinoma cells. *Cell Adhes Commun* **1**: 295–305

Silletti S and Raz A (1996) Regulation of autocrine motility factor receptor expression in tumor cell locomotion and metastasis. *Curr Top Microbiol Immunol* **213**: 137–169

Sporn MB and Roberts AB (1985) Autocrine growth factors and cancer. *Nature* **313**: 745–747

Sporn MB, Roberts AB, Wakefield LM and de Crombrugghe B (1987) Some recent advances in the chemistry and biology of transforming growth factor-β. *J Cell Biol* **105**: 1039–1045

Stoker M and Gherardi E (1991) Regulation of cell movement: the motogenic cytokines. *Biochem Biophys Acta* **1072**: 81–102

Stoker M and Perryman M (1985) An epithelial scatter factor released by embryo fibroblasts. *J Cell Sci* **77**: 209–223

Takaishi K, Sasaki T, Kato M, Yamori W, Kuroda S, Nakamura T, Takeichi M and Takai Y (1994) Involvement of rho p21 small GTP-binding protein and its regulatory protein in the HGF-induced cell motility. *Oncogene* **9**: 273–279

Ueda M, Fujii H, Yoshizawa K, Abe F and Ueki M (1996) Effects of sex steroids and growth factors on migration and invasion of endometrial adenocarcinoma SNG-M cell in vitro. *Jpn J Cancer Res* **87**: 524–533

Ueda M, Ueki M, Morimoto A, Fujii H, Yoshizawa K and Yanagisawa T (1997) Stimulatory effects of EGF and TGF-α on invasive activity and 5′-deoxy-5-fluorouridine sensitivity in uterine cervical carcinoma SKG-IIIb cells. *Int J Cancer* **72**: 1027–1033

Ullrich A and Schlessinger J (1990) Signal transduction by receptors with tyrosine kinase activity. *Cell* **61**: 203–212

van den Hooff A (1988) Stromal involvement in malignant growth. *Adv Cancer Res* **50**: 159–196

Watabe M, Matsumoto K, Nakamura T and Takeichi M (1993) Effect of hepatocyte growth factor on cadherin-mediated cell–cell adhesion. *Cell Struc Function* **18**: 117–124

Wehrle-Haller B and Weston JA (1997) Receptor tyrosine kinase-dependent neural crest migration in response to differentially localized growth factors. *Bioessays* **19**: 337–345

Weidner KM, Behrens J, Vanderkerckhove J and Birchmeier W (1990) Scatter factor: molecular characteristics and effect on the invasiveness of epithelial cells. *J Cell Biol* **111**: 2097–2108

Weidner KM, Arakaki N, Hartmann G, Vanderkerckhove J, Weingort S, Rieder H, Fonatsch C, Tsubouchi H, Hishida T, Daikuhara Y and Birchmeier W (1991) Evidence for identity of human scatter factor and human hepatocyte growth factor. *Proc Natl Acad Sci USA* **88**: 7001–7005

Welch DR, Fabba A and Nakajima M (1990) Transforming growth factor-β stimulates mammary adenocarcinoma cell invasion and metastatic potential. *Proc Natl Acad Sci USA* **87**: 7678–7682

Wernert N (1997) The multiple roles of tumour stroma. *Virchows Arch* **430**: 433–443

Wright JA and Huang A (1996) Growth factors in mechanisms of malignancy: roles for TGF-β and FGF. *Histol Histopathol* **11**: 521–536

Wright JA, Turley EA and Greenberg AH (1993) Transforming growth factor-β and fibroblast growth factor as promoters of tumour progression to malignancy. *Crit Rev Oncog* **4**: 473–492

Zarnegar R and Michalopoulas GK (1995) The many faces of hepatocyte growth factor: from haptopoiesis to hematopoiesis. *J Cell Biol* **129**: 1177–1180

Molecular Biology of the Cell
Vol. 9, 437–449, February 1998

参考論文

M Phase Phosphoprotein 10 Is a Human U3 Small Nucleolar Ribonucleoprotein Component

Joanne M. Westendorf,*†‡ Konstantin N. Konstantinov,§ Steven Wormsley,‖ Mei-Di Shu,¶ Naoko Matsumoto-Taniura,*# Fabienne Pirollet,† F. George Klier,* Larry Gerace,* and Susan J. Baserga@

Departments of *Cell and Molecular Biology, and §Molecular and Experimental Medicine, The Scripps Research Institute, La Jolla, California 92037; †Laboratoire du Cytosquelette, Commissariat à l'Energie Atomique, Institut National de la Santé et de la Recherche Médicale Unité 366, Département de Biologie Moléculaire et Structurale, Commissariat à l'Energie Atomique/Grenoble, 38054 Grenoble Cedex 9, France; ‖Department of Cell Biology, ¶The Howard Hughes Medical Institute, and @Departments of Therapeutic Radiology and Genetics, Yale University School of Medicine, New Haven, Connecticut 06520-8040

Submitted July 31, 1997; Accepted November 14, 1997
Monitoring Editor: Joseph Gall

We have previously developed a novel technique for isolation of cDNAs encoding M phase phosphoproteins (MPPs). In the work described herein, we further characterize MPP10, one of 10 novel proteins that we identified, with regard to its potential nucleolar function. We show that by cell fractionation, almost all MPP10 was found in isolated nucleoli. By immunofluorescence, MPP10 colocalized with nucleolar fibrillarin and other known nucleolar proteins in interphase cells but was not detected in the coiled bodies stained for either fibrillarin or p80 coilin, a protein found only in the coiled body. When nucleoli were separated into fibrillar and granular domains by treatment with actinomycin D, almost all the MPP10 was found in the fibrillar caps, which contain proteins involved in rRNA processing. In early to middle M phase of the cell cycle, MPP10 colocalized with fibrillarin to chromosome surfaces. At telophase, MPP10 was found in cellular structures that resembled nucleolus-derived bodies and prenucleolar bodies. Some of these bodies lacked fibrillarin, a previously described component of nucleolus-derived bodies and prenucleolar bodies, however, and the bulk of MPP10 arrived at the nucleolus later than fibrillarin. To further examine the properties of MPP10, we immunoprecipitated it from cell sonicates. The resulting precipitates contained U3 small nucleolar RNA (snoRNA) but no significant amounts of other box C/D snoRNAs. This association of MPP10 with U3 snoRNA was stable to 400 mM salt and suggested that MPP10 is a component of the human U3 small nucleolar ribonucleoprotein.

INTRODUCTION

During M phase of the cell cycle of higher eukaryotes, most cell structures undergo massive rearrangements to allow appropriate division of cellular components to both daughter cells. Often these structural changes involve breakdown of interphase structures into smaller subunits. For instance, when cells enter M phase, the nuclear envelope breaks down into vesicles, and the nuclear lamins, which form a stable lining on the nucleoplasmic surface of the nuclear envelope in interphase, disassemble (Gerace and Blobel, 1980; Ottaviano and Gerace, 1985). These events are regulated by M phase promoting factor, a kinase consisting of the $p34^{cdc2}$ catalytic subunit and a cyclin B regulatory

‡ Corresponding author, address for correspondence: Department of Molecular Pharmacology, Stanford University School of Medicine, Stanford, CA 94305-5332.
# Current address: Department of Biochemistry, Biomedical Research Center, Osaka University Medical School, Osaka, Japan.

subunit (Dunphy *et al.*, 1988; Gautier *et al.*, 1988, 1990; Draetta *et al.*, 1989; Labbé *et al.*, 1989; Meijer *et al.*, 1989; Heald and McKeon, 1990; Peter *et al.*, 1990; Ward and Kirschner, 1990). Consequently, lamins become phosphorylated and remain phosphorylated during M phase until telophase, when the nuclear lamina structure reforms. With the breakdown of the nucleus, many nuclear components become exposed to cytoplasmic enzymes that they do not encounter in interphase. This mixing of the nucleus with the cytoplasm could lead to some undesirable interactions that cells may work to avoid. Phosphorylation of cellular proteins could provide a means of shutting down interphase nuclear functions and disassembling nuclear structures.

Recently, we have developed a technique for identifying proteins that are phosphorylated during M phase and may be involved in some of the structural modifications that occur upon entry into M phase (Westendorf *et al.*, 1994). Our technique resulted in the identification of 10 novel proteins that are phosphorylated during M phase (Matsumoto-Taniura *et al.*, 1996). By immunofluorescence, each protein is found in its own characteristic locations within the cell. One of these proteins, M phase phosphoprotein 10 (MPP10), localized strongly to the nucleolus in interphase and to the chromosomes in M phase. This pattern of localization was similar to that exhibited by fibrillarin and several other nucleolar proteins (Yasuda and Maul, 1990; Gautier *et al.*, 1992, 1994; Medina *et al.*, 1995) and suggested that MPP10 might be involved in ribosome synthesis, assembly, or transport as are various other nucleolar proteins.

Autoantibodies to the protein fibrillarin have identified the U3 small nucleolar ribonucleoprotein (snoRNP), in vertebrates the most abundant of the snoRNPs (Lischwe *et al.*, 1985; Reimer *et al.*, 1987). In humans, it consists of an RNA component 217 nucleotides long complexed with at least six proteins, one of which is fibrillarin (Parker and Steitz, 1987; Lubben *et al.*, 1993; reviewed in Maxwell and Fournier, 1995; Venema and Tollervey, 1995), a protein found in a wide variety of organisms. Studies in both vertebrates and the yeast *Saccharomyces cerevisiae* have demonstrated a requirement for the U3 snoRNP in processing of precursors to the mature 18S rRNA (Savino and Gerbi, 1990; Hughes and Ares, 1991; Beltrame and Tollervey, 1992; Beltrame *et al.*, 1994; Beltrame and Tollervey, 1995; Hughes, 1996). It is likely that the U3 snoRNP acts as a rRNA chaperone, folding or presenting the precursor rRNA to the cleavage enzymes through direct base pairing between the small nucleolar RNA (snoRNA) and the pre-rRNA (Beltrame and Tollervey, 1995; Elela *et al.*, 1996; Hughes, 1996). Although the RNA–RNA interactions are fairly well characterized, the nature and role of the protein components remains unknown. Specifically, other than fibrillarin, no protein component of any vertebrate U3 snoRNP has been cloned and sequenced.

In this article, we describe the full-length coding sequence of MPP10 and further examine its role in nucleolar structure and function. Our results indicate that MPP10 colocalizes with fibrillarin under most cellular conditions and that, like fibrillarin, it is a component of the U3 snoRNP, which is involved in rRNA processing. Nevertheless, in contrast to fibrillarin, MPP10 is not a major component of ribonuclear particles containing snoRNAs other than U3, and MPP10 relocalizes to the nucleolus at the end of mitosis by a course distinct from that of fibrillarin.

MATERIALS AND METHODS

Cloning the 5′ cDNA Sequences of MPP10

To obtain the complete coding sequence for MPP10, several complementary procedures were used. In one method, the 284-bp 5′ end *Eco*RI–*Eco*RV restriction fragment from MPP10 clone 2 (Matsumoto-Taniura *et al.*, 1996) was labeled with [α-^{32}P]dCTP by the random-primer method and used to screen a total of 2×10^6 clones from two HeLa cDNA-containing λZAPII libraries, one from Stratagene and the other a gift from Dr. P. Chambon (Institut de Chimie Biologique, Strasbourg, France). In this way one cDNA, clone 10c8 containing positions from −17 to +217 (Figure 1A) was isolated from the library obtained from Dr. Chambon.

In the second method, 5′ rapid amplification of cDNA ends was performed on a λgt11 human placental cDNA library by using one oligonucleotide complementary to the vector and one complementary to MPP10 sequences near the 5′ end (Frohman, 1994). The vector primer (λgt11R) was 5′-TTGACACAGACCAACTGGTAATG and the MPP10 primer (MPP10R-2) was 5′-GTCCTCCTTGTCATCAGCCTCTATC. After a 7-min denaturation at 94°C, the polymerase chain reaction (PCR) was performed for 30 cycles (94°C, 45 s; 55°C, 45 s; 72°C, 45 s; on a Perkin Elmer–Cetus 2400 thermocycler. The 1.1-kb PCR fragment was cloned by TA cloning into the pCR2.1 vector (Invitrogen, San Diego, CA).

cDNAs were sequenced by the Sanger dideoxynucleotide method using custom primers and ^{35}S-labeled dATP or automated sequencing, which was performed with an Applied Biosystems 373A sequencer at the core facility at The Scripps Research Institute or an Applied Biosystems 373 Stretch sequencer at the W.M. Keck Foundation Biotechnology Resource Laboratory at Yale University. Sequences were analyzed with GCG and Intelligenetics programs and database searches were performed with the Blast program provided by the National Center for Biotechnology Information/National Institutes of Health.

Figure 1 (facing page). MPP10 cDNA and predicted amino acid sequence. (A) The cDNA and predicted amino acid sequences of MPP10 were determined as described in MATERIALS AND METHODS. The dotted underline indicates an upstream ATG in the 5′ noncoding sequence, the single underline indicates a stop codon in the same reading frame as the upstream ATG, the double underline indicates the poly(A) addition signal, and the stars indicate probable sites of MPM2-reactive phosphorylation (EMBL database accession number, X98494). (B) Probability of coiled-coil α-helix formation as determined by the program of Lupas *et al.* (1991).

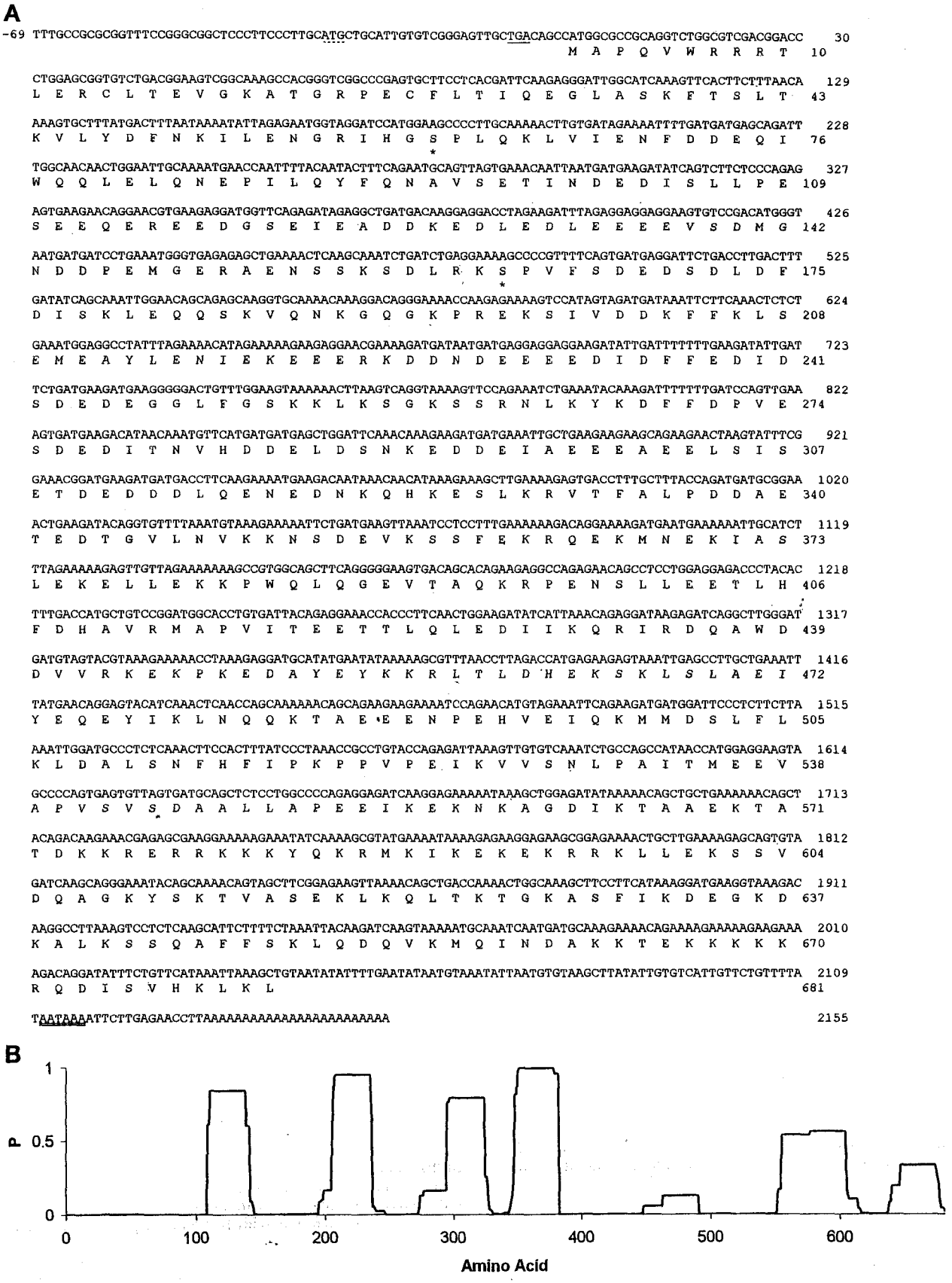
A
-69 TTTGCCGCGCGGTTTCCGGGCGGCTCCCTTCCCTTGCATGCTGCATTGTGTCGGGAGTTGCTGACAGCCATGGCGCCGCAGGTCTGGCGTCGACGGACC 30
M A P Q V W R R R T 10
CTGGAGCGGTGTCTGACGGAAGTCGGCAAAGCCACGGGTCGGCCCGAGTGCTTCCTCACGATTCAAGAGGGATTGGCATCAAAGTTCACTTCTTTAACA 129
L E R C L T E V G K A T G R P E C F L T I Q E G L A S K F T S L T 43
AAAGTGCTTTATGACTTTAATAAAATATTAGAGAATGGTAGGATCCATGGAAGCCCCTTGCAAAAACTTGTGATAGAAAATTTTGATGATGAGCAGATT 228
K V L Y D F N K I L E N G R I H G S P L Q K L V I E N F D D E Q I 76
TGGCAACAACTGGAATTGCAAAATGAACCAATTTTACAATACTTTCAGAATGCAGTTAGTGAAACAATTAATGATGAAGATATCAGTCTTCTCCCAGAG 327
W Q Q L E L Q N E P I L Q Y F Q N A V S E T I N D E D I S L L P E 109
AGTGAAGAACAGGAACGTGAAGAGGATGGTTCAGAGATAGAGGCTGATGACAAGGAGGACCTAGAAGATTTAGAGGAGGAGGAAGTGTCCGACATGGGT 426
S E E Q E R E E D G S E I E A D D K E D L E D L E E E E V S D M G 142
AATGATGATCCTGAAATGGGTGAGAGAGCTGAAAACTCAAGCAAATCTGATCTGAGGAAAAGCCCCGTTTTCAGTGATGAGGATTCTGACCTTGACTTT 525
N D D P E M G E R A E N S S K S D L R K S P V F S D E D S D L D F 175
GATATCAGCAAATTGGAACAGCAGAGCAAGGTGCAAAACAAAGGACAGGGAAAACCAAGAGAAAAGTCCATAGTAGATGATAAATTCTTCAAACTCTCT 624
D I S K L E Q Q S K V Q N K G Q G K P R E K S I V D D K F F K L S 208
GAAATGGAGGCCTATTTAGAAAACATAGAAAAAGAAGAGGAACGAAAAGATGATAATGATGAGGAGGAGGAAGATATTGATTTTTTTGAAGATATTGAT 723
E M E A Y L E N I E K E E E R K D D N D E E E E D I D F F E D I D 241
TCTGATGAAGATGAAGGGGGACTGTTTGGAAGTAAAAAACTTAAGTCAGGTAAAAGTTCCAGAAATCTGAAATACAAAGATTTTTTTGATCCAGTTGAA 822
S D E D E G G L F G S K K L K S G K S S R N L K Y K D F F D P V E 274
AGTGATGAAGACATAACAAATGTTCATGATGATGAGCTGGATTCAAACAAAGAAGATGATGAAATTGCTGAAGAAGAAGCAGAAGAACTAAGTATTTCG 921
S D E D I T N V H D D E L D S N K E D D E I A E E E A E E L S I S 307
GAAACGGATGAAGATGATGACCTTCAAGAAAATGAAGACAATAAACAACATAAAGAAAGCTTGAAAAGAGTGACCTTTGCTTTACCAGATGATGCGGAA 1020
E T D E D D D L Q E N E D N K Q H K E S L K R V T F A L P D D A E 340
ACTGAAGATACAGGTGTTTTAAATGTAAAGAAAAATTCTGATGAAGTTAAATCCTCCTTTGAAAAAAGACAGGAAAAGATGAATGAAAAAATTGCATCT 1119
T E D T G V L N V K K N S D E V K S S F E K R Q E K M N E K I A S 373
TTAGAAAAAGAGTTGTTAGAAAAAAAGCCGTGGCAGCTTCAGGGGGAAGTGACAGCACAGAAGAGGCCAGAGAACAGCCTCCTGGAGGAGACCCTACAC 1218
L E K E L L E K K P W Q L Q G E V T A Q K R P E N S L L E E T L H 406
TTTGACCATGCTGTCCGGATGGCACCTGTGATTACAGAGGAAACCACCCTTCAACTGGAAGATATCATTAAACAGAGGATAAGAGATCAGGCTTGGGAT 1317
F D H A V R M A P V I T E E T T L Q L E D I I K Q R I R D Q A W D 439
GATGTAGTACGTAAAGAAAAACCTAAAGAGGATGCATATGAATATAAAAAGCGTTTAACCTTAGACCATGAGAAGAGTAAATTGAGCCTTGCTGAAATT 1416
D V V R K E K P K E D A Y E Y K K R L T L D H E K S K L S L A E I 472
TATGAACAGGAGTACATCAAACTCAACCAGCAAAAAACAGCAGAAGAAGAAAATCCAGAACATGTAGAAATTCAGAAGATGATGGATTCCCTCTTCTTA 1515
Y E Q E Y I K L N Q Q K T A E E E N P E H V E I Q K M M D S L F L 505
AAATTGGATGCCCTCTCAAACTTCCACTTTATCCCTAAACCGCCTGTACCAGAGATTAAAGTTGTGTCAAATCTGCCAGCCATAACCATGGAGGAAGTA 1614
K L D A L S N F H F I P K P P V P E I K V V S N L P A I T M E E V 538
GCCCCAGTGAGTGTTAGTGATGCAGCTCTCCTGGCCCCAGAGGAGATCAAGGAGAAAAATAAAGCTGGAGATATAAAAACAGCTGCTGAAAAAACAGCT 1713
A P V S V S D A A L L A P E E I K E K N K A G D I K T A A E K T A 571
ACAGACAAGAAACGAGAGCGAAGGAAAAAGAAATATCAAAAGCGTATGAAAATAAAAGAGAAGGAGAAGCGGAGAAAACTGCTTGAAAAGAGCAGTGTA 1812
T D K K R E R R K K K Y Q K R M K I K E K E K R R K L L E K S S V 604
GATCAAGCAGGGAAATACAGCAAAACAGTAGCTTCGGAGAAGTTAAAACAGCTGACCAAAACTGGCAAAGCTTCCTTCATAAAGGATGAAGGTAAAGAC 1911
D Q A G K Y S K T V A S E K L K Q L T K T G K A S F I K D E G K D 637
AAGGCCTTAAAGTCCTCTCAAGCATTCTTTTCTAAATTACAAGATCAAGTAAAAATGCAAATCAATGATGCAAAGAAAACAGAAAAGAAAAAGAAGAAA 2010
K A L K S S Q A F F S K L Q D Q V K M Q I N D A K K T E K K K K K 670
AGACAGGATATTTCTGTTCATAAATTAAAGCTGTAATATATTTTGAATATAATGTAAATATTAATGTGTAAGCTTATATTGTGTCATTGTTCTGTTTTA 2109
R Q D I S V H K L K L 681
TAATAAAATTCTTGAGAACCTTAAAAAAAAAAAAAAAAAAAAAAAA 2155
B
P
1
0.5
0
0
100
200
300
400
500
600
Amino Acid

Figure 1.

In Vitro Translation of Full-Length MPP10 Protein

To make a clone containing a full-length MPP10 coding sequence, the 2000-bp *Bam*HI–*Eco*RI fragment from clone 2 was isolated and cloned into *Bam*HI/*Eco*RI-digested pBluescriptSK−. The resulting construct was then digested with *Not*I, and the ends were filled in with the Klenow fragment in the presence of dGTP. Then clone 10c8 was digested with *Psp*AI, and the ends were filled in with the Klenow fragment in the presence of dCTP. After cutting both the clone 2 and the clone 10c8 derivatives with *Bam*HI, the small fragment of 10c8 was cloned into the large fragment of the clone 2 derivative. The resulting plasmid containing bases −17 to +170 (see Figure 1A) of clone 10c8 and bases 171 to 2155 (see Figure 1A) of clone 2 were transcribed and translated in vitro with T3 RNA polymerase and the TNT system (Promega, Madison, WI) in the presence of [^{35}S]methionine.

Antibodies

Monoclonal antibody 72B9 against fibrillarin was a gift from Michael Pollard (Reimer *et al.*, 1987), the rabbit polyclonal antibody against recombinant p80-coilin was a gift from Ed Chan (Andrade *et al.*, 1991), the monoclonal antibody against the trimethylguanosine (TMG) cap was obtained from Oncogene Science (Manhassett, NY), and the Y-12 monoclonal antibody against Sm antigens was a gift from Joan Steitz (Lerner and Steitz, 1979). For antibodies to MPP10, guinea pigs were injected with a fusion protein consisting of T7 protein 10 fused to amino acids 58–681, and the resulting antisera were affinity purified as previously described (Matsumoto-Taniura *et al.*, 1996). Normal human serum was obtained from a young male volunteer.

Immunofluorescence by Light and Confocal Laser Scanning Microscopy

For immunofluorescence, HEp-2 cells were grown directly on glass coverslips (22 mm^2; Corning, Corning, NY) in six-well plates, rinsed briefly with phosphate-buffered saline (PBS; 10 mM phosphate), and then fixed at −20°C with methanol for 5 min followed by acetone for 2 min. Commercially available prefixed HEp-2 cell substrates (Bion, Park Ridge, IL) were also used. Primary antibodies were diluted in PBS and incubated with cells at 25°C for 1 h. For double labeling, purified guinea pig antibodies against MPP10 and murine monoclonal antibodies, characterized human serum, or rabbit polyclonal antibodies against other antigens were mixed together before incubation with cells. After three washes with PBS, the cells were incubated with fluorescein isothiocyanate-conjugated anti-guinea pig and rhodamine-conjugated anti-mouse, anti-human, or anti-rabbit (Caltag Laboratories, San Francisco; and Jackson ImmunoResearch Laboratories, West Grove, PA) for 1 h at 25°C, washed, and mounted on slides with an antifade mounting medium (Vectashield, Vector Laboratories, Burlingame, CA). Conventional epifluorescence microscopy was performed with an Olympus fluorescence microscope, and specimens were photographed with Kodak Ektachrome 400 film.

Microscopy was also performed with an MRC-600 confocal laser scanning instrument (Bio-Rad Laboratories, Cambridge, MA) fitted to a Zeiss Axiovert epifluorescence microscope with a ×63/1.4 numerical aperature oil-immersion lens. In most experiments, images were the product of 30 scans, each collected from a single focal plane (about 0.4 μm) and together averaged by the Kalman method with the Bio-Rad COMOS program. In the actinomycin D experiment, sequential optical planes were acquired along the *Z*-axis through the cultured cells, and the stored graphic files were collapsed to a single virtual image (Z-series projection) by using software provided by Bio-Rad Laboratories. Fluorescence images were collected simultaneously from the fluorescein and rhodamine channels; differential interference contrast images were collected subsequently. The images were digitized and imported into Adobe Photoshop 4.0 (Adobe Systems, Mountain View, CA) for further image processing.

Immunoprecipitation from HeLa Cells and In Vitro Translations

To precipitate in vitro-translated MPP10, a 20-μl TNT translation reaction of full-length MPP10 was diluted with 0.25 ml of high salt RIPA buffer [50 mM Tris-HCl, pH 8.0, 500 mM NaCl, 1% Triton X-100, 0.1% SDS, 0.5% sodium deoxycholate, 2 mM phenylmethylsulfonyl fluoride, 10 μg/ml aprotinin, 10 μg/ml leupeptin, 10 μg/ml pepstatin, 10 mM EDTA, 10 mM ethylene glycol-bis(β-aminoethyl ether)-*N,N,N',N'*-tetraacetic acid, 10 mM benzamidine, 10 mM tosyl arginylmethyl ester], and MPP10 was precipitated with 5 μl of MPP10 antiserum bound to 20 μl of protein A-Sepharose 6 MB. For precipitation of HeLa cell MPP10 protein, 4×10^7 exponentially growing HeLa cells were lysed with high salt RIPA and centrifuged at 100,000 × *g*, and MPP10 was precipitated with 10 μl of MPP10 antiserum bound to 40 μl of protein A-Sepharose 6 MB beads. After an overnight incubation, immunoprecipitates were washed three times with high salt RIPA, and bound proteins were eluted with SDS sample buffer. Samples were separated by SDS-PAGE and analyzed by immunoblot with anti-MPP10 and autoradiography.

Subcellular Fractionation

Fractionation of HeLa cells was performed according to Warner (1979) with the following modifications. The fractionation was performed at 4°C and all centrifugations were carried out in a JA-20 rotor (Beckman, Fullerton, CA) except where noted. HeLa cells (1×10^8 cells) were collected by centrifugation and washed two times with PBS. The cells were resuspended in 5 ml of buffer A (10 mM HEPES-KOH, pH 7.9, 1.5 mM $MgCl_2$, 10 mM KCl, and 0.5 mM dithiothreitol), swollen for 10 min on ice, then broken with 12–15 strokes of a tight fitting Dounce homogenizer, and centrifuged to pellet nuclei. The supernatant from this centrifugation was considered to be the cytoplasmic fraction and the pellet was termed "nuclei I."

To further purify the nuclei, the pellet was resuspended in 10 ml of buffer containing 10 mM Tris-Cl, pH 7.5, 3.3 mM $MgCl_2$, and 0.25 M sucrose and centrifuged for 5 min at 1000 rpm. The resulting pellet was resuspended in 2.5 ml of 10 mM $MgCl_2$ and 0.25 M sucrose, layered over 2.5 ml of 0.5 mM $MgCl_2$ and 0.35 M sucrose, and centrifuged for 10 min at 2500 rpm. The resulting pellet of purified nuclei was resuspended in 2.5 ml of 0.5 mM $MgCl_2$ and 0.35 M sucrose and sonicated (four or five times; 15 s) with a Branson sonifier (setting 1) to disrupt the nuclei. When disruption was complete, as determined by microscopy of a sample stained with Azure C (Muramatsu *et al.*, 1963), the sonicate (nuclei II) was layered over 2.5 ml of 0.5 mM $MgCl_2$ and 0.88 M sucrose and centrifuged for 15 min at 4000 rpm in an SW41 rotor (Beckman). The resulting pellet, which contained purified nucleoli, was resuspended in NET-2 (20 mM Tris-HCl, pH 7.5, 150 mM NaCl, 0.05% Nonidet P-40 [NP-40]), sonicated (five times; 30 s) at setting 3 of a Branson sonifier and centrifuged for 10 min at 10,000 rpm (12,000 × *g*). The supernatant was analyzed by SDS gel electrophoresis and immunoblot with anti-MPP10.

Immunoblotting

Proteins separated by SDS-PAGE were transferred to Immobilon-P or Hybond-N (Amersham, Arlington Heights, IL) and reacted with MPP10 antiserum at a dilution of 1:2000 to 1:10,000 in Tris-buffered saline containing Tween (50 mM Tris-HCl, pH 7.9, 150 mM NaCl, 0.1% Tween-20) with or without 5% nonfat dried milk. Bound antibodies were detected with horseradish peroxidase-conjugated anti-guinea pig antibody (Boehringer Mannheim, Indianapolis, IN, or Jackson ImmunoResearch Laboratories, West Grove, PA) at a dilution of 1:5000 and the ECL system (Amersham).

Small Nuclear Ribonucleoprotein (snRNP) Immunoprecipitations

Immunoprecipitations for detection of associated RNAs were performed essentially as described (Lerner *et al*, 1981). For direct RNA labeling, 10 μl of normal human serum, 40 μl of anti-fibrillarin culture supernatant (72B9) and 2.5 or 10 μl of affinity-purified MPP10 were bound to 4 mg of protein A-Sepharose. For Northern blot analysis of RNAs, the following antibodies were bound to 2.5 mg of protein A-Sepharose CL-4B for 16 h at 4°C: 10 μl of crude or affinity-purified anti-MPP10 polyclonal guinea pig serum, 100 μl of cell culture supernatant containing mouse monoclonal anti-fibrillarin (72B9), 10 μl of mouse ascites containing monoclonal anti-TMG plus 10 μl of rabbit anti-mouse IgG, or no added antibody (mock). The antibody–protein A-Sepharose CL-4B pellets were washed three times with NET-2 (20 mM Tris-HCl, pH 7.5, 150 mM NaCl, 0.05% NP-40). HeLa cells or mouse L cells (1×10^8 cells) were resuspended in NET-2 or NET-400 (20 mM Tris-HCl, pH 7.5, 400 mM NaCl, 0,05% NP-40), as indicated, and sonicated (five times; 30 s) at setting of 3 with a Branson sonifier. The sonicate was centrifuged for 10 min at 10,000 rpm (12,000 × *g*). The supernatant from this centrifugation was added to the washed antibody–protein A-Sepharose CL-4B pellets, mixed for 1 h at 4°C, and the pellets were washed with the buffer in which the extract was made.

RNA was recovered from the pellets by extraction with PCA (phenol:chloroform:isoamyl alcohol, 25:24:1) and ethanol precipitation. The recovered RNA was analyzed either by 3′-end-labeling with ^{32}P-labeled pCp and T4 RNA ligase (England *et al.*, 1980) or by Northern blotting with antisense RNA probes. In both cases, RNA was analyzed by denaturing gel electrophoresis.

Northern Blots

For Northern blots, RNAs purified from precipitates were electrophoresed on an 8% denaturing polyacrylamide gel and blotted to a Zeta-Probe membrane (Bio-Rad Laboratories; Kass *et al.*, 1987). Blots were hybridized with antisense RNAs complementary to U3, U2, and U1 or U8, produced as previously described (Black and Pinto, 1989; Baserga *et al.*, 1991).

RESULTS

Characterization of a Full-Length Coding Sequence for MPP10

cDNA clone 2 encoding the C-terminal portion of MPP10 was isolated by expression cloning of MPPs that are reactive with the phosphoepitope-specific monoclonal antibody MPM2 (Davis *et al.*, 1983; Westendorf *et al.*, 1994; Matsumoto-Taniura *et al.*, 1996). When clone 2 cDNA was transcribed into RNA and translated in vitro, the translation product migrated at 85 kDa (our unpublished observations), considerably faster than HeLa cell MPP10 protein, which migrates at 120 kDa (Matsumoto-Taniura *et al.*, 1996). To obtain sequences encoding the amino terminus of MPP10, we isolated cDNAs overlapping with clone 2 by screening cDNA libraries with labeled cDNA fragments and by PCR on cDNA libraries. Figure 1A presents a full-length coding sequence for MPP10, which consists of 69 nucleotides of 5′ noncoding sequence, a start codon that is surrounded by nucleotides found to be conducive to start of translation (Kozak, 1996), an in-frame stop codon, and 109 nucleotides of 3′ noncoding sequence. There is an additional ATG, which is in a poor

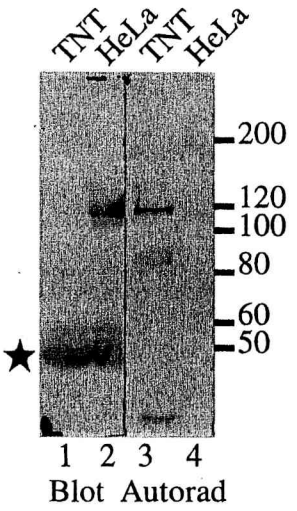

Figure 2. Comigration of MPP10 translated in vitro and MPP10 from Hela cells. MPP10 transcribed and translated in the presence of [^{35}S]methionine from a full-length cDNA coding sequence and MPP10 from HeLa cells were precipitated with anti-MPP10 serum, fractionated by SDS-PAGE, and immunoblotted with anti-MPP10 serum. Bound antibodies were detected by ECL (lanes 1 and 2), and radioactive MPP10 was detected by autoradiography (lanes 3 and 4). Positions of migration of molecular mass markers in kDa are indicated on the right; the star indicates the position of migration of IgG heavy chain.

context for start of translation, 5′ of the proposed start codon, but it is followed eight codons later by a stop codon in the same reading frame. When RNA transcribed from cDNA containing MPP10 cDNA sequences from positions −17 through the poly(A) tail is translated, the protein product comigrates with MPP10 immunoprecipitated from HeLa cells (Figure 2). This indicates that the full-length MPP10 protein is encoded by the long open reading frame of 681 codons shown in Figure 1A.

The sequence of full-length MPP10 predicts a protein of 78,868 Da, considerably less mass than the 120,000 Da indicated by its migration on SDS gels. T7 protein 10-MPP10 fusion protein also migrates anomalously slowly on gels (Matsumoto-Taniura *et al.*, 1996). This characteristic could be due to the extreme acidity of the protein; the predicted pI is 4.52. MPP10 contains acidic and basic stretches of amino acids, which are concentrated in portions of the protein that are predicted to have a high probability of being in coiled-coil α-helices (Lupas *et al.*, 1991; Figure 1B). The first stretch is 28 amino acids long, has a 0.84 predicted probability of forming a coiled-coil α-helix, and contains 18 acidic and 2 basic residues; the second is 29 long, has a 0.94 probability, and contains 16 acidic and 3 basic residues; the third is 28 long, has a 0.79 probability, and contains 14 acidic and 1 basic residues; the fourth is 35 long, has a 0.99 probability, and contains 8 acidic and 10 basic residues; the fifth is 50 long, has

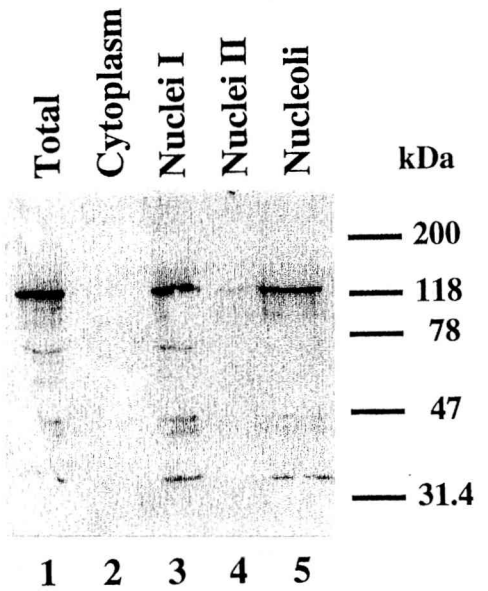

Figure 3. MPP10 in subcellular fractions of HeLa cells. First, HeLa cells were fractionated into cytoplasmic and nuclear fractions. Then, the crude nuclear fraction (Nuclei I) was further fractionated into nucleoplasm (Nuclei II) and nucleoli. Fractions representing an equal number of cells were separated by SDS-PAGE, transferred to Hybond-N, and reacted with anti-MPP10 serum. Bound antibodies were subsequently reacted with horseradish peroxidase-coupled secondary antibodies and detected with ECL. Positions of migration of molecular mass markers are indicated on the right.

a 0.55 probability, and contains 8 acidic and 23 basic residues; and the sixth is 28 long, has a 0.33 probability, and contains 4 acidic and 10 basic residues. Short stretches of probable coiled-coil α-helix such as these could be involved in intramolecular and/or intermolecular interactions (Lupas, 1996), and the charged amino acids found in these domains may also be involved in formation of structures. Acidic and basic stretches are found in many other nucleolar proteins also (Shaw and Jordan, 1995).

Although the sequence of MPP10 is not highly homologous to any known protein, database searches indicate weak relationships between MPP10 and the nucleolar protein nucleolin (22% identity), acid-rich proteins, and proteins containing coiled-coil α-helices. Interestingly, the sequence most similar to MPP10 found in GenBank is a yeast open reading frame identified by sequencing of the yeast genome. Experiments in yeast indicate that this gene, which is 30% identical to hMPP10, is likely to be the yeast homologue (Dunbar *et al.*, 1997). By comparison with a database of protein motifs, we find that MPP10 contains basic amino acid stretches that could represent nuclear localization sequences at amino acid positions 251–256, 574–579, 583–588, 592–597, and 666–671. The last four sequences are all within portions of the protein that have substantial potential to form coiled-coil α-helices. MPP10 contains two potential MPM2-reactive phosphorylation sites at amino acids 61 and 163 (Westendorf *et al.*, 1994; Matsumoto-Taniura *et al.*, 1996).

Characterization of Nucleolar MPP10

The nucleolar localization of MPP10 suggests that MPP10 is likely to be involved in generation of ribosomes. Possible functions include a role in rRNA processing, assembly of ribosomal subunits, and nucleocytoplamic transport of ribosomal components. To learn more about a possible role of MPP10 in these processes, the intracellular localization of MPP10 was examined in more detail. First, HeLa cells were fractionated into cytoplasmic and nuclear fractions after hypotonic lysis. Crude nuclei (nuclei I) were further purified and then subfractionated into nucleoplasm (nuclei II) and nucleoli (see MATERIALS AND METHODS). When fractions representing an equal number of cells were separated by SDS-PAGE and immunoblotted with antibodies to MPP10 (Figure 3), MPP10 was found in total cellular lysate (Figure 3, lane 1) and the nuclear (Figure 3, lane 3) and nucleolar (Figure 3, lane 5), but not the cytoplasmic (Figure 3, lane 2) and nucleoplasmic (Figure 3, lane 4) fractions.

Second, colocalization of MPP10 and a number of other nucleolar proteins in cultured cells was examined. In interphase cells, MPP10 staining overlapped with the nucleolar staining of fibrillarin, an abundant antigen of the fibrillar component of the nucleolus (Figure 4). Likewise, MPP10 colocalized to the nucleoli stained by antibodies to RNA polymerase I, the 90-kDa nucleolar organizer protein/upstream binding factor, and the PmScl and Th-To autoimmune antigens. To learn whether fibrillarin and MPP10 colocalize to a similar portion of the nucleolus, we treated cells with actinomycin D, which arrests rRNA transcription and causes the separation of the nucleolus into fibrillar caps containing proteins involved in rRNA processing and a granular region containing proteins involved in ribosome assembly and transport. In cells containing optimally segregated nucleoli, MPP10 primarily localized to the fibrillar caps as did fibrillarin, a protein known to be involved in rRNA processing (Figure 5). Further, merging of the confocal images of anti-MPP10 and anti-fibrillarin immunofluorescence indicated that portions of MPP10 and fibrillarin colocalize. Nevertheless, anti-MPP10 and anti-fibrillarin staining did not cover exactly the same parts of segregated nucleolus; some fibrillarin localized outside areas containing MPP10 and some MPP10 was found outside areas containing fibrillarin. Thus, the localization of MPP10 to the fibrillar caps of drug-segregated nucleoli indicates that MPP10 is likely to be involved in rRNA processing. Because some of the MPP10 colocalizes with fibrillarin, MPP10 may be in-

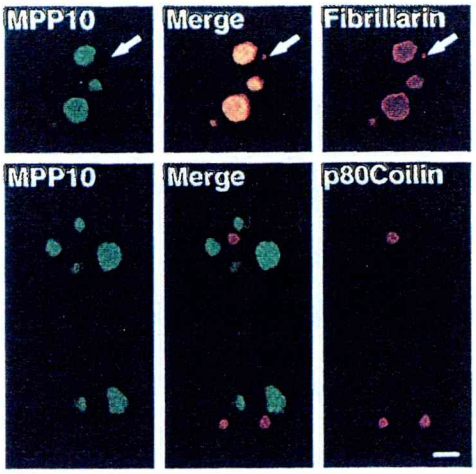

Figure 4. MPP10 colocalization with fibrillarin in the interphase nucleolus but not in the coiled body. Fixed human HEp-2 cells were stained with affinity-purified guinea pig anti-MPP10 and mouse anti-fibrillarin or anti-p80 coilin, and staining was detected with FITC-labeled anti-guinea pig and rhodamine-labeled anti-mouse or rabbit. Images were obtained by confocal microscopy. Bar, 4 μm.

volved in one or more of the processing steps that involves fibrillarin.

To further define the localization of MPP10, we examined coiled bodies, which contain numerous nucleolar proteins, including fibrillarin, as well as proteins involved in mRNA processing. Although the function of the coiled body is unknown, it can be stained specifically by antibodies to coilin, a protein found only in the coiled body. We never detected MPP10 staining in coiled bodies stained for either coilin or fibrillarin (Figure 4). This suggests that MPP10 does not participate in the functions of the coiled body.

Dynamics of MPP10 during the Cell Cycle

At the start of M phase, nucleoli break down, and only proteins involved in rRNA transcription remain associated with the rRNA genes. We have shown previously that after dissolution of the nucleolus in early M phase, MPP10, like fibrillarin, becomes associated with chromosomes (Matsumoto-Taniura *et al.*, 1996, see also Figure 6). MPP10 and fibrillarin continue to be near the chromosomes throughout metaphase and anaphase. In telophase, when the nuclear envelope re-

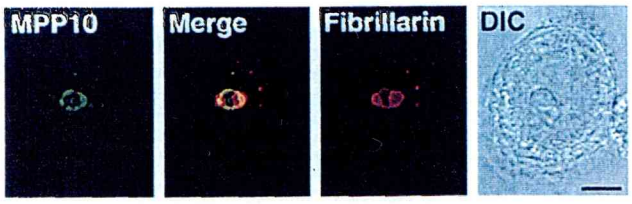

Figure 5. Localization of MPP10 and fibrillarin in cells treated with actinomycin D. HEp-2 cells were incubated with 0.1 μg/ml actinomycin D mannitol for 4 h. After drug treatment, cells were washed, fixed, and stained with affinity-purified guinea pig anti-MPP10 and mouse anti-fibrillarin, and staining was detected with FITC-labeled anti-guinea pig and rhodamine-labeled anti-mouse. Images were obtained by confocal microscopy. DIC, differential interference contrast microscopy. Bar, 5 μm.

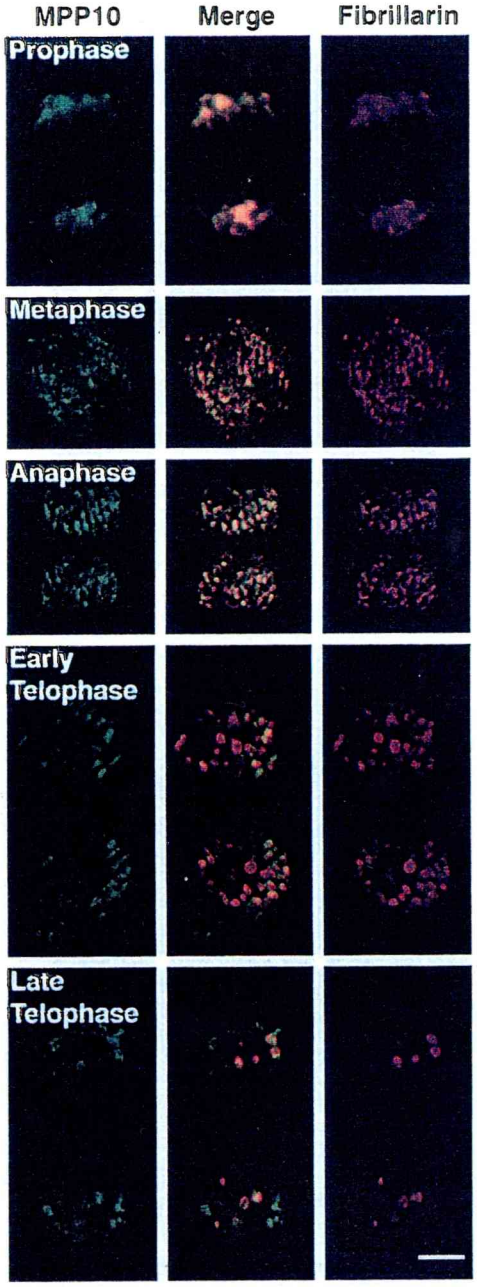

Figure 6. Localization of MPP10 and fibrillarin during M phase of the cell cycle. Fixed HEp-2 cells were stained with affinity-purified guinea pig anti-MPP10 and mouse anti-fibrillarin, and staining was detected with fluorescein-labeled anti-guinea pig and rhodamine-labeled anti-mouse. Images were obtained by confocal microscopy. Bar, 5 μm.

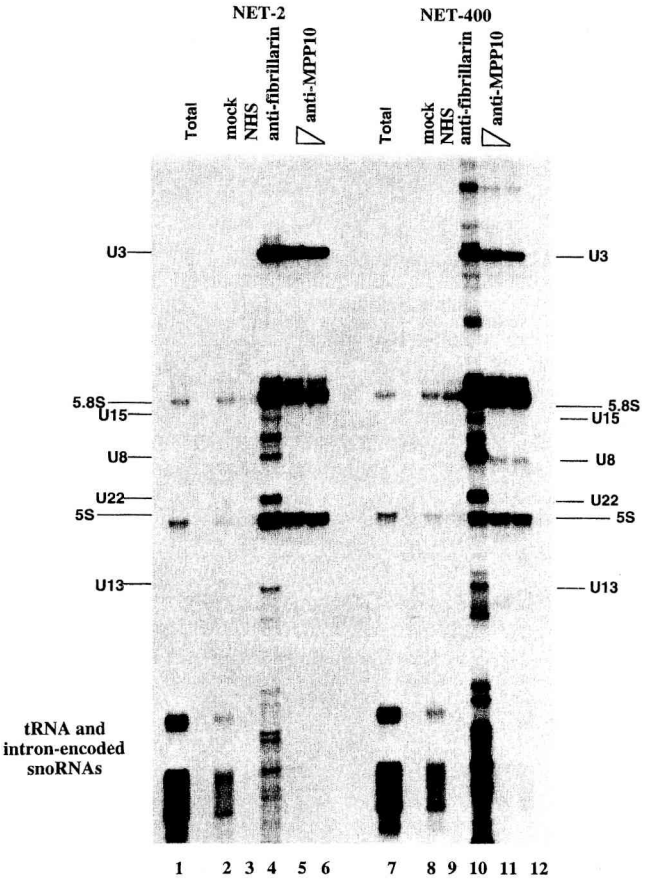

Figure 7. Immunoprecipitation of U3 snoRNA by anti-MPP10. Protein A beads were incubated with no antibodies (mock), normal human serum (NHS), mouse monoclonal antibodies (72B9) to fibrillarin (anti-fibrillarin), or affinity-purified guinea pig anti-MPP10 (anti-MPP10; 10 μl, lanes 5 and 11; 2.5 μl, lanes 6 and 12). The resulting beads were washed and incubated with HeLa cell sonicates. RNA from the resulting immunoprecipitates was purified, end-labeled with ^{32}P-labeled pCp, fractionated on 8% denaturing polyacrylamide gels, and autoradiographed. Lane 1 contains total RNA purified from 1% the number of cells used in the immunoprecipitations. The indicated positions of major RNAs were determined by comparison with the migration of pBR322 digested with *Msp*I, end-labeled, and denatured. We do not consider the presence of 5S and 5.8S rRNAs in the precipitates to be specific because these RNAs are found in precipitates of splicing snRNPs also.

forms, MPP10 and fibrillarin leave the chromosomal surfaces and are found concentrated in small cellular bodies (Figure 6). Two types of telophase bodies containing nucleolar constituents such as fibrillarin have been previously described. They are nucleolus-derived foci, which are present in the cytoplasm of late anaphase and early telophase cells, and prenucleolar bodies, which are present in the nucleus of telophase and early G_1 cells (Jiménez-García *et al.*, 1989, 1994; Azum-Gélade *et al.*, 1994; Medina *et al.*, 1995; Dundr *et al.*, 1997). We find, however, that the bodies containing MPP10 in telophase are distinct from most of the fibrillarin-containing bodies (Figure 6). At a time in telophase when the fibrillarin bodies are all within the nucleus, many of the MPP10 bodies are within the cytoplasm. Later, when fibrillarin is almost completely localized to the nucleoli, MPP10 is primarily found in nuclear structures resembling prenucleolar bodies. Thus, the reassociation of MPP10 with nucleoli is a distinct event, which is preceded by the arrival of fibrillarin.

Characterization of RNAs Found in MPP10 Immunoprecipitates

Localization of MPP10 to actinomycin D-segregated nucleolar fibrillar caps, where fibrillarin is found, suggests that MPP10 may be associated with a snoRNA involved in rRNA processing. To test this possibility, MPP10-containing complexes were immunoprecipitated from HeLa cell sonicates, and coprecipitated RNAs were purified and labeled at their 3′ ends with ^{32}P-labeled pCp (Figure 7). In the MPP10 immunoprecipitates, U3 was the only snoRNA found (Figure 7, lanes 5 and 6). Control immunoprecipitates with anti-fibrillarin contained large amounts of U3, U8, U22, U13 and many smaller box C/D snoRNAs (Figure 7, lane 4). The association of MPP10 with the U3 snoRNP remains stable in high salt (Figure 7, lanes 10–12). Nevertheless, there are a number of nonbox C/D snoRNAs that are visualized in the fibrillarin immunoprecipitation, indicating that the immunoprecipitations performed in high salt (400 mM) are less specific than those performed in low salt (150 mM). For this reason, we also consider the new RNA bands visualized in the MPP10 immunoprecipitations performed in high salt to be nonspecific. Thus, these findings suggest that MPP10 is a stably associated protein component of human U3 snoRNPs.

To further analyze the specificity of MPP10 association with U3 snoRNA, anti-MPP10, anti-TMG, and anti-fibrillarin antibodies were added to sonicates of HeLa cells, and the RNAs purified from the resulting immunoprecipitates were separated, blotted, and hybridized with probes for U1, U2, and U3 RNAs. RNA derived from the anti-MPP10 and anti-fibrillarin precipitates hybridized with only the U3 probe (Figure 8, lanes 4–6). In contrast, precipitates with anti-TMG, which recognizes the TMG cap of several small nuclear RNAs including the abundant U1 and U2 spliceosomal snRNAs and the U3 snoRNA, precipitated RNA that hybridized with all three probes (Figure 8, lane 3). When a U8 probe was used for hybridization, the U8 snoRNA was apparent in only the immunoprecipitations performed with anti-fibrillarin and anti-TMG cap antibodies. These results indicate further that MPP10 is found in U3 snoRNPs and, therefore, is likely to be involved in rRNA processing.

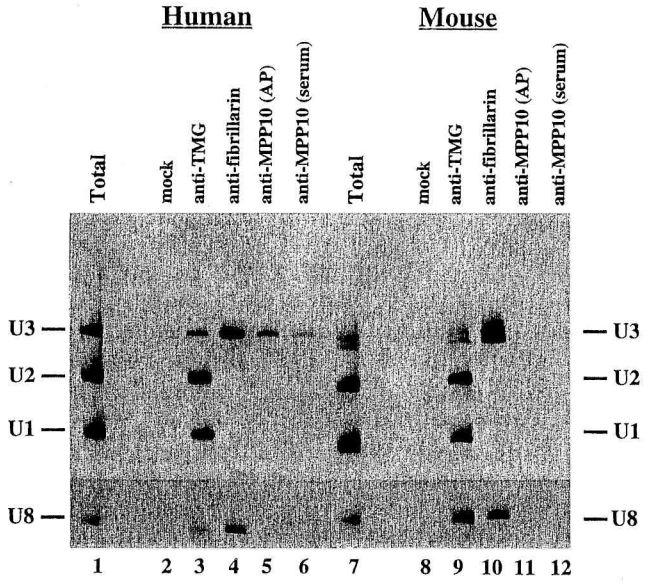

Figure 8. Human and mouse anti-MPP10 immunoprecipitations analyzed by Northern blot analysis. Protein A beads were incubated with no antibodies (mock), mouse monoclonal antibodies to the TMG cap (anti-TMG), mouse monoclonal antibodies (72B9) to fibrillarin (anti-fibrillarin), affinity-purified guinea pig anti-MPP10 (anti-MPP10; affinity purified, AP), or anti-MPP10 guinea pig serum (anti-MPP10 [serum]), washed, and incubated with HeLa (lanes 2–6) or mouse L (lanes 8–12) cell sonicates. RNA from immunoprecipitates was isolated, fractionated on 8% denaturing polyacrylamide gels, blotted to Zeta-Probe, and hybridized with U1, U2, and U3, or U8 probes. Lanes 1 and 7 contain total RNA from 10% the number of cells used in the immunoprecipitations.

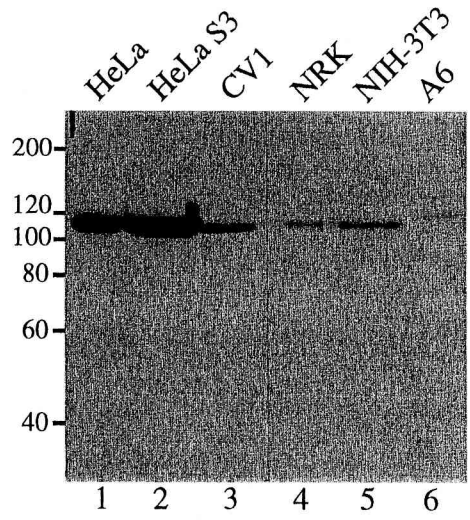

Figure 9. MPP10 in various vertebrate cells. Samples of cells lysed directly in SDS sample buffer were separated by SDS-PAGE and immunoblotted with guinea pig anti-MPP10 serum. Reactive proteins were detected with horseradish peroxidase-conjugated anti-guinea pig and ECL reagents. Lane 1, human HeLa cervical carcinoma cell line growing attached to culture dishes; lane 2, human HeLa cervical carcinoma cell line growing in suspension; lane 3, African green monkey CV1 kidney fibroblast cell line; lane 4, rat NRK kidney epithelial cell line; lane 5, mouse NIH 3T3 embryo fibroblastic cell line; lane 6, South African clawed toad A6 kidney epithelial cell line.

Conservation of MPP10 across Various Vertebrate Species

If MPP10 is involved in rRNA processing, an operation common to all cells, we would expect it to be conserved across various species. To learn whether there is a protein similar to MPP10 in cells other than human, we immunoblotted proteins from various animal cell lines with antibodies directed against amino acids 58 to 681. We found immunoreactive proteins approximately the same size as MPP10 in monkey, rat, mouse, and toad cells (Figure 9). From this, we conclude that an MPP10-like protein is present in diverse vertebrate species. In spite of the immuno-cross-reactivity we see by immunoblot, we find that the antibodies against human MPP10 do not recognize MPP10 in rat cells by immunofluorescence (our unpublished data) and are not able to immunoprecipitate U3 snoRNA from mouse cell sonicates (Figure 8, lanes 11 and 12). It is likely that most of the epitopes recognized by our antibodies are only exposed in denatured protein.

DISCUSSION

We have shown that MPP10, a protein whose cDNA was isolated on the basis of its ability to be phosphorylated by M phase kinases, is a nucleolar protein of unique properties. In our experiments, the majority of MPP10 colocalized with fibrillarin, a well-characterized nucleolar protein, under most conditions. Nevertheless, even though a portion of fibrillarin is found in the coiled body, a nuclear structure of unknown function, MPP10 was never detected in the coiled body stained with either anti-fibrillarin or anti-p80 coilin. Again, like fibrillarin, MPP10 localized to small cellular bodies similar to nucleolus-derived foci and prenucleolar bodies in early telophase of mitosis. Nonetheless, many of the nucleolus-derived foci and prenucleolar bodies in which fibrillarin is found did not contain MPP10, which arrived at the newly forming nucleolus later than fibrillarin. Finally, like those of fibrillarin, antibodies against MPP10 immunoprecipitated the U3 RNA. In contrast to immunoprecipitates of fibrillarin, however, those of MPP10 did not contain substantial amounts of any other snoRNA.

The properties of MPP10 suggest that it is involved in rRNA processing. This potential function for MPP10 was first indicated by its localization to the fibrillar caps of actinomycin D-segregated nucleoli, which contain proteins involved in rRNA processing (reviewed in Ochs, 1997). Much stronger evidence for MPP10 involvement in rRNA processing comes from our immunoprecipitation experiments; anti-MPP10 precipitates U3 snoRNA, which is necessary for pro-

cessing of 18S rRNA (Savino and Gerbi, 1990; Hughes and Ares, 1991; Beltrame and Tollervey, 1992; Beltrame *et al.*, 1994; Beltrame and Tollervey, 1995; Hughes, 1996). The final proof of MPP10 involvement in this event in vertebrates, however, is still lacking. We will need to deplete MPP10 from cell extracts and show that some rRNA processing step is lost. To date, we have not been able to do this because our antibodies do not immunoprecipitate U3 from mouse L cell sonicates. This experiment will require development of other antibodies to MPP10. Interestingly, depletion of the MPP10 homologue in yeast causes an 18S rRNA processing defect similar to that obtained on depletion of two other U3 snoRNP components (Dunbar *et al.*, 1997). Furthermore, mutations in yeast MPP10 suggest that it may be more directly involved in cleavage at the pre-rRNA A1 and A2 sites (Lee and Baserga, in press).

Because MPP10 is not detected in the coiled body, the functions of MPP10 that are similar to those of fibrillarin are likely to occur in the nucleolus, not the coiled body. As yet, the activities that are carried out in the coiled body and its relationship to the nucleolus are not understood. Nevertheless, overexpression of p80 coilin, the marker protein for the coiled body, disrupts nucleolar structure (Bohmann *et al.*, 1995), and U3 snoRNP components including fibrillarin and U3 snoRNA have been localized to the coiled body (Figure 4; Raska *et al.*, 1991; Jiménez-García *et al.*, 1994). The localization of U3 snoRNA to coiled bodies is, however, controversial; in other experiments using different probes, the U3 snoRNA was not observed in coiled bodies (Carmó-Fonseca *et al.*, 1993; Matera *et al.*, 1994). Therefore, although we do not observe any MPP10 in the coiled body, we cannot be certain that it is not present in that structure. If the presence of U3 RNA and absence of MPP10 in coiled bodies prove to be correct, then the U3 snoRNPs that are found in that structure must lack MPP10.

Because MPP10 was isolated on the basis of its ability to be phosphorylated by M phase kinases, and we have shown that MPP10 is phosphorylated in M phase, we suspect that phosphorylation may play a role in determining the M phase function, M phase distribution, or stability of MPP10. We note that the potential MPM2-reactive phosphorylation site at amino acid 163 is in a PEST sequence, a motif that regulates protein turnover (Rechsteiner and Rogers, 1996). Although we have found U3 associated with MPP10 immunoprecipitated from M phase cells (our unpublished results), we cannot be certain that these complexes are not formed after dephosphorylation of MPP10 in cell lysates. As yet, we have not found cell lysis conditions capable of maintaining both U3 snoRNP structure and MPP10 phosphorylation. Our ability to determine the role of phosphorylation in MPP10 function in M phase will be aided by identification of the kinases and phosphatases that act on MPP10.

Throughout M phase, nucleolar proteins involved in rRNA transcription remain with the nucleolar organizer (Scheer and Rose, 1984; Jiménez-García *et al.*, 1989; Chan *et al.*, 1991). In contrast, many other nucleolar proteins localize to chromosome surfaces in prophase through anaphase. In telophase and G1, they follow a pathway involving cytoplasmic nucleolus-derived foci and, subsequently, nuclear structures termed prenucleolar bodies, and, finally, reassociate with forming nucleoli when rRNA transcription resumes (Benavente *et al.*, 1987; Jiménez-García *et al.*, 1989, 1994; Oakes *et al.*, 1993; Azum-Gélade *et al.*, 1994; Hernandez-Verdun and Gautier, 1994; Medina *et al.*, 1995; Dundr *et al.*, 1997). Although both MPP10 and fibrillarin follow this general pattern of reassembly into nucleoli, we were surprised to find that the small bodies in which MPP10 was found in telophase did not always correspond to the bodies that contain fibrillarin. Our finding that MPP10 and fibrillarin do not colocalize to all the same telophase structures suggests a further layer of complexity to the process of nucleolar reformation. It is possible that nucleolus-derived foci and prenucleolar bodies process nucleolar components for relocalization to nucleoli and that, during nucleolar reformation, MPP10 passes through these structures at a different time from other nucleolar components.

To date, MPP10 is the only characterized vertebrate protein that has been shown to coimmunoprecipitate with U3 RNA but no significant amounts of other snoRNAs. Fibrillarin, the best-characterized protein of the U3 snoRNP, is also found in snoRNPs containing various other snoRNAs that are involved in processing 5.8S and 28S rRNA and rRNA methylation (Peculis and Steitz, 1993; Kiss-László *et al.*, 1996; Nicoloso *et al.*, 1996). We do not yet know whether fibrillarin and MPP10 are complexed together in the same U3 RNP, and we have not determined whether there is a pool of MPP10 that is not complexed with the U3 snoRNP. Furthermore, although MPP10 is tightly bound to U3 snoRNP, we have not been able to demonstrate direct binding of MPP10 to the U3 snoRNA (our unpublished observations). It may be that the association of MPP10 with the U3 snoRNA occurs via protein–protein interactions. The short stretches of potential coiled-coil α-helix found in MPP10 might mediate these intermolecular associations. As more protein components of nucleolar RNPs are characterized, it will be interesting to sort out which proteins are found in the same multi-protein complex.

MPP10 is one of what are likely to be many protein components of the vertebrate U3 snoRNP. [^{35}S]methionine and [^{32}P]orthophosphate labeling of HeLa cells followed by immunoprecipitation with anti-fibrillarin antisera indicates that there may be at least six protein

components of the U3 snoRNP, including the protein fibrillarin (Parker and Steitz, 1987). It is possible, however, that not all of these proteins are specific for the U3 RNP. For instance, we now know that fibrillarin is a component of many snoRNPs. By contrast, purification of the U3 snoRNP from hamster cells with anti-TMG and Mono Q anion-exchange chromatography yielded only three proteins, none of which were fibrillarin (Lubben *et al.*, 1993). Both these isolation protocols identified a 55-kDa protein that may be the mammalian homologue of the 56-kDa yeast U3 snoRNP Sof1 (Jansen *et al.*, 1993). The methods that have been used thus far for isolation of U3 snoRNPs may not, however, be adequate for identifying all its components. Glycerol gradients of HeLa extract indicate a size for the U3 monomeric snoRNP similar to that of the U1 mono-snRNP (12 S; Tyc and Steitz, 1989). Given that the vertebrate U1 snRNP has already been found to have 11 components (Fabrizio *et al.*, 1994), the U3 snoRNP may contain many more proteins that have not yet been identified.

ACKNOWLEDGMENTS

J.M.W. and F.P. are thankful for the support of Dr. Didier Job (Institut National de la Santé et de la Recherche Médicale U366, Commissariat à l'Energie Atomique, Grenoble), in whose laboratory part of the work reported herein was done. We thank the following individuals for materials: Dr. Pierre Chambon for the HeLa λZap cDNA library, Drs. Ludger Hengst and Steven Reed for the HeLa UniZap cDNA library, Drs. Michael Pollard and Eng Tan for the 72B9 anti-fibrillarin monoclonal, Dr. Ed Chan for the polyclonal anti-coilin, and Dr. Joan Steitz for the Y12 anti-Sm monoclonal. This work was supported by a grant from the National Institutes of Health to L.G. J.M.W. was supported by fellowships from the Association pour la Recherche sur la Cancer and the Fondation pour la Recherche Médicale. S.J.B and S.W. were supported by National Institutes of Health grant R29 GM5281. S.J.B. is a member of the Yale Cancer Center.

REFERENCES

Andrade, L.E.C., Chan, E.K.L., Raska, I., Peebles, C.L., Roos, G., and Tan, E.M. (1991). Human autoantibody to a novel protein of the nuclear coiled body: immunological characterization and cDNA cloning of p80 coilin. J. Exp. Med. *173*, 1407–1419.

Azum-Gélade, M.-C., Noaillac-Depeyre, J., Caizergues-Ferrer, M., and Gas, N. (1994). Cell cycle redistribution of U3 snRNA and fibrillarin. Presence in the cytoplasmic nucleolus remnant and in the prenucleolar bodies in telophase. J. Cell Sci. *107*, 463–475.

Baserga, S.J., Yang, X.W., and Steitz, J.A. (1991). An intact box C sequence is required for binding of fibrillarin, the protein common to the major family of nucleolar snRNPs. EMBO J. *10*, 2645–2651.

Black, D.L., and Pinto, A.L. (1989).U5 small nuclear ribonucleoprotein: RNA structure analysis and ATP-dependent interaction with U4/U6. Mol. Cell. Biol. *9*, 3350–3359.

Beltrame, M., Henry, Y., and Tollervey, D. (1994). Mutational analysis of an essential binding site for the U3 snoRNA in the 5′ external transcribed spacer of yeast pre-rRNA. Nucleic Acids Res. 22, 4057–4065.

Beltrame, M., and Tollervey, D. (1992). Identification and functional analysis of two U3 binding sites on yeast pre-ribosomal RNA. EMBO J. *11*, 1531–1542.

Beltrame, M., and Tollervey, D. (1995). Base pairing between U3 and the pre-ribosomal RNA is required for 18S rRNA synthesis. EMBO J. *14*, 4350–4356.

Benavente, R., Rose, K.M., Reimer, G., Hugle-Dorr, B., and Scheer, U. (1987). Inhibition of nucleolar reformation after microinjection of antibodies to RNA polymerase I into mitotic cells. J. Cell Biol. *105*, 1483–1491.

Bohmann, K., Ferreira, J.A., and Lamond, A.I. (1995). Mutational analysis of p80 coilin indicates a functional interaction between coiled bodies and the nucleolus. J. Cell Biol. *131*, 817–831.

Carmo-Fonseca, M., Ferreira, J., and Lamond, A.I. (1993). Assembly of snRNP-containing coiled bodies is regulated in interphase and mitosis–evidence that the coiled body is a kinetic nuclear structure. J. Cell Biol. *120*, 841–852.

Chan, E.K.L., Imai, H., Hamel, J.C., and Tan, E.M. (1991). Human autoantibody to RNA polymerase I transcription factor hUBF. Molecular identity of nucleolus organizer region autoantigen NOR-90 and ribosomal RNA upstream binding factor. J. Exp. Med. *174*, 1239–1244.

Davis, F.M., Tsao, T.Y., Fowler, S.K., and Rao, P.N. (1983). Monoclonal antibodies to mitotic cells. Proc. Natl. Acad. Sci. USA *80*, 2926–2930.

Draetta, G., Luca, F., Westendorf, J., Brizuela, L., Ruderman, J., and Beach, D. (1989). Cdc2 protein kinase is complexed with both cyclin A and B: evidence for proteolytic inactivation of MPF. Cell *56*, 829–838.

Dunbar, D.A., Wormsley, S., Agentis, T.M., and Baserga, S.J. (1997). Mpp10p, a U3 small nucleolar ribonucleoprotein component required for pre-18S rRNA processing in yeast. Mol. Cell. Biol. *17*, 5803–5812.

Dundr, M., Meier, U.T., Lewis, N., Rekosh, D., Hammarskjold, M.L., and Olson, M.O.J. (1997). A class of nonribosomal nucleolar components is located in chromosome periphery and in nucleolus-derived foci during anaphase and telophase. Chromosoma *105*, 407–417.

Dunphy, W.G., Brizuela, L., Beach, D., and Newport, J. (1988). The *Xenopus cdc2* protein is a component of MPF, a cytoplasmic regulator of mitosis. Cell *54*, 423–431.

Elela, S.A., Igel, H., and Ares, M., Jr. (1996). RNase III cleaves eukaryotic preribosomal RNA at a U3 snoRNP-dependent site. Cell *85*, 115–124.

England, T.E., Bruce, A.G., and Uhlenbeck, O.C. (1980). Specific labeling of 3′ termini of RNA with T4 RNA ligase. Methods Enzymol. *65*, 65–74.

Fabrizio, P., Esser, S., Kastner, B., and Luhrmann, R. (1994). Isolation of *S. cerevisiae* snRNPs: comparison of U1 and U4/U6.U5 to their human counterparts. Science *264*, 261–265.

Fritzler, M.J. (1997). Autoantibodies: diagnostic fingerprints and etiologic perplexities. Clin. Invest. Med. *20*, 50–66.

Frohman, M.A. (1994). On beyond classic RACE. PCR Methods Appl. *4*, s40–s58.

Gautier, T., Fomproix, N., Masson, C., Azum-Gélade, M.-C., Gas, N., and Hernandez-Verdun, D. (1994). Fate of specific nucleolar perichromosomal proteins during mitosis: cellular distribution and association with U3 snoRNA. Biol. Cell *82*, 81–93.

Gautier, J., Minshull, J., Lokha, M., Glotzer, M., Hunt, T., and Maller, J.L. (1990). Cyclin is a component of MPF from *Xenopus*. Cell *60*, 487–494.

Gautier, J., Norbury, C., Lokha, M., Nurse, P., and Maller, J. (1988). Purified maturation promoting factor contains the product of a *Xenopus* homolog of the fission yeast cell cycle control gene $cdc2^+$. Cell *54*, 433–439.

Gautier, T., Robert-Nicoud, M., Guilly, M.-N., and Hernandez-Verdun, D. (1992). Relocation of nucleolar proteins around chromosomes at mitosis. A study by confocal laser scanning microscopy. J. Cell Sci. *102*, 729–737.

Gerace, L., and Blobel, G. (1980). The nuclear envelope is reversibly depolymerized during mitosis. Cell *19*, 277–287.

Heald, R., and McKeon, F. (1990). Mutations of phosphorylation sites in lamin A that prevent nuclear lamina disassembly in mitosis. Cell *61*, 579–589.

Hernandez-Verdun, D., and Gautier, T. (1994). The chromosome periphery during mitosis. Bioessays *16*, 179–185.

Hughes, J.M.X. (1996). Functional base-pairing interaction between highly conserved elements of U3 small nucleolar RNA and the small ribosomal subunit RNA. J. Mol. Biol. *259*, 645–654.

Hughes, J.M.X., and Ares, M., Jr. (1991). Depletion of U3 small nucleolar RNA inhibits cleavage in the 5′ external transcribed spacer of yeast pre-ribosomal RNA and prevents formation of 18S ribosomal RNA. EMBO J. *10*, 4231–4239.

Jansen, R., Tollervey, D., and Hurt, E.C. (1993). A U3 snoRNP protein with homology to splicing factor PRP4 and G beta domains is required for ribosomal RNA processing. EMBO J. *12*, 2549–2558.

Jiménez-García, L.F., Rothblum, L.I., Busch, H., and Ochs, R.L. (1989). Nucleologenesis: use of non-isotopic in situ hybridization and immunocytochemistry to compare the localization of rDNA and nucleolar proteins during mitosis. Biol. Cell *65*, 239–246.

Jiménez-García, L.F., Segura-Valdez, M.d.L., Ochs, R.L., Rothblum, L.I., Hannan, R., and Spector, D.L. (1994). Nucleologenesis: U3 snRNA-containing prenucleolar bodies move to sites of active pre-rRNA transcription after mitosis. Mol. Biol. Cell *5*, 955–966.

Kass, S., Craig, N., and Sollner-Webb, B. (1987). Primary processing of mammalian rRNA involves two adjacent cleavages and is not species specific. Mol. Cell. Biol. *7*, 2891–2898.

Kiss-László, Z., Henry, Y., Bachellerie, J.-P., Caizergues-Ferrer, M., and Kiss, T. (1996). Site-specific ribose methylation of preribosomal RNA: a novel function for small nucleolar RNAs. Cell *85*, 1077–1088.

Kozak, M. (1996). Interpreting cDNA sequences: some insights from studies on translation. Mamm. Genome *7*, 563–574.

Labbé, J.-C., Capony, J.P., Caput, D., Cavadore, J.-C., Derancourt, J., Kaghdad, M., Lelias, J.-M., Picard, A., and Dorée, M. (1989). MPF from starfish oocytes at first meiotic metaphase is a heterodimer containing one molecule of cdc2 and one molecule of cyclin B. EMBO J. *8*, 3053–3058.

Lerner, M.R., Boyle, J.A., Hardin, J.A., and Steitz, J.A. (1981). Two novel classes of small ribonucleoproteins detected by antibodies associated with lupas erythematosus. Science *211*, 400–402.

Lerner, M.R., and Steitz, J.A. (1979). Antibodies to small nuclear RNAs complexed with proteins are produced by patients with systemic lupus erythematosus. Proc. Natl. Acad. Sci. USA *76*, 5495–5499.

Lischwe, M.A., Ochs, R.L., Reddy, R., Cook, R.G., Yeoman, L.C., Tan, E.M., Reichlin, M., and Busch, H. (1985). Purification and partial characterization of a nucleolar scleroderma antigen (M_r = 34,000; pI, 8.5) rich in N^G,N^G-dimethylarginine. J. Biol. Chem. *260*, 14304–14310.

Lubben, B., Marshallsay, C., Rottman, N., and Luhrmann, R. (1993). Isolation of U3 snoRNP form CHO cells: a novel 55-kDa protein binds to the central part of U3 snoRNA. Nucleic Acids Res. *21*, 5377–5385.

Lupas, A. (1996). Coiled coils: new structures and new functions. Trends Biochem. Sci. *21*, 375–382.

Lupas, A., VanDyke, M., and Stock, J. (1991). Predicting coiled-coils from protein sequences. Science *252*, 1162–1164.

Matera, A.G., Tycowski, K.T., Steitz, J.A., and Ward, D.C. (1994). Organization of small nucleolar ribonucleoproteins (snornps) by fluorescence in situ hybridization and immunocytochemistry. Mol. Biol. Cell *5*, 1289–1299.

Matsumoto-Taniura, N., Pirollet, F., Monroe, R., Gerace, L., and Westendorf, J.M. (1996). Identification of novel M phase phosphoproteins by expression cloning. Mol. Biol. Cell *7*, 1455–1469.

Maxwell, E.S., and Fournier, M.J. (1995). The small nucleolar RNAs. Annu. Rev. Biochem. *64*, 897–934.

Medina, F.J., Cerdido, A., and Fernández-Gómez, M.E. (1995). Exp. Cell Res. *221*, 111–125.

Meijer, L., Arion, D., Golsteyn, R., Pines, J., Brizuela, L., Hunt, T., and Beach, D. (1989). Cyclin is a component of the sea urchin egg M-phase specific histone H1 kinase. EMBO J. *8*, 2275–2282.

Muramatsu, M., Smetana, K., and Busch, H. (1963). Quantitative aspects of isolation of nucleoli of the Walker carcinosarcoma and liver of the rat. Cancer Res. *25*, 693–697.

Nicoloso, M., Qu, L.-H., Michot, B., and Bachellerie, J.-P. (1996). Intron-encoded, antisense small nucleolar RNAs: the characterization of nine novel species points their direct role as guides for the 2′-*O*-ribose methylation of rRNAs. J. Mol. Biol. *160*, 178–195.

Oakes, M., Nogi, Y., Clark, M.W., and Nomura, M. (1993). Structural alterations of the nucleolus in mutants of *Saccharomyces cerevisiae* defective in RNA polymerase I. Mol. Cell. Biol. *13*, 2441–2455.

Ochs, R.L. (1997). Methods used to study structure and function of the nucleolus. Methods Cell Biol. (*in press*).

Ottaviano, Y., and Gerace, L. (1985). Phosphorylation of the nuclear lamins during interphase and mitosis. J. Biol. Chem. *260*, 624–632.

Parker, K.A., and Steitz, J.A. (1987). Structural analyses of the human U3 ribonucleoprotein particle reveal a conserved sequence available for base-pairing with pre-rRNA. Mol. Cell. Biol. *7*, 2899–2913.

Peculis, B.A., and Steitz, J.A. (1993). Disruption of U8 nucleolar snRNA inhibits 5.8S and 28S rRNA processing in the *Xenopus* oocyte. Cell *73*, 1233–1245.

Peter, M., Nakagawa, J., Doreé, M., Labbé, J.C., and Nigg, E.A. (1990). In vitro disassembly of the nuclear lamina and M phase-specific phosphorylation of lamins by cdc2 kinase. Cell *61*, 591–602.

Raska, I., Andrade, L.E. C., Ochs, R.L., Chan, E.K. L., Chang, C.-M., Roos, G., and Tan, E.M. (1991). Immunological and ultrastructural studies of the nuclear coiled body with autoimmune antibodies. Exp. Cell Res. *195*, 27–37.

Rechsteiner, M., and Rogers, S.W. (1996). PEST sequences and regulation by proteolysis. Trends Biochem. Sci. *21*, 267–271.

Reimer, G., Pollard, K.M., Penning, C.A., Ochs, R.L., Lischwe, M.A., Busch, H., and Tan, E.M. (1987). Monoclonal antibody from a (New Zealand black × New Zealand white) F_1 mouse and some human scleroderma sera target an M_r 34,000 nucleolar protein of the U3 RNP particle. Arthritis Rheum. *30*, 793–800.

Savino, R., and Gerbi, S.A. (1990). In vivo disruption of *Xenopus* U3 snRNA affects ribosomal RNA processing. EMBO J. *9*, 2299–2308.

Scheer, U., and Rose, K.M. (1984). Localization of RNA polymerase I in interphase cells and mitotic chromosomes by light and electron microscopic immunocytochemistry. Proc. Natl. Acad. Sci. USA *81*, 1431–1435.

Shaw, P.J., and Jordan, E.G. (1995). The nucleolus. Annu. Rev. Cell Dev. Biol. *11*, 93–121.

Tyc, K., and Steitz, J.A. (1989). U3, U8 and U13 comprise a new class of mammalian snRNPs localized to the cell nucleolus. EMBO J. *8*, 3113–3119.

Venema, J., and Tollervey, D. (1995). Processing of pre-ribosomal RNA in *Saccharomyces cerevisiae*. Yeast *11*, 1629–1650.

Ward, G.E., and Kirschner, M.W. (1990). Identification of cell cycle-regulated phosphorylation sites on nuclear lamin C. Cell *61*, 561–577.

Warner, J.R. (1979). Distribution of newly formed ribosomal proteins in HeLa cell fractions. J. Cell Biol. *80*, 767–772.

Westendorf, J.M., Rao, P.N., and Gerace, L. (1994). Cloning of cDNAs for M phase phosphoproteins recognized by the MPM2 monoclonal antibody and determination of the phosphorylated epitope. Proc. Natl. Acad. Sci. USA *91*, 714–718.

Yasuda, Y., and Maul, G.G. (1990). A nucleolar auto-antigen is part of a major chromosomal surface component. Chromosoma *99*, 152–160.

Molecular Biology of the Cell
Vol. 7, 1455–1469, September 1996

参考論文

Identification of Novel M Phase Phosphoproteins by Expression Cloning

Naoko Matsumoto-Taniura,*† Fabienne Pirollet,*‡ Robert Monroe,*§ Larry Gerace,* and Joanne M. Westendorf*‡‖

*Departments of Cell and Molecular Biology, The Scripps Research Institute, La Jolla, California 92037; and ‡Laboratoire du Cytosquelette Commissariat à l'Energie Atomique, Institut National de la Santé et de la Recherche Médicale Unité 366, Département de Biologie Moléculaire et Structurale, CEA/Grenoble, 38054 Grenoble Cedex 9, France

Submitted March 22, 1996; Accepted July 9, 1996
Monitoring Editor: Mitsuhiro Yanagida

Using an expression cloning technique, we isolated cDNAs for eight M phase phosphoproteins (MPPs 4–11). We then used affinity-purified antibodies to fusion proteins to characterize the intracellular localization and some biochemical properties of these proteins and two others that we identified previously (MPPs 1–2). Each antibody immunoprecipitated one or two protein species of a characteristic size ranging from 17,000 to 220,000 Da. Each MPP, when immunoprecipitated from lysates of M phase cells, was reactive with MPM2, a monoclonal antibody that recognizes a group of related M phase phosphorylation sites, including F-phosphoT-P-L-Q. This reactivity indicated that all the MPPs encoded genuine M phase phosphoproteins. When antibodies to the MPPs were used for immunofluorescence microscopy, each anti-MPP gave a characteristic pattern of localization. In interphase, several of the MPPs were nuclear proteins, whereas others were cytoplasmic or distributed throughout the cell. Three MPPs were strikingly localized to interphase structures: MPP7 to centers of DNA replication, MPP9 to the Golgi complex, and MPP10 to nucleoli. In mitosis, most of the MPPs were distributed throughout the cells. Further studies of the 10 MPPs, most of which are previously undescribed, are expected to provide new understandings of the process of cell division.

INTRODUCTION

A family of cyclin-dependent kinases (cdks) drives progression through the cell cycle by phosphorylating numerous cellular proteins (Draetta, 1994; Heichman and Roberts, 1994; Hunt and Sherr, 1994; Hunter and Pines, 1994; King *et al.*, 1994; Nurse, 1994; O'Connell and Nurse, 1994; Sherr, 1994). These kinases consist of two subunits: a catalytic subunit that is related to the yeast cdc2/CDC28 gene and a cyclin regulatory subunit. The catalytic subunit is present throughout the cell cycle, and the cyclin subunit, which is required for activity, appears and disappears at a time appropriate to its function. The activity of cyclin-dependent kinases is further regulated by phosphorylation and dephosphorylation of the catalytic subunit (Coleman and Dunphy, 1994) and by binding to several small peptide kinase inhibitors (Elledge and Harper, 1994). Although much information has accumulated on regulation of cdk activity, less is now known about the kinase substrates that perform cell-cycle progression.

The first known cyclin-dependent kinase, $p34^{cdc2}$, associates primarily with cyclin B to generate M phase-promoting factor (MPF; Dunphy *et al.*, 1988; Gautier *et al.*, 1988, 1990; Draetta *et al.*, 1989; Labbé *et al.*, 1989, Meijer *et al.*, 1989), which causes G2 phase cells to enter M phase. Upon progression into M phase, many proteins, which include mitotic regulators and interphase structural proteins, become hyper-

Present addresses: †Department of Biochemistry, Biomedical Research Center, Osaka, Japan; §Present address: Children's Hospital, Harvard Medical School, Boston, MA 02115.
‖ Corresponding author: Laboratoire du Cytosquelette CEA, INSERM U366, DBMS, CEA/Grenoble, 17 rue des Martyrs, 38054 Grenoble Cedex 9, France.

phosphorylated by MPF or other activated M phase kinases (Maller *et al.*, 1977; Karsenti *et al.*, 1987; Lohka *et al.*, 1987). These M phase phosphoproteins, many of which have not yet been identified, permit disassembly of interphase structures and generation of M phase enzymatic activities and structures.

A subset of the M phase phosphoproteins (at least 40 polypeptides) is reactive with MPM2 (Davis *et al.*, 1983), a monoclonal antibody that recognizes a set of related phosphorylation sites, including F-phosphoT-P-L-Q (Westendorf *et al.*, 1994). The MPM2-reactive phosphoproteins, which are abundant in M phase cells and strongly reduced in interphase cells, can be generated by phosphorylation of pre-existing interphase proteins (Kuang *et al.*, 1989). As a group, MPM2-reactive phosphoproteins are present throughout the M phase cell but are most concentrated in several structures involved in M phase functions, including centrosomes, kinetochores, spindle fibers, the chromosomal axis, and the midbody (Vandre *et al.*, 1984; Hirano and Mitchison, 1991). Because addition of MPM2 to centrosomes prevents microtubule nucleation in vitro (Centonze and Borisy, 1990), the concentration of MPM2-reactive proteins in spindle poles is suggested to be of functional importance. Furthermore, when cells are microinjected with MPM2, entry into (Kuang *et al.*, 1989) and exit from M phase (Davis and Rao, 1987) are inhibited. Recently, a molecular basis for these results has been suggested; MPM2-reactive forms of cdc25, a tyrosine phosphatase, and wee1, a kinase, have been shown to be involved in activation of MPF (Kuang *et al.*, 1994; Mueller *et al.*, 1995), and cyclin destruction activity has been shown to be MPM2-reactive (King *et al.*, 1995), probably because of an MPM2-reactive ubiquitin-protein ligase subunit CDC27, which contains several potential MPM2 binding sites. Several other proteins, including topoisomerase II (Taagepera *et al.*, 1993), MAP4 (Vandre *et al.*, 1991), and nimA (Ye *et al.*, 1995), known to have M phase functions have also been shown to be MPM2 antigens. It seems likely that phosphorylation of these and other proteins at MPM2 sites imparts key M phase functions.

We have originated a method for cloning cDNAs encoding proteins that are efficient substrates for M phase kinases that act at MPM2 sites, and in this manner we have identified two novel proteins (Westendorf *et al.*, 1994). In this paper, we have isolated cDNA clones for eight more proteins, most of which have not yet been described. Further, for each of the 10 proteins, we have produced fusion proteins that were then used to generate specific antisera. These antisera have allowed us to characterize biochemical properties and the intracellular localization of these 10 proteins in interphase and M phase. Importantly, we are now able to show that all of the proteins are authentic MPM2 antigens in vivo during M phase. Among them are molecules with a possible role in regulating structure and functions of nucleoli, Golgi, and DNA replication centers.

MATERIALS AND METHODS

Isolation of M Phase Phosphoproteins (MPP) cDNAs

cDNAs were isolated essentially as described previously (Westendorf *et al.*, 1994). Protein replica filters of λ cDNA libraries were incubated with extracts of M phase HeLa cells to phosphorylate substrate proteins, washed, and incubated with the phospho-epitope-binding antibody MPM2. Immunoreactivity was detected with horseradish peroxidase anti-mouse (Clontech, Palo Alto, CA) and 4-chloro-1-napthol. The following improvements were made to the procedure. Before reaction with M phase cell extracts for isolation of MPPs 4–11, replica filters were denatured with 6 M guanidine in buffer A (25 mM HEPES, 25 mM NaCl, and 5 mM $MgCl_2$) and renatured by incubation with four successive twofold dilutions of the guanidine solution with buffer A containing 0.5 mM dithiothreitol (DTT). This improved the kinase substrate accessibility of MPP protein expressed in λ plaques. For the kinase incubations using extracts of M phase cells, 1 μM microcystin LR was substituted for NaF and $Na_4P_2O_7$, which were found to inhibit kinase activity in the extract. Finally, 1.5 M NaCl was added to the MPM2 incubation to decrease background antibody binding. To allow selection of cDNAs different from those already isolated, we compared the positive plaques of the protein replica filters reacted with M phase cell extracts and MPM2 with the positives obtained with a second replica filter hybridized with probes corresponding to our previously isolated cDNAs by standard procedures (Sambrook *et al.*, 1989).

Preparation of Bacterially Expressed MPPs

All MPPs were fused to T7 protein 10, and all of those except MPP1 also contained a hexahistidine (his) tag. MPP1 and MPP2 fusion proteins were prepared as described previously (Westendorf *et al.*, 1994). Vectors encoding his-tagged protein 10–MPP fusion proteins for MPP5, 6, and 9 were prepared exactly as described for MPP2. Vectors encoding the other MPP fusion proteins were prepared as follows. MPP7 cDNA, which contained internal *Eco*RI sites, was amplified from λ DNA, subcloned into the pCRII vector (Invitrogen, San Diego, CA), excised with *Hin*dIII and *Eco*RV, and ligated to *Hin*dIII-cut GEMEX1HIS. The ends of the resulting linear product of this ligation were blunted with mung bean nuclease and recircularized. MPP8 cDNA, which lacked a 5′ *Eco*RI site, was amplified from λ DNA, subcloned into the pCRII vector, methylated at *Eco*RI sites, excised together with 61 base pairs (bp) of vector DNA with *Bst*XI, blunted with T4 DNA polymerase, ligated to 12 mer *Eco*RI linkers, and cloned into the *Eco*RI site of GEMEX1HIS. MPP10 cDNA was subcloned into the *Eco*RI site of pBluescript, excised with *Bam*HI (which resulted in a 144 bp 5′ end deletion), blunted with T4 DNA polymerase, ligated to 10 mer *Eco*RI linkers, and cloned into the *Eco*RI site of GEMEX1HIS. MPP11 cDNA, which contained internal *Eco*RI sites, was amplified from λ DNA and subcloned into the pCRII vector. The largest *Eco*RI (starting at bp 607) fragment was excised, blunted with T4 DNA polymerase, ligated to 8-mer *Bam*HI linkers, and cloned into GEMEX1HIS-*Bam*HI (GEMEX1HIS modified by digesting with *Eco*RI, blunting with T4 DNA polymerase, and ligating in an 8-mer *Bam*HI linker). The MPP4 cDNA insert 4-3 was subcloned into GEMEX2, but because of a 5′ stop codon, it was not fused to protein 10. This construct was used for production of a nonfusion protein, which was used for immunization. Subsequently, a PCR primer containing an *Eco*RI site and the region surrounding the apparent start codon and the T3 promoter primer were used to produce a PCR product lacking the 5′ stop. This PCR

product was cut with *Eco*RI and subcloned into pGEMEX1HIS. This construct was used for preparation of an affinity column for purification of antisera. Plasmids were transfected into JM109(DE3) or BL21plysS (Glass *et al.*, 1993) and grown in minimal media plus casamino acids and 200 μg/ml ampicillin at 30 or 37°C. Just before induction, cells were centrifuged and resuspended in media containing fresh ampicillin and 1–10 mM isopropyl-β-D-thiogalactopyranoside. Cells were centrifuged and resuspended in 6 M guanidine for purification on Probond resin, according to the manufacturer's instructions (Invitrogen, San Diego, CA). MPP4 that was not fused to protein 10 HIS was isolated from bacterial inclusion bodies, purified by SDS-PAGE, and electroluted from gel slices.

Production of Antisera

Guinea pigs were injected intramuscularly and subcutaneously with bacterially expressed MPP proteins in Freund's complete adjuvant and boosted five times with MPP proteins in Freund's incomplete adjuvant. Terminal bleeds were by cardiac puncture 7–10 d after the final injection. For each protein, antisera were generated in two guinea pigs, and for all of the MPPs except MPP9, antisera from both animals gave similar immunofluorescent patterns. For MPP9, antibodies from one of the animals were reactive almost exclusively with protein 10. Antibodies were purified on affinity columns containing fusion proteins (1 mg/ml) coupled to cyanogen bromide-activated Sepharose CL4 beads (Pharmacia, Piscataway, NJ), as described by the manufacturer. One-half milliliter aliquots of antisera were bound to 1–2 ml of beads and eluted with 3 M potassium thiocyanate, 0.5 M NH_4OH, 5 mg/ml bovine serum albumin, or 4.9 M $MgCl_2$. For some experiments, antisera were passed over beads containing a heterologous protein 10 fusion protein to remove cross-reacting antibodies before purification on homologous protein 10 fusion protein beads.

Immunoprecipitation

HeLa S3 cells were grown as spinner cultures in Joklik's media containing 10% equine serum. M phase cells (85–98%, as determined by staining with lacto-orcein) were produced by treating exponentially growing cultures with 0.1 μg/ml nocodazole for 18–24 h. Most of the immunoprecipitations were performed by lysing cells at a concentration of 10^7 per milliliter in high-salt RIPA, which contained 50 mM Tris-HCl pH 8.0, 500 mM NaCl, 1% Triton X-100, 0.1% SDS, 0.5% sodium deoxycholate, 2 mM phenylmethylsulfonyl fluoride (PMSF), 10 μg/ml aprotinin, 10 μg/ml leupeptin, 10 μg/ml pepstatin, 10 mM EDTA, 10 mM ethylene glycol bis(β-aminoethyl)ether-*N,N,N',N'*-tetra-acetic acid (EGTA), 10 mM benzamidine, 10 mM tosylarginyl methyl ester (TAME), 50 mM NaF, 10 mM tetrasodium pyrophosphate, 1 mM sodium orthovanadate, 80 mM β-glycerophosphate, and 500 nM to 5 μM microcystin LR. Others were performed by first lysing cells in hot 50 mM Tris-HCl, pH 7.4, 0.4% SDS, 10 mM EDTA, 10 mM EGTA, 10 mM benzamidine, 50 mM NaF, 10 mM tetrasodium pyrophosphate, 1 mM sodium orthovanadate, 10 mM TAME, and 80 mM β-glycerophosphate and then adding appropriate stock solutions to yield final concentrations of 2% Triton X-100, 2 mM PMSF, 10 μg/ml aprotinin, 10 μg/ml leupeptin, 10 μg/ml pepstatin, and 2–5 μM microcystin LR. Lysates were centrifuged at 100,000 × *g* and 20–40 μg of antibody cross-linked to cyanogen bromide-activated Sepharose CL4B, or protein A Sepharose 6 MB was added to 10^7 or 10^8 cell equivalents of lysate. After a 2 h to overnight incubation at 4°C, beads were washed three times with immunoprecipitation buffer, and bound protein was eluted with SDS sample buffer. In some experiments, after washing with immunoprecipitation buffer, the beads were further washed with 40 mM 1,4-piperazinediethanesulfonic acid (PIPES) buffer, pH 6.0, and incubated with 0.2 U of potato acid phosphatase in the same buffer for 15–60 min before addition of SDS sample buffer.

Immunoblotting

Proteins were separated by SDS-PAGE, blotted to supported nitrocellulose in 50 mM Tris, 380 mM glycine, 0.3% SDS, and 20% methanol or Immobilon-P in 25 mM Tris, 180 mM glycine, reacted with primary antibodies overnight at 4°C, reacted with secondary antibodies conjugated to horseradish peroxidase for 1–2 h, and detected by enhanced chemiluminescence reagents (Amersham, Arlington Heights, IL).

Immunofluorescence

HeLa, CV1, or mycNAGT I HeLa (Nilsson *et al.*, 1993) cells were grown on coverslips in DMEM plus 10% fetal bovine serum and nonessential amino acids (plus 450 μg/ml Geneticin for the mycNAGT I HeLa cells) and fixed in methanol at −20°C for 10 min or in 4% formaldehyde, PBS, and 1 mM $MgCl_2$ at room temperature for 6–30 min, followed by permeabilization with 0.2% Triton X-100, PBS. Generally, formaldehyde and methanol fixations gave similar results, and, therefore, results of only one fixation, the one that gave the strongest antibody reaction or best preserved the structures stained by the antibody, are shown. Fixed cells were blocked with 0.2% gelatin in PBS and incubated with primary antibodies (2–10 μg/ml) for 1–2 h at room temperature or overnight at 4°C. After washing, cells were incubated with cyanine3-labeled donkey anti-guinea pig (Jackson ImmunoResearch, West Grove, PA) for 30 min to 2 h at room temperature, stained with 1 μg/ml Hoechst 33258, and mounted in PBS, 50% glycerol, or MOWIOL. For double immunofluorescence with anti-myc (mouse) or MPM2 (mouse), cells were incubated with the two primary antibodies, followed by both secondary antibodies (cya3-labeled donkey anti-guinea pig and fluorescein-labeled donkey anti-mouse). For double immunofluorescence with anti-MPP7 and anti-BrdU (bromodeoxyuridine), rapidly growing, unsynchronized cells were incubated for 10 min with 10 μM BrdU, fixed with formaldehyde, and stained as described above with anti-MPP7 and cyanine3-labeled anti-guinea pig. Then cells were again fixed with formaldehyde for 6 min, treated with 4 N HCl for 10 min, washed with PBS, and stained with fluorescein-labeled anti-BrdU (Becton Dickinson, San Jose, CA).

Fractionation

HeLa S3 cells (exponentially growing and nocodazole-arrested M phase) grown as for immunoprecipitations were harvested by centrifugation, washed with 10 mM HEPES, pH 7.4, 10 mM KCl, 150 mM NaCl, 1.5 mM $MgCl_2$, and lysed by nitrogen cavitation in two pellet volumes of 10 mM HEPES, pH 7.4, 10 mM KCl, 250 mM sucrose, 2 mM $MgCl_2$, 5 μM microcystin LR, 2 mM PMSF, 10 μg/ml leupeptin, 10 μg/ml pepstatin, 10 mM TAME, 10 mM benzamidine, 5 μM E-64, 1 mM EDTA, and 10 μg/ml aprotinin. Cell lysates were loaded onto 30% sucrose and centrifuged at 800 × *g* to obtain the nuclear pellet. The nuclear-free lysate above the 30% sucrose layer was collected, and part of it was centrifuged at 39,000 rpm in a Beckman Ti70 rotor for 1 h to obtain cytosol and crude high-speed pellets. The remaining portion was brought to 1.4 M sucrose, layered underneath 0.25 M sucrose, and centrifuged at 25,000 rpm in a Beckman SW28 rotor for 1.5 h. The membrane fraction at the interface between the two layers was collected, diluted to 0.25 sucrose, and centrifuged at 39,000 rpm in a Beckman Ti70 rotor for 1 h. Portions of the membrane pellets were further fractionated by resuspension at 2 mg/ml in 0.5 M NaCl or 0.1 M NaOH and 1 mM DTT, incubation on ice for 15 min, and centrifugation at 70,000 rpm in a Beckman TLA rotor for 30 min. Samples of unfractionated cell extract, nuclear pellet, cytosol, crude high-speed pellet, gradient pellet, and membranes containing 25 μg protein and the supernatants and pellets from salt and alkaline fractionation of 25 μg of membranes were subjected to SDS-PAGE and immunoblot procedures.

RESULTS

Expression Screening Isolates cDNAs for MPM2-reactive Phosphoproteins

We improved our previous protocol (Westendorf *et al.*, 1994) for isolating cDNAs encoding MPM2-reactive phosphoproteins (MPPs) by using microcystin LR as phosphatase inhibitor during phosphorylation of phage plaque proteins with M phase cell extracts. In addition, we improved the accessibility of protein kinase substrates bound to nitrocellulose by pretreatment of filters with denaturing solutions of guanidine hydrochloride. This permitted us to isolate a total of 30 cDNA clones (Tables 1 and 2). Cross-hybridization experiments and the sequences of the 5′ and 3′ termini of each clone indicated that we have isolated cDNAs for 16 different mRNAs. Ten of these encoded previously undescribed proteins, MPP 1–2, and MPP 4–11 (Table 1), which we further characterized in this study. The other six sequences encoded known proteins (Table 2: casein kinase II β-subunit, ribosomal protein L18a, and the 33-kDa laminin binding protein) or did not clearly encode any human protein (Table 2: 3′ noncoding sequences of cofilin; X-1, which encodes a partial open reading frame (ORF) of 226 amino acids with 39% identity to a segment of *Escherichia coli* DNA helicase II and may be of bacterial origin; and X-2, an uncharacterized sequence containing many *Eco*RI sites). Further sequencing of the clones for MPPs 4–11 indicated that the predicted protein sequences of all MPPs except MPP8 have one or more 5-amino-acid strings that correspond to sequences previously shown to be reactive with MPM2 (Table 3; Westendorf *et al.*, 1994). This finding strengthens our method for cloning MPM2-reactive phosphoproteins and the sequence that we have determined for binding of MPM2.

To study further the 10 previously undescribed proteins, we made T7 protein 10 fusion proteins, most of which contained a six histidine tag, to allow easy purification on a metal chelate column. As shown in Figure 1 and previously described for MPP1 and MPP2 fusion proteins (Westendorf *et al.*, 1994), all of the fusion proteins were at least partially degraded owing to their extreme sensitivity to proteolysis. Nev-

Table 1. Characteristics of cDNA clones for MPPs 1–2 and 4–11

MPP	Library[a]	Clone	Length cDNA (bp)	A tail?	5′stop before ORF?	Amount of protein encoded by ORF (kDa)	Size HeLa protein (by IP)	Intracellular localization, interphase	Intracellular localization, M phase
1	HeLa λZap	6-1	2565	no	no	66	220	cytoplasmic foci and cytoplasm	cytoplasmic foci and cytoplasm
2	MOLT4λgt11	5-3	1659	yes	no	24	120	nucleus	mitotic centrosomes and spindle, cytoplasmic foci, and cytoplasm
4	HeLa λZap	4-3	2042	no	yes	66	90, 110	nucleus and nucleolus	cytoplasm
	HeLa λZap	5-1	1386	no	yes	48			
	MOLT4λgt11	14	1373	no	yes	43			
5	MOLT4λgt11	3	687	no	no	12	130	cytoplasmic foci, cytoplasm, and nucleus	cytoplasmic foci and cytoplasm
6	MOLT4λgt11	6	1017	yes	no	20	17	nucleus and nucleolus	cytoplasm
		13	1099	yes	no	20			
7	MOLT4λgt11	7	2200 (744)[b]	yes[b]	no	9	75	centers of DNA replication, nucleus	cytoplasm
8	MOLT4λgt11	8	918	no	no	35	130	nucleus	cytoplasm
9	MOLT4λgt11	9	925	yes	no	24	150, 160	Golgi	cytoplasm
10	MOLT4λgt11	2	2130	yes	no	78	120	nucleolus	perichromosomal plaques
11	MOLT4λgt11	14	1859	yes	no	67	130	cytoplasmic foci, cytoplasm, and nucleus	cytoplasmic foci and cytoplasm

[a] The origins of cDNA libraries: HeLa λZap, Drs. Helena Richardson and Steven Reed; MOLT4λgt11, Dr. Kevin Sullivan.

[b] The first "A tail" occurs after nucleotide 744 of the clone.

Table 2. Characteristics of other cDNAs whose encoded proteins become MPM2 antigens

Protein	Library[a]	Clone	Length cDNA (bp)	Portion of Protein Encoded
Casein Kinase II β (regulatory) subunit[c] (242aa)	MOLT4λgt11	4	1200	aa −42 to 242[d]
ribosomal protein L18a[e] (175aa)	MOLT4λgt11	5	300	aa 121 to 175
laminin binding protein[f] (295aa)	MOLT4λgt11	1-1	345	aa 222 to 295
	MOLT4λgt11	1-2	200	ND[b]
	MOLT4λgt11	2-1	312	aa 223 to 295
	MOLT4λgt11	3-1	679	aa 105 to 295
	MOLT4λgt11	4-1	342	aa 222 to 295
	MOLT4λgt11	5-2	448	aa 177 to 295
	MOLT4λgt11	9-1	349	aa 221 to 295
3′ noncoding sequence of cofilin[g] (166 aa)	MOLT4λgt11	1	550	63nt beyond aa166 codon to A tail
	MOLT4λgt11	10	650	aa 160 to A tail
	MOLT4λgt11	11	500	123 nt beyond aa166 codon to A tail
	MOLT4λgt11	12	450	126 nt beyond aa166 codon to A tail
X-1[h]	HeLa λgt11	4	2284	226 C terminal aa
		3	1835	222 C terminal aa
		16	2260	218 C terminal aa
X-2	HeLa λZap	4-2	3000	ND[b]

[a] The origins of cDNA libraries: HeLa λZap, Drs. Helena Richardson and Steven Reed; MOLT4λgt11, Dr. Kevin Sullivan; HeLa λgt11, Clontech.

[b] The cDNA sequence was not determined. Laminin binding protein clone 1-2 was identified by cross-hybridization with the other clones. Clone 4-2 did not hybridize with any other isolated clones.

[c] A. Voss, U. Wirkner, R. Jacobi, N. Hewitt, C. Schwager, J. Zimmermann, W. Ansorge, and W. Pyerin (1991). Structure of the gene encoding human casein kinase II subunit beta. J. Biol. Chem. *266*, 13706–13711.

[d] The 126 nt of 5′ "noncoding" sequence contain no inframe stop codons.

[e] Y. Aoyama, Y.-L. Chan, O. Meyuhas, and I.G. Wool. (1989). The primary structure of rat ribosomal protein L18a. FEBS Lett. *247*, 242–246.

[f] H. Yow, J.M. Wong, H.S. Chen, C. Lee, G.D. Steele, Jr., and L.B. Chen. (1988). Increased mRNA expression of a laminin-binding protein in human colon carcinoma: complete sequence of a full-length cDNA encoding the protein. Proc. Natl. Acad. Sci. USA *85*, 6394–6398.

[g] K. Ogawa, M. Tashima, Y. Yumoto, T. Okuda, H. Sawada, M. Okuma, and Y. Maruyama. (1990). Coding sequence of human placental cofilin cDNA. Nucleic Acids Res. *18*, 7169.

[h] The X1 clones contain two apparent ORFs in one cDNA. The first ORF contains 2 regions with 94% (18 of 19 amino acids) and 100% (9 of 9 amino acids) identity to replicative protein motifs V and VI, respectively. T.C. Hodgman. (1988). A new superfamily of replicative proteins. Nature *333*, 22–23; the second has 39% identity with *E. coli*. DNA ligase. The presence of two ORFs in a cDNA of eukaryotic origin is an uncommon occurrence and suggests that these clones may be bacterial contaminants of the HeLa cDNA library. The accession number for X-1 is X98266.

ertheless, if the largest fusion protein band is compared with the size of the T7 protein 10 fusion partner (40 kDa), the sequences contained in the cDNA clones are found to code for ~10-110 kDa of MPP protein (Figure 1). For most of the clones, the apparent amount of protein mass present in the fusion protein is almost the same as that derived from the predicted amino acid sequence (Figure 1 and Table 1). For MPP10, by contrast, there seems to be substantially more protein mass in the fusion protein (130 kDa) than would be predicted from the sequence (78–5 kDa not included in fusion protein + 40 kDa protein 10 = 113 kDa). This could be due to anomalous migration of a highly charged protein. Purified fusion proteins for MPPs 1–2 and 4–11 were injected into guinea pigs to generate antisera, all of which were purified on MPP fusion protein affinity columns for use in the following experiments.

Each MPP cDNA Encodes a Human Protein(s) of a Characteristic Size(s)

To determine the molecular size of the proteins in cells, we immunoprecipitated lysates of 10^7 to 10^8 exponentially growing HeLa cells with each anti-MPP and reacted immunoblots of the immunoprecipitates with homologous antibodies (Figure 2). The blots indicate that the MPPs are HeLa cell proteins of various sizes from 17,000 to 220,000 Da. Their molecular sizes are MPP1, 220,000; MPP2, 120,000; MPP4, 90,000 and 110,000; MPP5, 130,000; MPP6, 17,000 (and, possibly, a minor high molecular weight species); MPP7, 75,000;

Table 3. Potential MPM2 binding sites in MPPs 1 to 2 and 4 to 11.

cDNA Clone	Potential MPM2 sites–TP	Potential MPM2 sites–SP
MPP1	FT_{374}PLQ*	HS_{486}PSI
	TT_{390}PVT*	SS_{533}PID
	AT_{421}PRT	
MPP2	KT_{58}PIK	FS_{96}PVQ*
	ST_{69}PSK	ES_{130}PQP*
	RT_{78}PES	SS_{151}PSD
	LT_{85}PPA*	GS_{162}PEP
	TT_{120}PLQ*	
MPP4	IT_{368}PMK*	TS_{173}PVV
	ST_{504}PSA	KS_{382}PSK
	DT_{596}PLA	
MPP5	ET_{51}PRQ	PS_{65}PLQ*
		AS_{78}PVV
		VS_{92}PWP*
MPP6	IT_{158}PIK*	
MPP7	TT_{23}PRR	GS_{65}PPE
	LT_{30}PLK*	
	DT_{36}PPS	
	ST_{48}PST	
	ET_{58}PGD	
MPP8	KT_{107}PRK	DS_{45}PFP
	QT_{158}PKG	
	LT_{227}PEE	
MPP9	LT_{11}PVT*	ST_{2}PTK
	VT_{130}PQG	YS_{18}PKR
	QT_{185}PQI	RS_{22}PKE
		LS_{28}PGF
		SS_{41}PIR
		PS_{171}PGG
MPP10		GS_{52}PLQ
		KS_{154}PVF*
MPP11	FT_{197}PVF*	
	AT_{500}PSE	
	FT_{513}PWT*	
	NT_{534}PER	

Amino acid numbering begins with the first 5′ inframe amino acid coded for all clones except MPP4, which contains a stop codon before the open reading frame and is numbered from the start methionine. All TP and SP sites within each protein are listed.

* Starred sequences are identical to or closely resemble sequences previously shown to be reactive with MPM2 in that each of the five positions in the string contains an amino acid previously identified in the corresponding position of MPM2-reactive sequences (Westendorf *et al.*, 1994). MPM2 binding at any site also depends on phosphorylation on the T or S and the number of reactive sites within the protein. The accession numbers for the cDNAs are as follows: MPP1, L16782; MPP2, L16783; MPP4, X98264 (clones 14 and 5-1) and X98265 (clone 4-3); MPP5, X98261; MPP6, X98263; MPP7, X98262; MPP8, X98259; MPP9, X98258; MPP10, X98494; and MPP11, X98260.

MPP8, 70,000 and 130,000; MPP9, 150,000 and 160,000; MPP10, 120,000; MPP11, 130,000. The multiple molecular species recognized by antibodies to MPPs 4, 8, and 9 could be due to the existence of multiple genes, alternatively spliced mRNAs, proteolysis (despite the use of many protease inhibitors), or various phosphorylation states. For MPP8, the 70-kDa species is never seen in immunoblots of total cell lysates and is likely

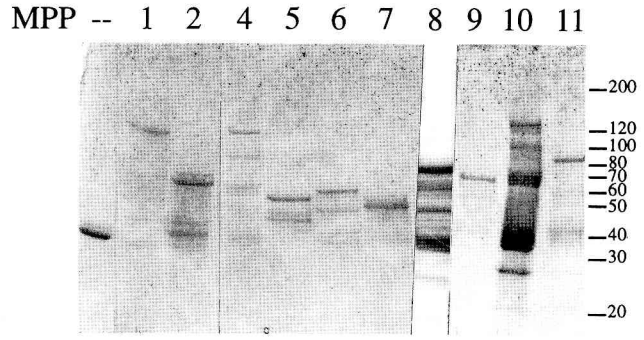

Figure 1. Fusion proteins for cloned MPPs. Fusion proteins produced and purified as discussed in MATERIALS AND METHODS were subjected to electrophoresis on an SDS gel and stained with Coomassie blue. The far left lane contains protein 10 not fused with an MPP protein. The other lanes contain the protein 10 fusion protein for the indicated MPP. Migration of molecular weight markers in kDa is indicated on the right.

to be a proteolytic product of full-length MPP8. For MPP4 and MPP9, phosphorylation is apparently not responsible for multiple molecular species, because dephosphorylation of protein from exponentially growing cells with a phosphatase of broad specificity (potato acid phosphatase) does not change the sizes of the two proteins (MPP4, our unpublished observations; MPP9, Figure 3). The reported molecular weights of all HeLa cell MPPs, which, like their bacterial fusion proteins, are very sensitive to proteolytic degradation, will be reassessed when full-length sequences for each protein are known.

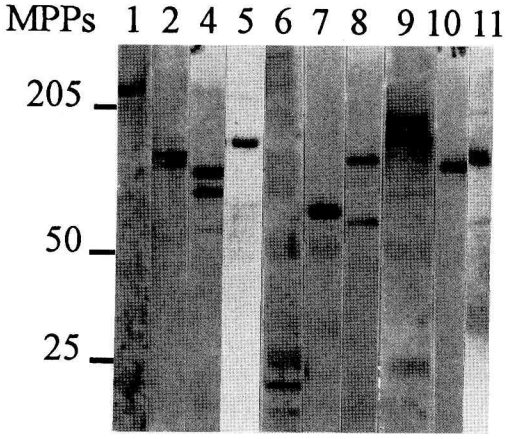

Figure 2. Immunoprecipitation of MPPs from extracts of exponentially growing HeLa cells. MPPs were immunoprecipitated with affinity-purified antibodies from lysates of exponentially growing HeLa cells in high-salt RIPA buffer. Lane, antibody, and cell equivalents: 1, αMPP1, 10^8; 2, αMPP2, 10^7; 3, αMPP4, 10^8; 4, αMPP5, 10^8; 5, αMPP6, 10^8; 6, αMPP7, 10^8; 7, αMPP8, 10^7; 8, αMPP9, 10^8; 9, αMPP10, 10^7; 10, αMPP11, 10^8. In the MPP8 precipitate, the 70-kDa band is apparently an artifact of immunoprecipitation, because it is never seen in immunoblots of whole-cell extracts. Migration of molecular weight markers in kDa is indicated on the left.

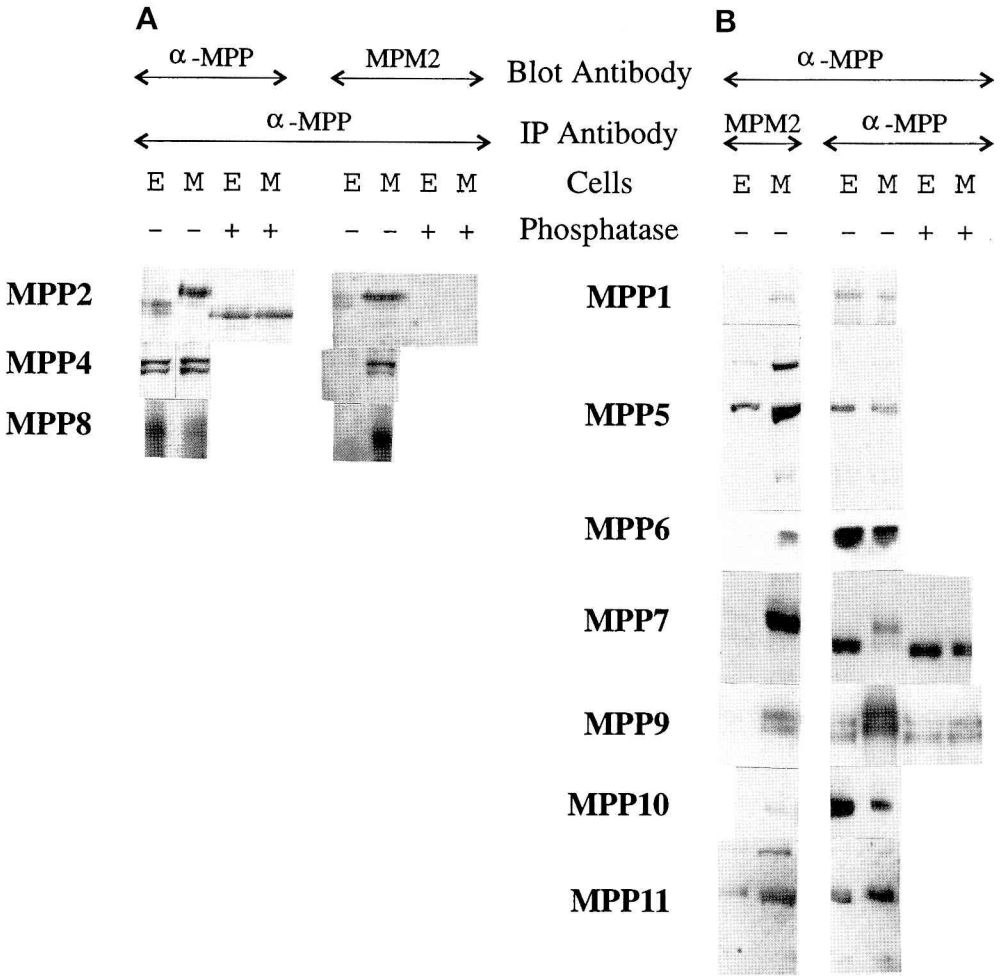

Figure 3. MPM2 reactivity of MPPs immunoprecipitated from extracts of HeLa cells. (A) MPPs were immunoprecipitated (IP) from lysates of exponentially growing (E) or M phase (M) HeLa cells with MPM2 or antibodies directed against an MPP (α-MPP). Immunoprecipitated proteins were separated by SDS-PAGE, and immunoblots were reacted with the α-MPP indicated at the left. (B) MPPs immunoprecipitated with α-MPP as described above were separated by SDS-PAGE, and immunoblots were incubated with MPM2 or the α-MPP indicated at the left. (A and B) When the protein from M phase cells was larger than the protein from exponentially growing cells (MPP2, MPP7, and MPP9), immunoprecipitation pellets were treated with a broad specificity phosphatase, as described in MATERIALS AND METHODS, before addition of SDS sample buffer.

Each MPP Is Reactive with MPM2 in M Phase

To learn whether the proteins encoded by the cDNAs were MPM2-reactive phosphoproteins in vivo, we performed one of the two following types of experiments. In the first type of experiment, MPP proteins were immunoprecipitated from exponentially growing and M phase cells with MPP antibodies. Then, one-half of the resulting immunoprecipitates were immunoblotted with MPP antibodies and the other one-half with MPM2 (Figure 3A). The MPM2 reactivity of MPPs 2, 4, and 8 could be visualized clearly with this procedure. For each of these MPPs, the respective anti-MPP reacted approximately equally well with the MPP precipitated from exponentially growing and M phase cells, whereas MPM2 reacted much more strongly with the MPP precipitated from M phase cells. The other MPPs could not be clearly visualized with MPM2 by this protocol, possibly because they are dephosphorylated in cell lysates even in the presence of phosphatase inhibitors, or of too low abundance to be detected with MPM2 after precipitation with anti-MPP. Therefore, a second procedure was used to analyze their reactivity with MPM2 during M phase. Proteins were immunoprecipitated from lysates of exponentially growing or M phase cells with MPM2 or MPP antibodies and detected on immunoblots with antibodies against MPPs (Figure 3B). For each of these MPPs the anti-MPP precipitates from exponentially growing and M phase cells were approximately equally reactive with the respective anti-MPP on immunoblots. In contrast, the MPM2 precipitates from M phase cells were more strongly reactive with anti-MPP than those from exponentially growing cells. Thus, the results of these experiments indicate that all the MPPs are immunoreactive with MPM2 in M phase cells.

For most of the MPPs, the gel mobilities of the polypeptides from exponentially growing and M phase cells (including the MPM2-reactive species) are indistinguishable (Figure 3). Nevertheless, in M phase cells compared with exponentially growing cells, the gel mobilities of MPP2, MPP7, and MPP9 are substantially decreased, and these slowly migrating forms of the proteins are MPM2-reactive (Figure 3). For MPP2 and MPP9, the shifts are equivalent to ~20 kDa; for

MPP7, the observed shift is variable, but in some of our unpublished observations the shift is as much as 90 kDa. These mobility changes can be reversed by treatment with a broad specificity phosphatase (potato acid phosphatase), which also destroys reactivity with MPM2 (Figure 3). All detectable molecules of MPP2, MPP7, and MPP9 are shifted in mobility, indicating that phosphorylation in M phase is quantitative. Interestingly, MPP2 also seems to be phosphorylated in interphase, because a small shift in size of the interphase protein is seen after dephosphorylation. In addition, immunoprecipitation with MPM2 permits detection of additional protein species of 50,000, 65,000, and 200,000 daltons for MPP5 and of 80,000 and 200,000 daltons for MPP11. The origin of these other anti-MPP–reactive protein species for MPPs 5 and 11 is uncertain, but some could be due to proteolysis and dephosphorylation artifacts.

Although all the MPPs are reactive with MPM2 in M phase, they differ in the strength of reactivity with MPM2 and the conditions required for maintaining MPM2 reactivity. For instance, most of the MPPs react with MPM2 only in M phase, but MPP5 and MPP11 also react more weakly with MPM2 in interphase (Figure 3). Also, MPP6, which contains only one potential MPM2 site, was found to be an MPM2 antigen only when precipitated from a cell lysate containing 5 μM microcystin LR, whereas MPP2, which contains nine potential sites, was an MPM2 antigen when precipitated from lysates containing only 500 nM microcystin LR (Figure 3; our unpublished observations). Further, MPP10, which contains only S-P, as opposed to T-P, sites was less strongly reactive with MPM2 than most of the other MPPs, possibly because MPM2 reacts more strongly with T-P sites than S-P sites (Zhao *et al.*, 1989; Westendorf *et al.*, 1994).

Each MPP Is Localized to Characteristic Cell Structures

When MPP proteins were studied by immunofluorescence microscopy, a diverse range of localization patterns was obtained. For each protein, similar results were obtained with HeLa (human) and CV1 (African green monkey) cells. The antibody staining patterns were also confirmed by preincubation with protein 10 alone, which did not alter the staining, or protein 10-MPP fusion protein, which diminished or abolished staining.

Antibodies to MPPs 1, 2, 5, and 11 all recognize some punctate cytoplasmic foci as well as diffuse staining during at least part of the cell cycle. Anti-MPP1 labeled punctate cytoplasmic foci in both interphase and mitotic cells (Figure 4). In mitotic cells, the staining was concentrated near the mitotic spindle (Figure 4) and, in some interphase cells, the centrosomes (our unpublished observations). In both interphase and mitotic cells, MPP5 and MPP11 were distributed throughout the cell, including the nuclei, in fine punctate foci (Figure 4). In some mitotic cells, MPP5 and MPP11 seemed to be associated with the mitotic spindle.

MPP2 was localized throughout the nucleus except for the nucleoli in interphase (Figure 4). The nuclear localization of MPP2 was difficult to preserve in fixed cells and was obtained only after lengthy fixation with paraformaldehyde. After fixation with methanol or shorter fixations with paraformaldehyde, anti-MPP2 yielded punctate cytoplasmic labeling. A nuclear localization of MPP2 in interphase was consistent with the results of our subcellular fractionation experiments. In cells entering M phase, some MPP2 became concentrated at centrosomes (Figure 4; white arrows in MPP2 interphase panel), and in later stages of M phase, MPP2 was present at the centrosome, in the spindle, and in punctate foci throughout the cell.

MPP4, MPP6, MPP8, and MPP10 were localized to the nucleus in interphase (Figure 5). MPP4 and MPP6 were distributed throughout the nucleus and showed a modest concentration in nucleoli, whereas MPP8 was excluded from the nucleoli, and MPP10 was almost entirely nucleolar. In mitosis, MPP10 adhered to the chromosomes in a manner similar to the nucleolar protein fibrillarin (Yasuda and Maul, 1990); in contrast, MPP4, MPP6, and MPP8 were present throughout the mitotic cell (Figure 5).

MPP7 was localized to distinct spots within the nuclei of some cells and was diffusely localized throughout the nuclei of other cells (Figures 6 and 7). During M phase it was distributed throughout the cells (our unpublished data). When centers of DNA replication were labeled by a 10-min treatment with bromodeoxyuridine, which incorporates into DNA that is being synthesized, and were detected with antibodies to bromodeoxyuridine, the MPP7 spots corresponded exactly to the positions in which DNA was being replicated (Figure 6). Because MPM2 also stains spots within the nucleus (Vandre *et al.*, 1984), it was of interest to know whether the MPM2 reactivity of interphase nuclei was due to MPP7 present in DNA replication centers. Double immunofluorescence with MPM2 and MPP7, however, indicates that the MPM2 and MPP7 spots are not the same (Figure 7). Furthermore, whereas the MPP7 spots are present only in S phase cells, the MPM2 spots are present in all interphase cells. Apparently, the MPP7 associated with centers of DNA replication is not the predominant source of interphase nuclear MPM2 reactivity. This observation is also supported by the data in Figure 3, indicating that MPP7 is not an MPM2 antigen of exponentially growing (92–97% interphase) cells.

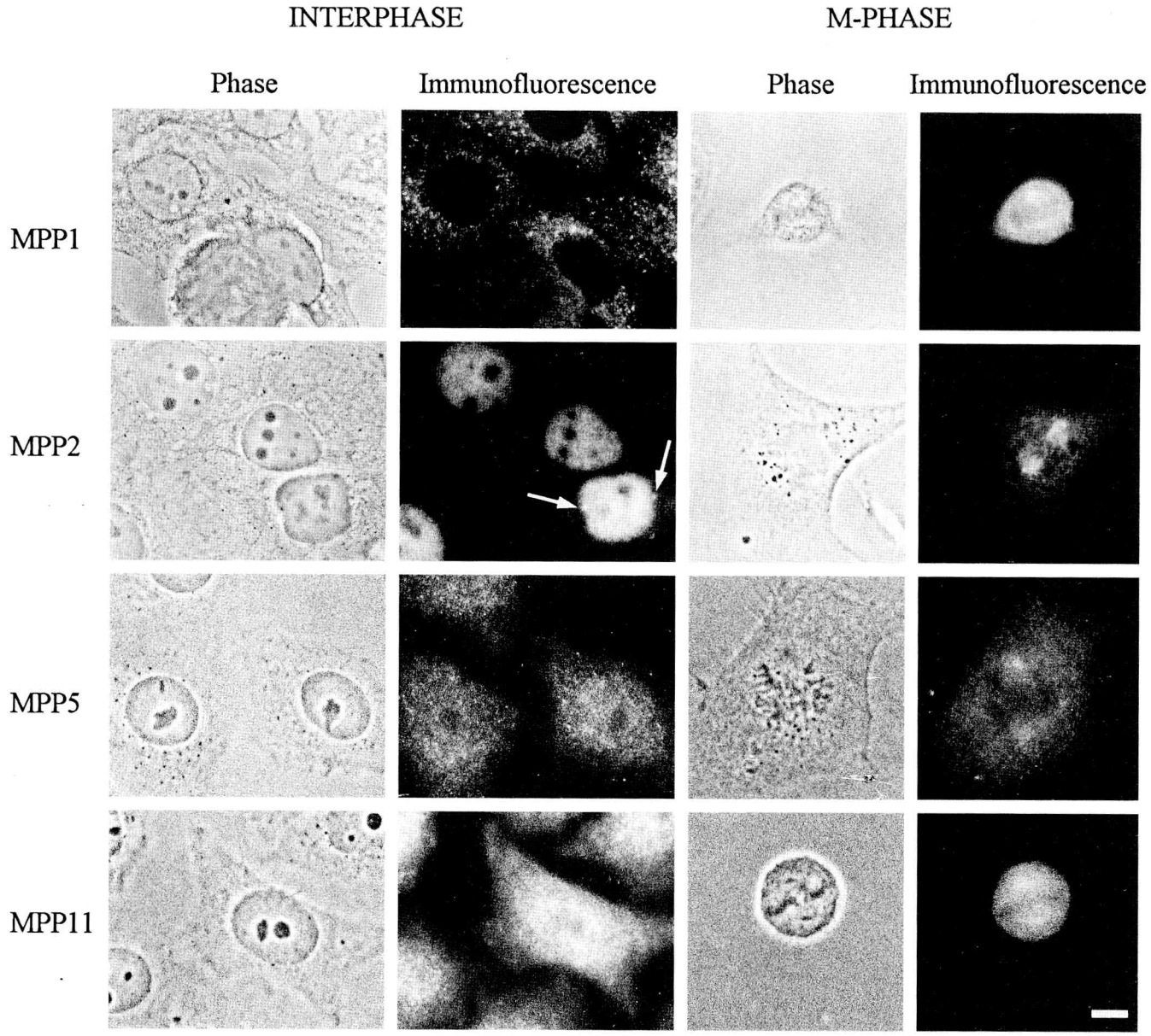

Figure 4. Immunofluorescent localizations of MPP1, MPP2, MPP5, and MPP11. Cells (HeLa or CV1) were grown on coverslips, fixed with formaldehyde, and stained as described in MATERIALS AND METHODS. Antiserum, Interphase (I) or M phase (M), and cell line: αMPP1, I, HeLa; αMPP1, M, CV1; αMPP2, I, CV1; αMPP2, M, CV1; αMPP5, I, HeLa; αMPP5, M, CV1; αMPP11, I, HeLa; and αMPP11, M, HeLa. The arrows in the αMPP2 interphase panel indicate αMPP2-staining centrosomes of a prophase cell. The location of the centrosomes was confirmed by double immunofluorescence staining with anti-tubulin. Bar, 2 μ.

In interphase, much of the HeLa cell MPP9 was localized to the Golgi complex (Figure 8). When compared with the localization of myc-tagged *N*-acetylglucosaminyl transferase I (NAGT I; Nilsson *et al.*, 1993), a transmembrane protein of the medial Golgi, MPP9 staining was found to overlap strongly with that of NAGT I. In cell fractionation experiments designed to confirm the localization of MPP9 to membranes, MPP9 was found in membrane fractions from which it was partially released by 0.5 M NaCl and totally removed by 0.1 M NaOH. These characteristics indicate that MPP9 is a peripheral membrane protein. There was also cytoplasmic background staining with anti-MPP9; this was probably due to the presence of some MPP9 in the cytosol as was observed in cell fractionation experiments. In mitosis, MPP9 was dispersed throughout the cell and did not localize to the Golgi fragments containing NAGT I (Figure 8).

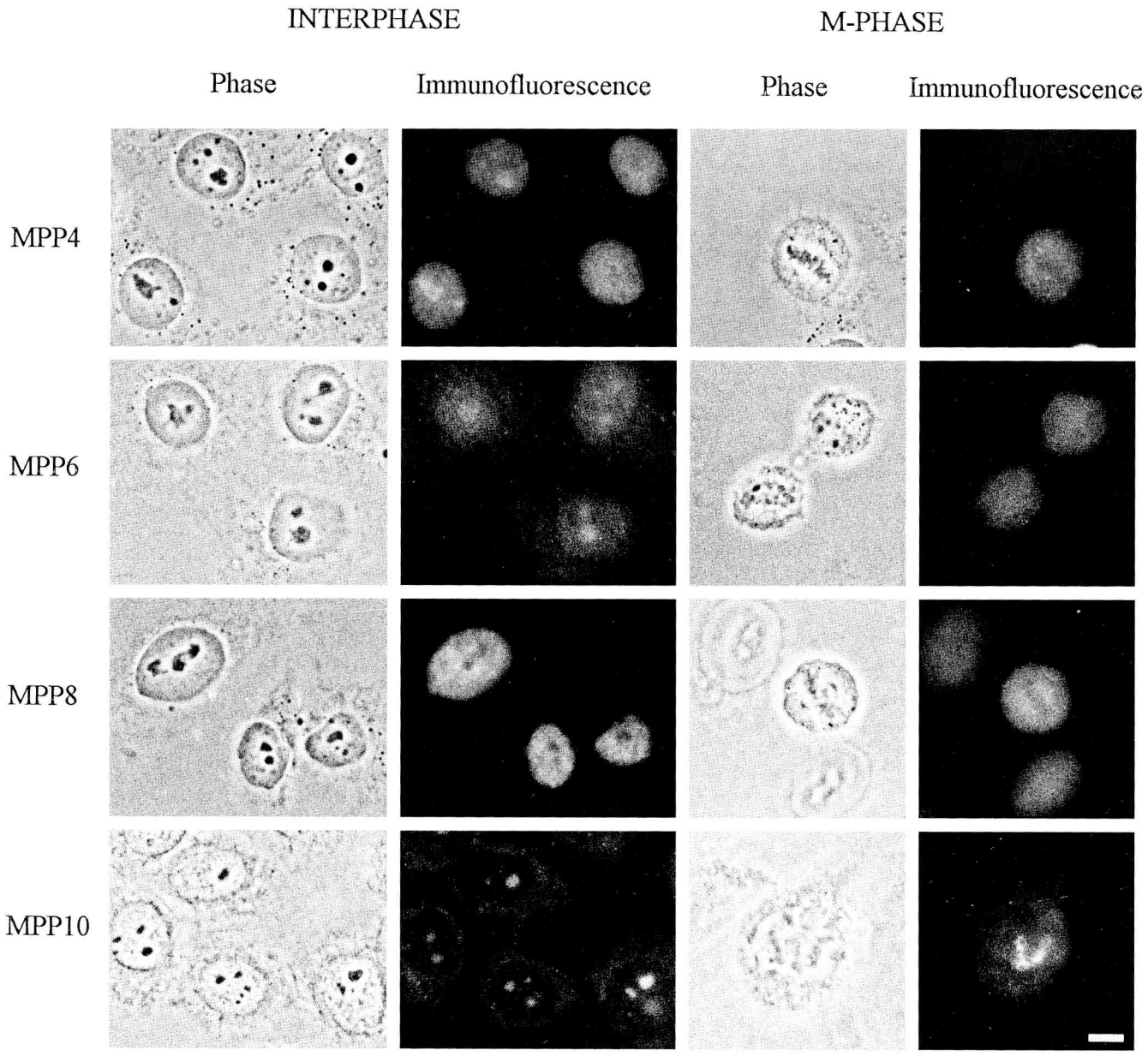

Figure 5. Immunofluorescent localizations of MPP4, MPP6, MPP8, and MPP10. HeLa cells were grown on coverslips, fixed with formaldehyde (Form) or methanol (Meth), and stained as described in MATERIALS AND METHODS. Antiserum, Interphase (I) or M phase (M), and fixation: αMPP4, I, Form; αMPP4, M, Form; αMPP6, I, Form; αMPP6, M, Form; αMPP8, I, Form; αMPP8, M, Form; αMPP10, I, Meth; and αMPP10, M, Meth. Bar, 2 μ.

DISCUSSION

Using our recently developed technique for isolation of proteins containing the phosphoepitope bound by MPM2, we have successfully isolated cDNAs for eight additional proteins (MPPs 4–11). After production of antibodies to protein fragments encoded by these cDNA clones and two previously isolated clones (for MPPs 1–2) (Westendorf *et al.*, 1994), we detect one or two major polypeptides for each MPP in HeLa cell lysates. Moreover, when each MPP protein is immunoprecipitated from extracts of M phase HeLa cells, the protein in the precipitate reacts with MPM2. This reactivity indicates that the MPPs are M phase phosphoproteins as well as MPM2-reactive phosphoproteins and demonstrates that our method is capable of isolating genuine M phase phosphoproteins.

Immunofluorescence microscopy indicates that each MPP has a characteristic pattern of localization. In

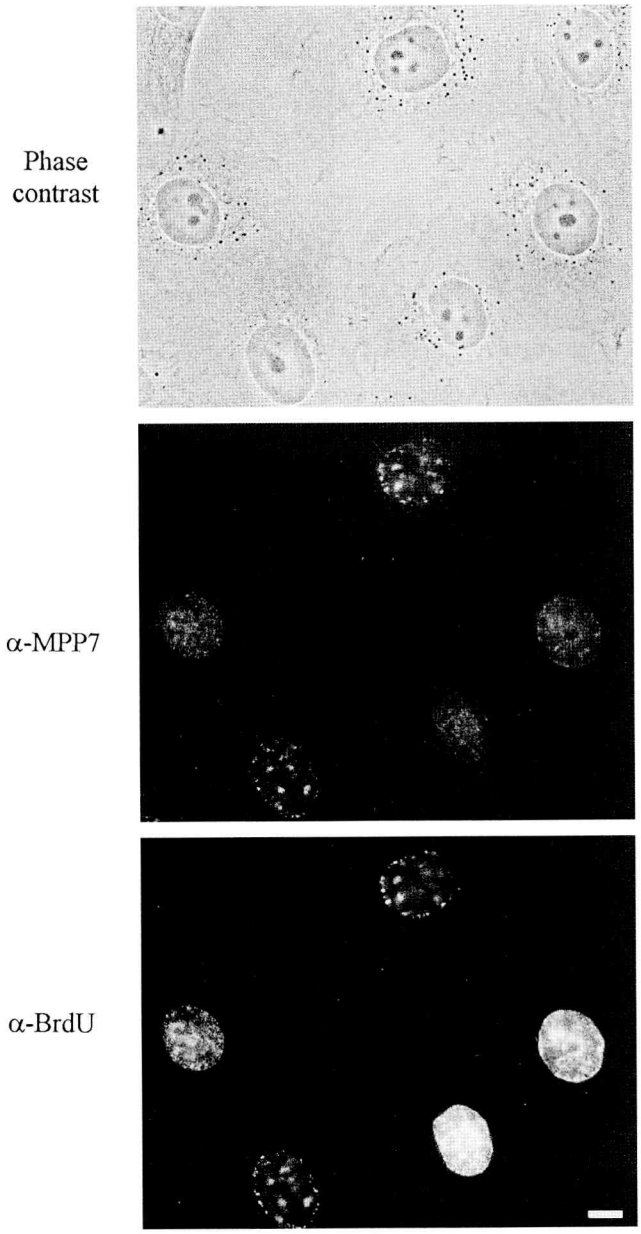

Figure 6. Immunofluorescent localization of MPP7 to centers of DNA replication. HeLa cells grown on coverslips were incubated with BrdU for 10 min and stained with anti-MPP7 and anti-BrdU as described in MATERIALS AND METHODS. Bar, 2 μ.

interphase, MPPs are present in the cytoplasm, the nucleus, the nucleolus, the centers of DNA replication, and the Golgi apparatus. In mitosis, as expected from the pattern of immunofluorescence seen with MPM2, most of the MPPs are spread throughout the cell, in some cases in punctate foci. Nonetheless, MPP2 may account for some of the MPM2 immunofluorescence associated with the centrosome and MPP10 for some of the chromosomal immunofluorescence. Therefore, the MPPs that we have isolated have the properties expected of MPM2-reactive M phase phosphoproteins, and their localization to various cell structures suggests that they will provide clues about how several cell structures and processes are regulated during mitosis.

Although the characterization of the MPPs has been performed almost entirely in HeLa cells, which were derived from a cervical carcinoma, and CV1 cells, a nontransformed kidney epithelial cell line, most of the MPPs are probably not confined to cells of epithelial origin. cDNAs encoding MPPs 2 and 4–11 were isolated from a cDNA library derived from MOLT4 lymphoblastic leukemia cells (Table 1). This limited survey of cell lines suggests that the MPPs are present in rapidly growing cells of various origins. Further characterization of the MPPs in other normal and transformed cells will be necessary to have a clear understanding of the relationship of each to cell growth and differentiation.

The localization of each MPP provides broad hints about its specific interphase function and how that might be altered in M phase. For instance, MPPs 4, 6, 8, and 10 are nuclear during interphase. Phosphorylation in M phase may turn off their nuclear functions to prevent inappropriate interactions with non-nuclear proteins. Alternatively, M phase phosphorylation might confer an M phase-specific function on these proteins.

Four of the MPPs—MPP1, MPP2, MPP5, and MPP11— are associated with punctate foci that are dispersed throughout the cell. Because these MPPs sometimes localize to centrosomes or the mitotic spindle, some of the structures seen as punctate foci may have a microtubule-related function. Currently, we are investigating the nature and activity of these structures.

The localizations of MPP7 and MPP9 point to functions within specific cell structures. MPP9, which localizes to the Golgi apparatus, may regulate Golgi structure or function. MPP7 is localized to centers of DNA replication during S phase and, therefore, is suggested to have a role in that process. Consistent with this localization, the sequence of MPP7 is identical to a subunit of a chromatin assembly factor essential for incorporation of histones into newly synthesized DNA (Kaufman *et al.*, 1995). Our data indicate further that this complex is appropriately localized to centers of DNA replication and is phosphorylated at mitosis.

While this manuscript was in preparation, a protein sequence 94% identical to MPP11 was deposited in the database. This protein, MIDA1, is related to the yeast Z-DNA binding protein zuotin and associates with the transcription factor Id (Shoji *et al.*, 1995). The migration of MIDA1 at 74 kDa on gels corresponds well with the predicted size of MIDA1 but contrasts with the migration of HeLa MPP11 on gels (130 kDa). This discrepancy could be due to an N terminal extension,

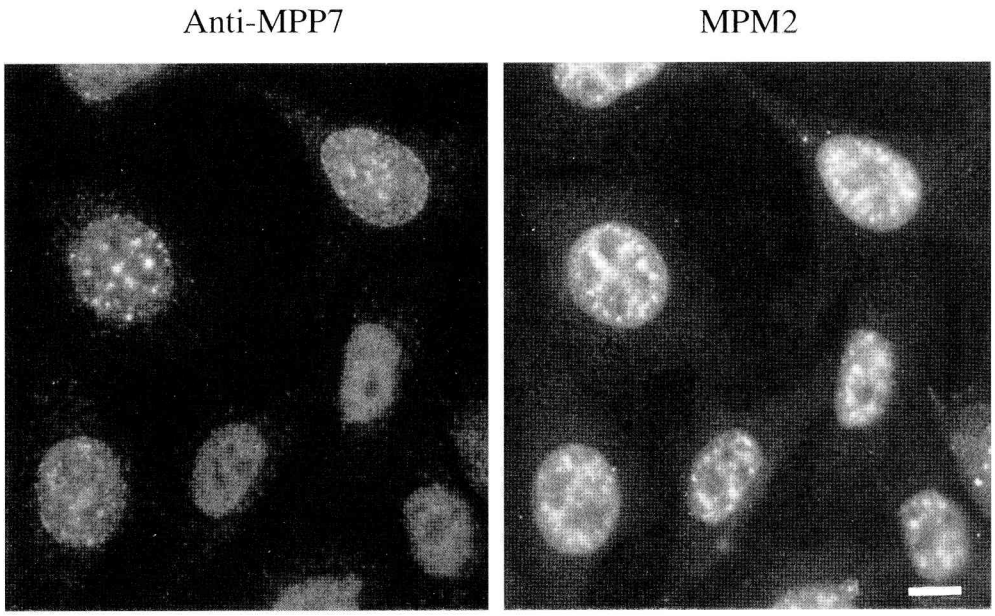

Figure 7. Comparison of MPP7 and MPM2 nuclear immunofluorescence. HeLa cells grown on coverslips were fixed with formaldehyde and stained with anti-MPP7 and MPM2 as described in MATERIALS AND METHODS. Bar, 2 μ.

anomalous migration, or phosphorylation of the human protein.

MPP4 is the human homologue of a previously described *Xenopus* double-stranded RNA binding protein whose function is unknown (Bass *et al.*, 1994). Our data indicate that this protein is also present in human cells, in which it is localized to the nucleus and undergoes phosphorylation in M phase.

Other than MPPs 4, 7, and 11, the sequences of the MPP cDNAs have not provided much information about the functions of the proteins. Further study of the MPPs will require full-length cDNA clones and their encoded protein sequences, which may also provide more clues about their functions.

We have previously defined the phosphorylation site for MPM2 to be a set of related phosphorylation sites, including F-phosphoT-P-L-Q (Westendorf *et al.*, 1994). The sequence of each of the MPPs except MPP8 contains at least one site corresponding to our previous description of potential MPM2 binding sites. MPP8 does, however, have four sequences with the central T/S-P of the MPM2 motif. Because many related peptide sequences are able to bind MPM2 and our previous selection of peptides capable of binding to MPM2 was not exhaustive, it is likely that at least one of the T/S-P sites of MPP8 will, when phosphorylated, bind to MPM2. Recently, a site for MPM2 binding that does not contain a proline has been described in MAP kinase (Taagepera *et al.*, 1994). A sequence corresponding to this site is not found in MPP8 or any of the MPPs. Interestingly, the corresponding site in MAP kinase of neuronal cells does contain a proline (Mohit *et al.*, 1995). If the secondary structure, possibly a beta turn, of this key regulatory site of MAP kinase is conserved, it may be that the MPM2-reactive site of MAP kinase is not really so different from the sites found in other MPM2-reactive proteins. Like the site in MAP kinase, MPM2-reactive phosphorylation sites of MPPs may be responsible for alterations of activity during M phase. Further biochemical studies will be needed to define the precise sites that are phosphorylated in these proteins during M phase and which of these are essential for MPM2 binding and, importantly, alterations of function.

In our screening efforts, we also isolated cDNAs for three known proteins. Interestingly, one of them is the casein kinase II β (regulatory) subunit, which previously has been shown to be phosphorylated during mitosis (Litchfield *et al.*, 1992). This further confirms the validity of our method for identification of mitotic phosphoproteins and indicates that casein kinase II may be part of the cascade of activation of protein kinases that occurs during mitosis. We do not know the significance of the isolations of cDNAs for ribosomal protein L18a or "laminin-binding protein," two proteins associated with ribosomes (Aoyama *et al.*, 1989; Auth and Brawerman, 1992). If these proteins are phosphorylated in vivo, phosphorylation could regulate the amount or kinds of proteins that are synthesized. As yet, we have no evidence that these two proteins are, indeed, phosphorylated in cells. The portion of the laminin-binding protein that is contained in our clones does not have a sequence corresponding to any previously defined M phase MPM2 binding site (Taagepera *et al.*, 1994; Westendorf *et al.*, 1994). Furthermore, it contains no central T/S-P motifs, but, like the MAP kinase site, the site in laminin-binding protein does not seem to be M phase-specific; laminin

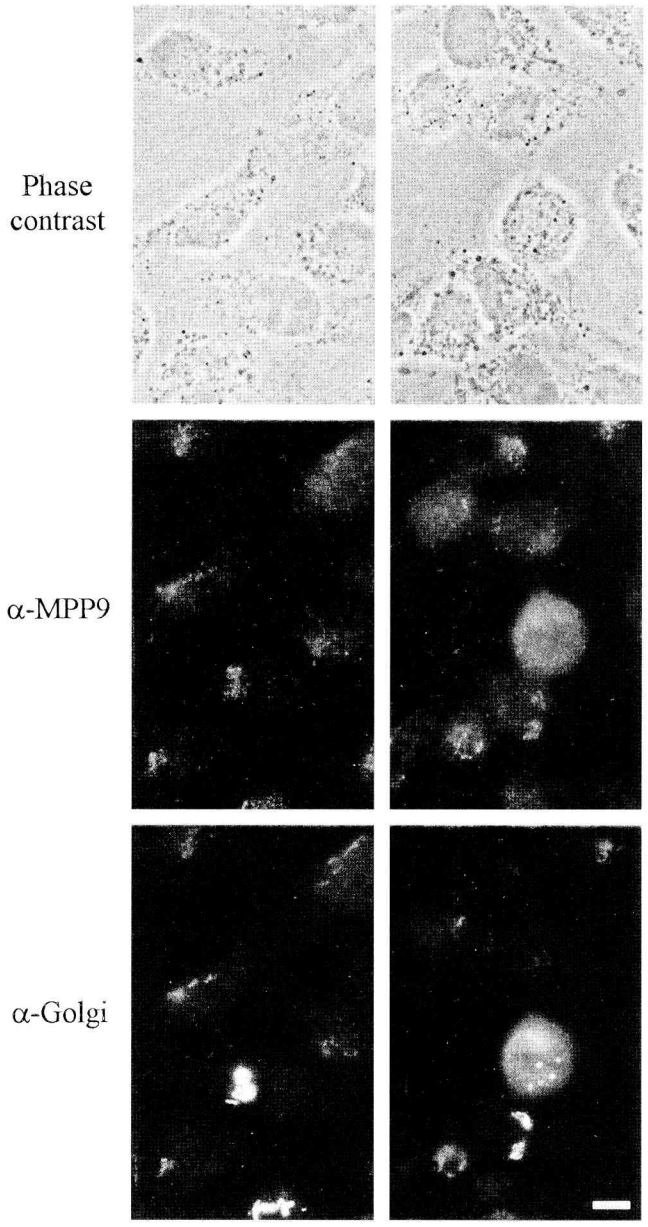

Figure 8. Immunofluorescent localization of MPP9 to the Golgi apparatus. HeLa mycNAGT I cells (Nilsson *et al.*, 1993) were grown on coverslips, fixed with formaldehyde, and stained with anti-MPP9 and anti-myc as described in MATERIALS AND METHODS. Bar, 2 μ.

binding protein fusion protein is phosphorylated to acquire MPM2 reactivity equally well by interphase and M phase extracts of HeLa cells (our unpublished observations). Perhaps the phosphorylation site of laminin-binding protein has a secondary structure similar to that of the proline-containing sites.

So far, four or five kinases have been shown to phosphorylate substrates on sites that, when phosphorylated, become MPM2 antigens. We have shown previously that MPP1 and MPP2 are phosphorylated primarily by different kinases of M phase extracts. For MPP1, the primary kinase seems to be $p34^{cdc2}$, whereas for MPP2, it is another, uncharacterized kinase. By phosphorylating *Xenopus* antigens on blots, Kuang and Ashorn (1993) have isolated two kinases, MAP kinase and a second, novel kinase, that yield MPM2 reactivity. One of these two kinases might be the major kinase that phosphorylates MPP2. In addition, working with MAP kinase as substrate, Tagepera *et al.* (1994) have shown that the activity of MAP kinase kinase can lead to MPM2 reactivity. This kinase may, however, phosphorylate only MAP kinase and no other substrates. The other MPPs, whose kinases have not yet been examined, will also be useful for examining the specificity of various M phase kinases and possibly purifying novel kinases. Likewise, the MPPs will be useful for identifying phosphatases involved in exit from M phase.

In conclusion, our results indicate that a broad range of M phase phosphoproteins can be identified by our expression cloning method. We are now in a position to study the functions of the MPPs that we have characterized in interphase and M phase and discover their roles in the process of cell division.

ACKNOWLEDGMENTS

We thank Dr. Didier Job, in whose laboratory the final experiments of this study were performed, for his generous support. We thank the following for materials: Drs. Jian Kuang and Potu Rao for the MPM2 antibody, Drs. Helena Richardson and Steven Reed for the HeLa λZap cDNA library, Dr. Kevin Sullivan for the λgt11 MOLT4 library, Drs. Dalia Resnitzky and Steven Reed for BrdU and anti-BrdU, and Drs. William Balch and Graham Warren for the mycNAGT I cells. We acknowledge the excellent technical assistance of Mona Razik and Lisa Cunningham. This work was supported by a grant from the National Institutes of Health (PO-46006) to L.G. We also gratefully acknowledge support from the G. Harold and Leila Y. Mathers Charitable Foundation. J.M.W. was supported by fellowships from the National Institutes of Health, the Association pour la Recherche sur la Cancer, and the Fondation pour la Recherche Médicale. F.P. was supported by Institut National de la Santé et de la Recherche Médicale (INSERM) and additional funding from the Association pour la Recherche sur la Cancer and the Fondation pour la Recherche Médicale. This work was also supported by INSERM funds awarded to Dr. Didier Job.

REFERENCES

Aoyama, Y., Chan, Y.-L., Meyuhas, O., and Wool, I.G. (1989). The primary structure of rat ribosomal protein L18a. FEBS Lett. *247*, 242–246.

Auth, D., and Brawerman, G. (1992). A 33-kDa polypeptide with homology to the laminin receptor: component of translation machinery. Proc. Natl. Acad. Sci. USA *89*, 4368–4372.

Bass, B.L., Hurst, S.R., and Singer, J.D. (1994). Binding properties of newly identified *Xenopus* proteins containing dsRNA-binding motifs. Curr. Biol. *4*, 301–314.

Centonze, V.E., and Borisy, G.G. (1990). Nucleation of microtubules from mitotic centrosomes is modulated by a phosphorylated epitope. J. Cell Sci. *95*, 405–411.

Coleman, T.R., and Dunphy, W.G. (1994). Cdc2 regulatory factors. Curr. Opin. Cell Biol. *6*, 877–882.

Davis, F.M., and Rao, P.N. (1987). Antibodies to mitosis-specific phosphoproteins. In: Molecular Regulation of Nuclear Events in Mitosis and Meiosis, ed. R.A. Schlegel, M.S. Halleck, and P.N. Rao, New York: Academic Press, 259–293.

Davis, F.M., Tsao, T.Y., Fowler, S.K., and Rao, P.N. (1983). Monoclonal antibodies to mitotic cells. Proc. Natl. Acad. Sci. USA *80*, 2926–2930.

Draetta, G.F. (1994). Mammalian G1 cyclins. Curr. Opin. Cell Biol. *6*, 842–846.

Draetta, G., Luca, F., Westendorf, J., Brizuela, L., Ruderman, J., and Beach, D. (1989). Cdc2 protein kinase is complexed with both cyclin A and B: evidence for proteolytic inactivation of MPF. Cell *56*, 829–838.

Dunphy, W.G., Brizuela, L., Beach, D., and Newport, J. (1988). The *Xenopus cdc2* protein is a component of MPF, a cytoplasmic regulator of mitosis. Cell *54*, 423–431.

Elledge, S.J., and Harper, J.W. (1994). Cdk inhibitors: on the threshold of checkpoints and development. Curr. Opin. Cell Biol. *6*, 847–852.

Gautier, J., Minshull, J., Lohka, M., Glotzer, M., Hunt, T., and Maller, J.L. (1990). Cyclin is a component of MPF from *Xenopus*. Cell *60*, 487–494.

Gautier, J., Norbury, C., Lohka, M., Nurse, P., and Maller, J. (1988). Purified maturation-promoting factor contains the product of a *Xenopus* homolog of the fission yeast cell-cycle control gene $cdc2^+$. Cell *54*, 433–439.

Glass, C.A., Glass, J.R., Taniura, H., Hasel, K.W., Blevitt, J.M., and Gerace, L. (1993). The alpha-helical rod domain of human lamins A and C contains a chromatin binding site. EMBO J. *12*, 4413–4424.

Heichman, K.A., and Roberts, J.M. (1994). Rules to replicate by. Cell *79*, 557–562.

Hirano, T., and Mitchison, T.J. (1991). Cell-cycle control of higher order chromatin assembly around naked DNA in vitro. J. Cell Biol. *115*, 1479–1489.

Hunt, T., and Sherr, C.J. (1994). Cell multiplication. Editorial overview: checks and balances. Curr. Opin. Cell Biol. *6*, 833–835.

Hunter, T., and Pines, J. (1994). Cyclins and cancer II: cyclin D and CDK inhibitors come of age. Cell *79*, 573–582.

Karsenti, E., Bravo, R., and Kirschner, M. (1987). Phosphorylation changes associated with the early cell cycle in *Xenopus* eggs. Dev. Biol. *119*, 442–453.

Kaufman, P.D., Kobayashi, R., Kessler, N., and Stillman, B. (1995). The p150 and p60 subunits of chromatin assembly factor I: a molecular link between newly synthesized histones and DNA replication. Cell *81*, 1105–1114.

King, R.W., Jackson, P.K., and Kirschner, M.W. (1994). Mitosis in transition. Cell *79*, 563–571.

King, R.W., Peters, J.-M., Tugendreich, S., Rolfe, M., Hieter, P., and Kirschner, M.W. (1995). A 20S complex containing CDC27 and CDC16 catalyzes the mitosis-specific conjugation of ubiquitin to cyclin B. Cell *81*, 2279–2288.

Kuang, J., and Ashorn, C. (1993). At least two kinases phosphorylate the MPM-2 epitope during *Xenopus* oocyte maturation. J. Cell Biol. *123*, 859–868.

Kuang, J., Ashorn, C.L., Gonzalez-Kuyvenhoven, M., and Penkala, J.E. (1994). cdc25 is one of the MPM-2 antigens involved in the activation of maturation-promoting factor. Mol. Biol. Cell *5*, 135–145.

Kuang, J., Zhao, J.Y., Wright, D.A., Saunders, G.F., and Rao, P.N. (1989). Mitosis-specific monoclonal antibody MPM-2 inhibits *Xenopus* oocyte maturation and depletes maturation-promoting activity. Proc. Natl. Acad. Sci. USA *86*, 4982–4986.

Labbé, J.-C., Capony, J.P., Caput, D., Cavadore, J.-C., Derancourt, J., Kaghdad, M., Lelias, J.-M., Picard, A., and Dorée, M. (1989). MPF from starfish oocytes at first meiotic metaphase is a heterodimer containing one molecule of cdc2 and one molecule of cyclin B. EMBO J. *8*, 3053–3058.

Litchfield, D.W., Lüscher, B., Lozeman, F.J., Eisenman, R.N., and Krebs, E.G. (1992). Phosphorylation of casein kinase II by p34cdc2 in vitro and at mitosis. J. Biol. Chem. *267*, 13943–13951.

Lohka, M.J., Kyes, J.L., and Maller, J.L. (1987). Metaphase protein phosphorylation in *Xenopus laevis* eggs. Mol. Cell. Biol. *7*, 760–768.

Maller, J., Wu, M., and Gerhart, J.C. (1977). Changes in protein phosphorylation accompanying maturation of *Xenopus laevis* oocytes. Dev. Biol. *58*, 295–312.

Meijer, L., Arion, D., Golsteyn, R., Pines, J., Brizuela, L., Hunt, T., and Beach, D. (1989). Cyclin is a component of the sea urchin egg M phase-specific histone H1 kinase. EMBO J. *8*, 2275–2282.

Mohit, A.A., Martin, J.H., and Miller, C.A. (1995). P493F12 kinase: a novel MAP kinase expressed in a subset of neurons in the human nervous system. Neuron *14*, 67–78.

Mueller, P.R., Coleman, T.R., and Dunphy, W.G. (1995). Cell-cycle regulation of a *Xenopus* wee1-like kinase. Mol. Biol. Cell *6*, 119–134.

Nilsson, T., Pypaert, M., Hoe, M.H., Slusarewicz, P., Berger, E.G., and Warren, G. (1993). Overlapping distribution of two glycosyltransferases in the Golgi apparatus of HeLa cells. J. Cell Biol. *120*, 5–13.

Nurse, P. (1994). Ordering S phase and M phase in the cell cycle. Cell *79*, 547–550.

O'Connell, M.J., and Nurse, P. (1994). How cells know they are in G1 or G2. Curr. Opin. Cell Biol. *6*, 867–871.

Sambrook, J., Fritsch, E.F., and Maniatis, T. (1989). Molecular Cloning, A Laboratory Manual, Cold Spring Harbor, NY: Cold Spring Harbor Laboratory Press.

Sherr, C.J. (1994). G1 phase progression: cycling on cue. Cell *79*, 551–555.

Shoji, W., Inoue, T., Yamamoto, T., and Obinata, M. (1995). MIDA1, a protein associated with Id, regulates cell growth. J. Biol. Chem. *270*, 24818–24825.

Taagepera, S., Dent, P., Her, J.-H., Sturgill, T.W., and Gorbsky, G.J. (1994). The MPM-2 antibody inhibits mitogen-activated protein kinase activity by binding to an epitope containing phosphothreonine-183. Mol. Biol. Cell *5*, 1243–1251.

Taagepera, S., Rao, P.N., Drake, F.H., and Gorbsky, G.J. (1993). DNA topoisomerase II alpha is the major chromosome protein recognized by the mitotic phosphoprotein antibody MPM-2. Proc. Natl. Acad. Sci. USA *90*, 8407–8411.

Vandre, D.D., Centonze, V.E., Peloquin, J., Tombes, R.M., and Borisy, G.G. (1991). Proteins of the mammalian mitotic spindles: phosphorylation/dephosphorylation of MAP-4 during mitosis. J. Cell Sci. *98*, 577–588.

Vandre, D.D., Davis, F.M., Rao, P.N., and Borisy, G.G. (1984). Phosphoproteins are components of mitotic microtubule organizing centers. Proc. Natl. Acad. Sci. USA *81*, 4439–4443.

Westendorf, J.M., Rao, P.N., and Gerace, L. (1994). Cloning of cDNAs for M phase phosphoproteins recognized by the MPM2 monoclonal antibody and determination of the phosphorylated epitope. Proc. Natl. Acad. Sci. USA *91*, 714–718.

Yasuda, Y., and Maul, G.G. (1990). A nucleolar auto-antigen is part of a major chromosomal surface component. Chromosoma *99*, 152–160.

Ye, X.S., Xu, G., Pu, R.T., Fincher, R.R., McGuire, S.L., Osmani, A.H., and Osmani, S.A. (1995). The NIMA protein kinase is hyperphosphorylated and activated downstream of $p34^{cdc2}$/cyclin B: coordination of two mitosis-promoting kinases. EMBO J. *14*, 986–994.

Zhao, J.-Y., Kuang, J., Adlakha, R.C., and Rao, P.N. (1989). Threonine phosphorylation is associated with mitosis in HeLa cells. FEBS Lett. *249*, 389–395.

Journal of Neurochemistry
Raven Press, Ltd., New York

参考論文

Different Natures of Supersensitivity of Adenylate Cyclase Stimulated by Calcitonin Gene-Related Peptide and Isoproterenol in Rat Diaphragm After Denervation and Reserpine Treatment

Naoko Matsumoto, Xiao-Bing Wang, and Shuji Uchida

Department of Pharmacology I, Osaka University School of Medicine, Osaka, Japan

Abstract: In skeletal muscles, calcitonin gene-related peptide (CGRP) released from motor nerve terminals and humoral catecholamines stimulate adenylate cyclase (AC) and enhance muscle contraction. The effects of denervation and treatment with reserpine on twitch contraction and the AC system in rat diaphragm were investigated. The basal levels of twitch contraction and AC activity of the diaphragm of rats were both increased 2 weeks after phrenic nerve denervation but were not altered by treatment with reserpine. Reserpine treatment provoked supersensitivity of AC to isoproterenol, without affecting the response to CGRP. On the other hand, denervation decreased the activation of AC and enhancement of twitch contraction by CGRP, without affecting the responses to isoproterenol. These data suggest that denervation causes up-regulation of AC as a result of loss of CGRP release from nerve terminal and that depletion of catecholamines by reserpine treatment supersensitizes the responses at the β-adrenoceptor level. Thus, nervous and humoral factors regulate the AC system in striated muscle by different mechanisms. **Key Words:** Calcitonin gene-related peptide—Striated muscle—Adenylate cyclase—Denervation—Reserpinization. **Matsumoto N. et al.** Different natures of supersensitivity of adenylate cyclase stimulated by calcitonin gene-related peptide and isoproterenol in rat diaphragm after denervation and reserpine treatment. *J. Neurochem.* **58,** 357–361 (1992).

Adrenergic stimulation influences several metabolic and physiological processes in skeletal muscle, including glycogenolysis (Gross and Mayer, 1975), Na^+,K^+ transport (Hays et al., 1974), and twitch contraction (Bowman and Nott, 1969). β-Adrenoceptors, located on the plasma membranes of skeletal muscle (Reddy and Engel, 1979), are coupled with adenylate cyclase (AC) through activation of stimulatory guanine nucleotide-binding regulatory protein (G_s) (Smith, 1984). This system is thought to be driven by humoral catecholamines.

Calcitonin gene-related peptide (CGRP), a peptide consisting of 37 amino acids, is widely distributed in the CNS and the PNS. In striated muscle, CGRP enhances the rate of desensitization of nicotinic acetylcholine (ACh) receptors (Mulle et al., 1988) through activation of AC. Among its long-term actions are an increase in the number of ACh receptors (Fontaine et al., 1986; New and Mudge, 1986) and a suppression of the sprouting of motor nerve terminals induced by chronic blockade of nerve–muscle activity (Tsujimoto and Kuno, 1988). This peptide was shown to colocalize with ACh in motor nerve terminals (Takami et al., 1985*a*). In murine phrenic nerve–hemidiaphragm preparations, CGRP increased the twitch contraction induced by nerve or transmural stimulation in a dose-dependent manner (Takami et al., 1985*b*; Kobayashi et al., 1987; Ohhashi and Jacobowitz, 1988). Electrical stimulation of the phrenic nerve caused release of a CGRP-like immunoreactive substance and an increase in cyclic AMP content in rat phrenic nerve–diaphragm preparations (Uchida et al., 1990). These reports sup-

Received January 3, 1991; revised manuscript received May 16, 1991; accepted June 13, 1991.

Address correspondence and reprint requests to Dr. S. Uchida at Department of Pharmacology I, Osaka University School of Medicine, 2-2, Yamada-Oka, Suita, Osaka 565, Japan.

The present address of Dr. N. Matsumoto is Osaka Research Laboratory, Sawai Pharmaceutical Co., Ltd., 8-14, Ikue, 1-chome, Asahi-ku, Osaka 535, Japan.

Abbreviations used: AC, adenylate cyclase; ACh, acetylcholine; CGRP, calcitonin gene-related peptide; EP, end-plate; G_s, stimulatory guanine nucleotide-binding regulatory protein; TME buffer, 10 m*M* Tris-maleate buffer (pH 7.4) containing 5 m*M* EDTA.

port the view that CGRP is a neuromodulater coexisting with ACh in nerve endings of phrenic nerve in this preparation.

Previously we demonstrated that denervation caused heterologous supersensitization of AC in rat gastrocnemius muscle (Hashimoto et al., 1989). We also showed that denervation increases the basal levels of contraction and AC activity but decreases enhancement of twitch contraction and AC by CGRP (Matsumoto et al., 1990). These observations are unique if the changes in AC on denervation are caused by disappearance of CGRP.

In the present study, we examined whether the AC system is regulated by nervous and humoral systems by similar or different mechanisms. For this purpose, we investigated the effects of denervation and reserpine treatment, which depletes storage pools of catecholamines, on twitch contraction and the AC system in rat diaphragm.

MATERIALS AND METHODS

Preparation

Male Sprague–Dawley rats, 6 weeks old and weighing 150–200 g, were used. The left hemidiaphragm was denervated by section of the left phrenic nerve at the level of CVI with the animal under pentobarbital anesthesia. Control rats were subjected to a sham operation. Half of each group of rats was then treated with reserpine (1 mg/kg) intraperitoneally once a day for 14 days, and the other half was treated with 0.9% NaCl. This treatment with reserpine is sufficient to deplete catecholamines from the tissue and to cause increased responsiveness to catecholamines (Fleming and Trendelenburg, 1961; Hawthorn and Broadley, 1982). After 2 weeks, the rats were killed by decapitation, and their left hemidiaphragms were used for experiments.

Measurement of twitch contraction

The phrenic nerve–left hemidiaphragm preparation was mounted in a 5-ml organ bath containing Krebs–Ringer bicarbonate solution at 37°C and continuously aerated with 5% CO_2 in O_2. A load (~0.5 g) was applied, and the strip was stimulated transmurally with rectangular pulses (0.25 Hz, 1 ms in duration, supramaximal voltage).

The twitch contraction was measured isometrically. When twitch responses became steady, the dose-dependent effects of rat CGRP and isoproterenol were examined by adding the compounds cumulatively. The changes in tension observed in experiments are expressed as percent increases in tension over that developed by electrical stimulation during the control period.

Preparation of membranes of striated muscle

Muscle of the left hemidiaphragm was excised, cut up with scissors, and homogenized for 30 s in a microhomogenizer in 10 volumes of cold 10 m*M* Tris-maleate buffer (pH 7.4) containing 5 m*M* EDTA (TME buffer). The homogenate was strained through nylon mesh and centrifuged twice for 10-min periods at 15,000 *g*. The pellets were suspended in a suitable volume of TME buffer at an appropriate concentration for AC assay.

The phrenic nerve–hemidiaphragm preparation was cut into 2-mm-wide strips from end to end along the region of nerve ending as end-plate (EP)-rich regions (Wessler and Kilbinger, 1986), and the other part of the left hemidiaphragm was used as the EP-free region. Membranes of these regions were prepared as described above.

Assay of AC

The AC activity in membranes of rat striated muscle was determined by measuring the synthesis of cyclic AMP from ATP in an incubation mixture containing 80 m*M* Tris-maleate (pH 7.4) buffer, 1 m*M* 3-isobutyl-1-methylxanthine, 0.5 μM GTP, 6 m*M* $MgSO_4$, 0.5 m*M* EGTA, 1.5 m*M* ATP, and 20 μg of membrane protein suspended in TME buffer, with the indicated concentration of rat CGRP or isoproterenol, in a total volume of 100 μl. The incubation mixture was preincubated for 2 min at 37°C, and then the reaction was started by addition of ATP with the indicated concentration of rat CGRP or isoproterenol. After 10 min, the reaction was stopped by addition of 25 μl of 0.5 *M* HCl and cooling. The mixture was centrifuged, and cyclic AMP in the supernatant was quantified by radioimmunoassay (Honma et al., 1977). Assays were performed in duplicate.

Protein content measurement

Protein content was determined by the method of Lowry et al. (1951) with bovine serum albumin as the standard.

Statistical analysis

Data are expressed as mean ± SEM values. Statistical analysis was carried out by Student's *t* test.

Materials

Synthetic rat CGRP was purchased from the Peptide Institute (Osaka, Japan). Apoplone (Daiichi Pharmaceuticals) was used as reserpine. A cyclic AMP assay kit was obtained from Yamasa Shouyu Co. (Chiba, Japan).

RESULTS

Twitch contractions on transmural stimulation of denervated and reserpinized diaphragm

On transmural stimulation in fixed conditions (pulse width of 1.0 ms and frequency of 0.25 Hz), the mean ± SEM tension developed was 40.4 ± 6.2 g/g of tissue. After denervation, the contraction force was increased about twofold, to 76.7 ± 4.9 g/g of tissue. On the other hand, treatment with reserpine for 2 weeks did not affect the contraction force of either normal (31.3 ± 1.0 g/g of tissue) or denervated (60.8 ± 6.1 g/g of tissue) muscle (Fig. 1).

Effects of CGRP and isoproterenol on twitch contraction in denervated and reserpinized diaphragm

CGRP enhanced the twitch contraction of normal muscle (maximal increase of ~20% at 1 μM). Denervation almost completely abolished the enhancement of twitch contraction by CGRP, but reserpine treatment did not alter the effect of CGRP significantly in either normal or denervated diaphragm (Fig. 2A).

Isoproterenol enhanced twitch contraction of denervated muscle and normal muscle similarly and dose

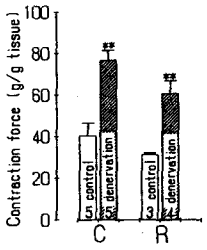

FIG. 1. Effects of denervation and reserpine treatment on twitch contraction. Twitch contraction by transmural stimulation was measured isometrically in diaphragms isolated from rats 14 days after phrenic nerve denervation or a sham operation and then daily treatment with reserpine (1 mg/kg) (R) or saline as a control (C). Contraction is expressed as force (g) per 1 g of tissue, measured isometrically. The numerals in the columns represent numbers of experiments. Data are mean ± SEM (bars) values. Results significantly different from the corresponding value for normal muscle are indicated: $^{**}p < 0.01$.

dependently (maximal increase of ~40% increase). In denervated, but not normal muscle, reserpine treatment shifted the dose–response curve of isoproterenol to the left (Fig. 2B).

Effects of CGRP and isoproterenol on AC activity in membranes

Denervation increased the basal activity of AC significantly from 2.66 ± 0.14 to 3.86 ± 0.3 pmol/mg of protein/min. Treatment with reserpine did not affect the basal activity of AC (Fig. 3).

CGRP activated AC dose-dependently in both normal and denervated muscle, but the activation was significantly less in denervated muscle (maximal increase of 81%) than in control muscle (maximal increase of 120%). Reserpine treatment had no effect on the activation of AC by CGRP (Fig. 4).

AC activation by isoproterenol was not affected significantly by denervation. Treatment with reserpine resulted in supersensitivity of the AC activity to isoproterenol: 10 μM isoproterenol increased the AC activity to 3.3-fold the basal level in untreated muscle and to 4.1-fold the basal level in reserpinized muscle (Fig. 4).

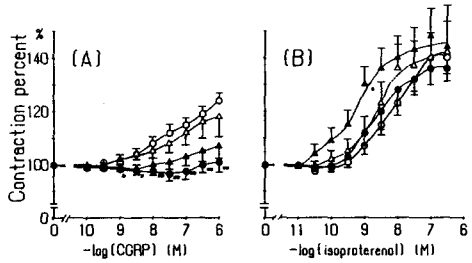

FIG. 2. Enhancement of twitch contraction by CGRP and isoproterenol in normal and denervated muscle with or without reserpine treatment. Data are expressed as percent increases in isometric tension induced by (**A**) CGRP or (**B**) isoproterenol over the basal level. Results are for normal (open symbols) and denervated (closed symbols) muscles, treated with saline as a control (circles; normal n = 8, denervated n = 12) or reserpine (triangles; normal n = 9, denervated n = 9). Data are mean ± SEM (bars) values. Results significantly different from the corresponding value for normal muscle are indicated: $^{*}p < 0.05$, $^{**}p < 0.01$.

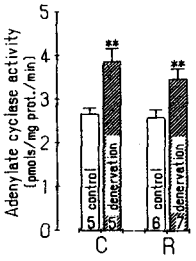

FIG. 3. Effects of denervation and reserpine treatment on basal activities of AC. Basal activities of AC were measured in membranes from normal and denervated muscles, treated with saline (C) or reserpine (R). The numerals in the columns represent numbers of experiments. Data are mean ± SEM (bars) values. Results significantly different from the corresponding value for normal muscle are indicated: $^{**}p < 0.01$.

AC activity in EP-rich and -free regions of diaphragm

The basal activities of AC in the EP-rich and -free regions were similar: 1.06 ± 0.23 and 1.17 ± 0.17 pmol/mg of protein/min, respectively. CGRP activated AC more in the EP-rich region (3.6-fold increase at 10 μM) than in the EP-free region (2.3-fold increase), but isoproterenol activated AC similarly in the two regions (5.4- and 5.9-fold, respectively) (Fig. 5).

After denervation, the basal levels of AC activity were similarly increased in the EP-rich (29% increase) and -free (33% increase) regions. The response of AC to CGRP in the EP-rich region decreased to the level in the EP-free region, and the latter did not change. On the other hand, the response of AC to isoproterenol was not changed by denervation in either region (Fig. 6).

DISCUSSION

In this work we demonstrated that denervation increased the basal levels of AC and twitch contraction and decreased the activation of AC and enhancement of twitch contraction by CGRP, without affecting the responses to isoproterenol. These results were essen-

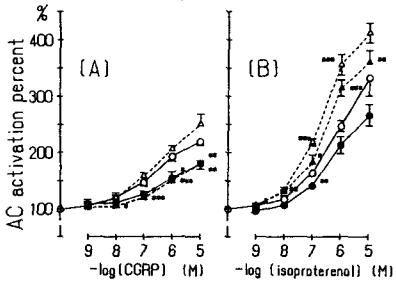

FIG. 4. Effects of CGRP and isoproterenol on AC activity in normal and denervated muscles, with and without reserpine treatment. Data are expressed as percent increases in AC activated by (**A**) CGRP or (**B**) isoproterenol over the basal level. Results are for normal (open symbols) and denervated (closed symbols) muscles, treated with saline (circles; normal n = 5, denervated n = 5) or reserpine (triangles; normal n = 6, denervated n = 7). Data are mean ± SEM (bars) values. Results significantly different from the corresponding value for normal muscle are indicated: $^{*}p < 0.05$, $^{**}p < 0.01$, $^{***}p < 0.001$. Results significantly different from the corresponding value for saline-treated muscle are also indicated: $^{\#}p < 0.05$, $^{\#\#}p < 0.01$, $^{\#\#\#}p < 0.001$.

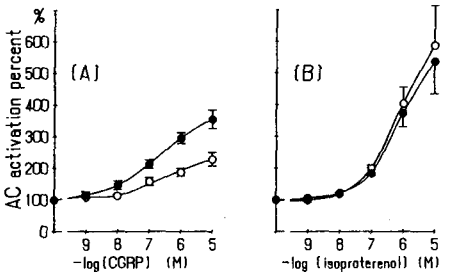

FIG. 5. Effects of CGRP and isoproterenol on AC activity in EP-free and -rich regions. Data are expressed as percent increases in AC activated by **(A)** CGRP or **(B)** isoproterenol over the basal level. The AC activities of membranes from the EP-free (○) and -rich (●) regions were measured. The basal AC activity was 1.17 ± 0.17 pmol/mg of protein in the EP-free region and 1.06 ± 0.23 pmol/mg of protein in the EP-rich region. Data are mean ± SEM (bars) values (n = 4).

tially consistent with our previous findings (Hashimoto et al., 1989; Matsumoto et al., 1990). On the other hand, reserpine treatment provoked supersensitivity of AC to a β-adrenergic agonist, without affecting the response to CGRP. However, it did not affect the basal levels of AC and twitch contraction.

These findings suggest that denervation caused up-regulation of the responses at the AC level, whereas reserpinization caused their up-regulation at the β-adrenoceptor level. We found previously that denervation of motor nerves caused nonspecific, not CGRP-specific, supersensitivity to AC in rat gastrocnemius muscle (Hashimoto et al., 1989) and rat diaphragm (Matsumoto et al., 1990). These findings suggest that denervation increased the level of AC, not the number of CGRP receptors.

In contrast, the finding that the responses to CGRP were decreased after denervation suggests a decrease in the number of CGRP receptors. Therefore, we tried to quantify CGRP receptors. We found that human ^{125}I-CGRP bound specifically to a preparation of rat diaphragm with a K_D value of 3×10^{-9} M (data not shown). The amount of this specific binding was not affected by denervation. However, this binding did not seem to indicate that the CGRP receptor coupled with AC because the K_D value differed from the affinities measured by AC activity and twitch contraction and because the binding was not affected by guanine nucleotides, which usually decrease the affinity of agonist binding to receptors coupled with GTP-binding proteins.

Reserpine treatment seemed to increase the number of β-adrenoceptors in this tissue. Pretreatment with reserpine is reported not to alter either the density or the K_D of β_2-adrenoceptors in gastrocnemius muscle membranes from the guinea pig (Elfellah and Reid, 1989). In this study we did not investigate the receptor binding, but it is possible that preparations from different species or different parts of the body show different characteristics of binding.

As shown in Figs. 2 and 4, responses to isoproterenol in twitch contraction and cyclic AMP content were larger than those to CGRP. The ED_{50} value of isoproterenol for twitch contraction was lower than that for the increase in cyclic AMP content, whereas those of CGRP were similar. This nonlinear relationship between elevation of the cyclic AMP level and enhancement of twitch contraction by isoproterenol may be explained by the spare receptor theory: the mechanism of amplification and saturation (Furchgott and Bursztyn, 1967; Takeyasu et al., 1979). That is, a low concentration of isoproterenol induces a very slight increase in cyclic AMP content that is not detectable by our methods, and this may have elicited the enhancement of twitch contraction, whereas a submaximal level of cyclic AMP may have caused the full activation. Supersensitivity of enhancement of twitch contraction by isoproterenol was observed only on reserpine treatment plus denervation, although activation of AC by isoproterenol was increased by reserpine treatment alone. As predicted from the spare receptor theory, supersensitivity as the result of change in the ED_{50} may require a large increase in efficacy between receptor activation and muscle contraction and so may become significant only when the levels of both the β-receptor and AC are increased by reserpine treatment and denervation. The reason why CGRP did not show those phenomena may be a small and localized increase in cyclic AMP content by CGRP.

We showed here that the decrease in CGRP-activated AC level after denervation was prominent in the EP-rich region. Specific CGRP binding has been shown by ^{125}I-CGRP autoradiography to be localized at the neuromuscular junction in the bulbocavernosus (Popper and Micevych, 1989). This is consistent with our finding that the EP-rich region showed higher sensitivity to CGRP than the EP-free region. The activation of AC by CGRP was observed even in the EP-free region, although it was smaller than that in the EP-rich region. It might be due to the contamination of nerve

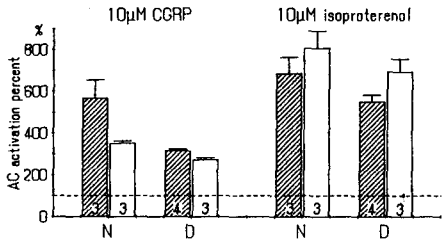

FIG. 6. Effects of CGRP and isoproterenol on AC activity in EP-free and -rich regions of normal and denervated muscle. Data are expressed as percent increases in AC activated by 10 μM CGRP or 10 μM isoproterenol over the basal level. The AC activities of membranes from the EP-free (□) and -rich (▨) regions of normal (N) and denervated (D) muscle were measured. The numerals in the columns represent numbers of experiments. Data are mean ± SEM (bars) values.

ending in the EP-free region or to the broader presence of CGRP receptors than nicotinic ACh receptors.

Our study suggested that denervation caused a reduction in the number or sensitivity of CGRP receptors in the EP, concomitantly with an increase in the number of AC molecules. On the other hand, sensitivity to isoproterenol was as high in the EP-free region as in the EP-rich region, a result suggesting humoral control of the β-adrenergic system in skeletal muscle.

We found in this work that reserpine treatment caused supersensitivity of AC activity to isoproterenol but not to CGRP. On the other hand, denervation induced an increase in the basal activity of AC and subsequent muscle contraction. These findings suggest that depletion of catecholamines supersensitizes the responses at the β-adrenoceptor level and that denervation causes an increase in the response at the level of AC activity, possibly as a result of loss of CGRP release from nerve terminals. Thus, it is probable that the AC system of striated muscle is regulated by two different mechanisms of control: hormonal and nervous.

Acknowledgment: This study was supported in part by a grant from the Nakatomi Foundation and by a grant-in-aid for Scientific Research from the Ministry of Education, Science and Culture of Japan.

REFERENCES

Bowman W. C. and Nott M. W. (1969) Actions of sympathomimetic amines and their antagonists on skeletal muscle. *Pharmacol. Rev.* **21**, 27–72.

Elfellah M. S. and Reid J. L. (1989) Regulation of β_1- and β_2-adrenoceptors following chronic treatment with β-adrenoceptor antagonists. *Eur. J. Pharmacol.* **173**, 85–92.

Fleming W. W. and Trendelenburg U. (1961) The development of supersensitivity to norepinephrine after pretreatment with reserpine. *J. Pharmacol. Exp. Ther.* **133**, 41–51.

Fontaine B., Klarsfeld A., Hökfelt T., and Changeux J.-P. (1986) Calcitonin gene-related peptide, a peptide present in spinal cord motoneurons, increases the number of acetylcholine receptors in primary cultures of chick embryo myotubes. *Neurosci. Lett.* **71**, 59–65.

Furchgott R. F. and Bursztyn P. (1967) Comparison of dissociation constants and of relative efficacies of selected agonists acting on parasympathetic receptors. *Ann. NY Acad. Sci.* **144**, 882–899.

Gross S. R. and Mayer S. E. (1975) Phosphorylase kinase mediating the effects of cyclic AMP in muscle. *Metabolism* **24**, 369–380.

Hashimoto K., Watanabe Y., Uchida S., and Yoshida H. (1989) Increase in the amount of adenylate cyclase in rat gastrocnemius muscle after denervation. *Life Sci.* **44**, 1887–1895.

Hawthorn M. H. and Broadley K. J. (1982) β-Adrenoceptor ligand binding and supersensitivity to isoprenaline of ventricular muscle after chronic reserpine pretreatment. *Naunyn Schmiedebergs Arch. Pharmacol.* **320**, 240–245.

Hays E. T., Dwyer T. M., Horowicz P., and Swift J. G. (1974) Epinephrine action on sodium fluxes in frog striated muscle. *Am. J. Physiol.* **227**, 1340–1347.

Honma M., Satoh T., Takezawa J., and Ui M. (1977) An ultrasensitive method for the simultaneous determination of cyclic AMP and cyclic GMP in small-volume samples from blood and tissue. *Biochem. Med.* **18**, 257–273.

Kobayashi H., Hashimoto K., Uchida S., Sakuma J., Takami K., Tohyama M., Izumi F., and Yoshida H. (1987) Calcitonin gene related peptide stimulates adenylate cyclase activity in rat striated muscle. *Experientia* **43**, 314–316.

Lowry O. H., Rosebrough N. J., Farr A. L., and Randall R. J. (1951) Protein measurement with the Folin phenol reagent. *J. Biol. Chem.* **193**, 265–275.

Matsumoto N., Uchida S., Wang X.-B., and Yoshida H. (1990) Effect of denervation of the phrenic nerve on the action of calcitonin gene-related peptide in rat diaphragm. *Life Sci.* **47**, 547–555.

Mulle C., Benoit P., Pinset C., Roa M., and Changeux J.-P. (1988) Calcitonin gene-related peptide enhances the rate of desensitization of the nicotinic acetylcholine receptor in cultured mouse muscle cells. *Proc. Natl. Acad. Sci. USA* **85**, 5728–5732.

New H. V. and Mudge A. W. (1986) Calcitonin gene-related peptide regulates muscle acetylcholine receptor synthesis. *Nature* **323**, 809–811.

Ohhashi T. and Jacobowitz D. M. (1988) Effects of calcitonin gene-related peptide on neuromuscular transmission in the isolated rat diaphragm. *Peptides* **9**, 613–617.

Popper P. and Micevych P. E. (1989) Localization of calcitonin gene-related peptide and its receptors in a striated muscle. *Brain Res.* **496**, 180–186.

Reddy N. B. and Engel W. K. (1979) In vitro characterization of skeletal muscle β-adrenergic receptors coupled to adenylate cyclase. *Biochim. Biophys. Acta* **585**, 343–359.

Smith P. B. (1984) Developmental alterations in guanine nucleotide regulation of the β-adrenergic receptor-adenylate cyclase system of skeletal muscle. *J. Biol. Chem.* **259**, 7294–7299.

Takami K., Kawai Y., Shiosaka S., Lee Y., Girgis S., Hillyard C. J., MacIntyre I., Emson P. C., and Tohyama M. (1985*a*) Immunohistochemical evidence for the coexistence of calcitonin gene-related peptide- and choline acetyltransferase-like immunoreactivity in neurons of the rat hypoglossal, facial and ambiguus nuclei. *Brain Res.* **328**, 386–389.

Takami K., Kawai Y., Uchida S., Tohyama M., Shiotani Y., Yoshida H., Emson P. C., Girgis S., Hillyard C. J. and MacIntyre I. (1985*b*) Effect of calcitonin gene-related peptide on contraction of striated muscle in the mouse. *Neurosci. Lett.* **60**, 227–230.

Takeyasu K., Uchida S., Wada A., Maruno M., Lai R. T., Hata F., and Yoshida H. (1979) Experimental evidence and dynamic aspects of spare receptor. *Life Sci.* **25**, 1761–1722.

Tsujimoto T. and Kuno M. (1988) Calcitonin gene-related peptide prevents disuse-induced sprouting of rat motor nerve terminals. *J. Neurosci.* **8**, 3951–3957.

Uchida S., Yamamoto H., Iio S., Matsumoto N., Wang X.-B., Yonehara N., Imai Y., Inoki R., and Yoshida H. (1990) Release of calcitonin gene-related peptide-like immunoreactive substance from neuromuscular junction by nerve excitation and its action on striated muscle. *J. Neurochem.* **54**, 1000–1003.

Wessler I. and Kilbinger H. (1986) Release of [^{3}H]acetylcholine from a modified rat phrenic nerve-hemidiaphragm preparation. *Naunyn Schmiedebergs Arch. Pharmacol.* **334**, 357–364.

参考論文

FUNCTIONS OF A CO-TRANSMITTER, CALCITONIN GENE-RELATED PEPTIDE, ON THE NEUROMUSCULAR JUNCTION

SHUJI UCHIDA, KENJI TAKAMI, HIDEYUKI KOBAYASHI, KAZUYA HASHIMOTO AND NAOKO MATSUMOTO

Department of Pharmacology 1, School of Medicine, Osaka University, Nakanoshima 4-3-57, Kitaku, Osaka 530, Japan

INTRODUCTION

Calcitonin gene-related peptide (CGRP) is a peptide that is synthesized in nervous tissues by a different processing of the messenger RNA for calcitonin (Amara et al.,1982; Rosenfeld et al.,1983) . A wide, but non-random distribution of CGRP-like immunoreactive structures in the central and peripheral nervous system has been demonstrated by immunohistochemistry and radioimmunoassay (Rosenfeld et al.,1983; Gibson et al.,1984; Kawai et al.,1985). CGRP has been shown to cause physiological responses and to have specific binding sites, suggesting that it is a neurotransmitter or neuromodulator.

Among these nervous systems, motor neurons and motor nerve terminals have been shown by immunohistochemistry and in situ hybridization to contain CGRP with acetylcholine, so we have been interested in the function of CGRP in signal transduction at neuromuscular junctions (Takami et al.,1985A; Fontaine et al.,1986; New and Mudge,1986; Gibson et al.,1988).

Many neuropeptides including CGRP are known to co-exist with classical neurotransmitters and are called "co-transmitters". However, the physiological significance of these co-transmitters is not yet clear. Neuromuscular junctions in which acetylcholine and CGRP are co-existent seemed a very good system for studying the significance of co-transmitters because the innervation of skeletal muscles is simple, the tissue is homogeneous and it is easy to detect physiological and biochemical responses.

Another reason that we are interested in this subject is that CGRP may be a trophic factor. Destruction of a motor nerve is known to cause drastic changes in the structure and metabolism of the skeletal muscle cells that it innervates. The main changes observed are atrophy of the muscle cells, decrease in insulin-dependent glucose uptake, increase in the amount of nicotinic acetylcholine receptors and changes in the properties of ion channels, etc., most of which are thought to be due to disuse of the denervated muscles. However, some of these changes may be caused by disappearance of a tropic factor. So, it seemed very interesting to study the effects of CGRP on these changes after denervation.

Neuroreceptor Mechanisms in Brain, Edited by S. Kito *et al.*
Plenum Press, New York, 1991

In this report, we describe the release of CGRP by nerve stimulation and the short- and long-term effects of CGRP on contraction and the adenylate cyclase system in skeletal muscle cells.

I.EFFECTS OF CGRP ON CONTRACTION AND THE ADENYLATE CYCLASE SYSTEM IN SKELETAL MUSCLE

In mouse and rat phrenic nerve-diaphragm preparations, CGRP caused dose-dependent increase in twitch contraction by nerve and direct stimulations (Fig.1,2) (Takami et al.,1985B; Uchida et al.,1990). The ED_{50} value of CGRP was about $3x10^{-8}$ M and the increase in contraction at 10^{-6} M CGRP was about 30% more than the basal contraction. This stimulatory effect of CGRP was observed even in the presence of curare and propranolol, suggesting a direct action of CGRP on skeletal muscle cells.

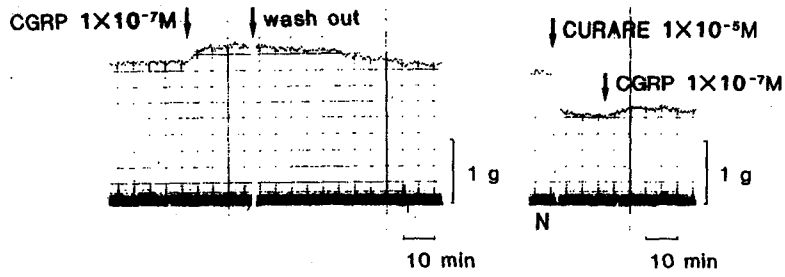

Fig.1 Effect of CGRP on striated muscle contraction under nerve stimulation (left) and on direct stimulation (right) of the phrenic nerve-diaphragm preparation of mice.

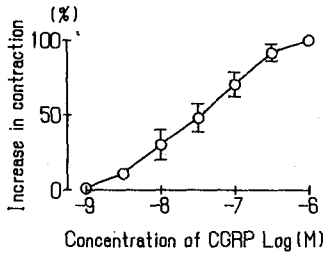

Fig.2 Dose-dependence of effect of CGRP on twitch contraction of rat diaphragm induced by direct stimulation.
CGRP was added to the medium cumulatively and increase of the contraction at 1 μM CGRP was taken as 100 % increase.

Fig. 3 shows that CGRP increased the cyclic AMP content of diaphragm muscle cells dose-dependently, which is consistent with its effect on twitch contraction (Takami et al.,1986). CGRP elevated the cyclic AMP content within 1 min after its addition, which is fast enough to cause the

increase in twitch contraction. The elevation of cyclic AMP content was due to activation of adenylate cyclase in the membranes by CGRP. Muscle cell membranes had a specific binding site for CGRP with a similar affinity as the ED_{50} values for activation of adenylate cyclase and stimulation of twitch contraction (Kobayashi et al.,1987).

These results suggest that CGRP binds to specific receptors on cell membranes and then activates adenylate cyclase. Activation of twitch contraction by CGRP seemed to be mainly due to elevation of the cyclic AMP content because dibutyryl-cyclic AMP, 8-bromo-cyclic AMP or phosphodiesterase inhibitors also caused activation of twitch contraction.

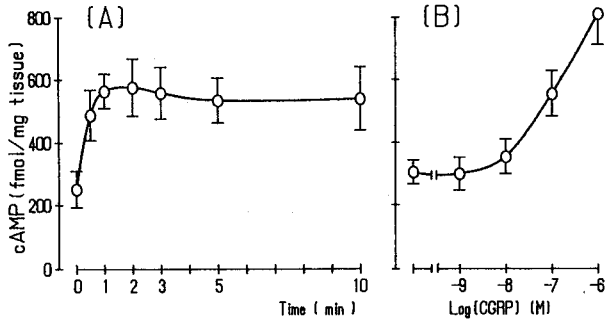

Fig.3 Time course (A) and dose response curve (B) of CGRP-induced elevation of cyclic AMP levels in mouse diaphragm.
A) After 5 min preincubation, 0.1μM CGRP was added at 0 min. B) The diaphragm was incubated for 3 min in Krebs-Ringer solution containing various concentrations of CGRP.

II.RELEASE OF CGRP FROM MOTOR NERVE TERMINAL BY NERVE EXCITATION

For confirmation of the physiological significance of CGRP as a neurotransmitter or neuromodulator, its release on nerve excitation must be demonstrated. Electrical stimulation of the phrenic nerve or membrane depolarization by high K^+ medium increased the content of CGRP-like immunoreactive substance (CGRP-LIS) in the medium in rat phrenic nerve-hemidiaphragm preparations.(Fig.4,A and B). This increased release was not observed in Ca^{++}-free medium (Fig.4, C and D), indicating that release of CGRP-LIS from nerve terminals on tetanic stimulation was Ca^{++}-dependent.

Fig.5A shows the Ca^{++}-dependent increase in the cyclic AMP level after phrenic nerve stimulation in the presence of a phosphodiesterase inhibitor. Addition of antiserum against human CGRP to the medium prevented the increase in cyclic AMP content without affecting the cyclic AMP content in the resting state (Fig.5B).

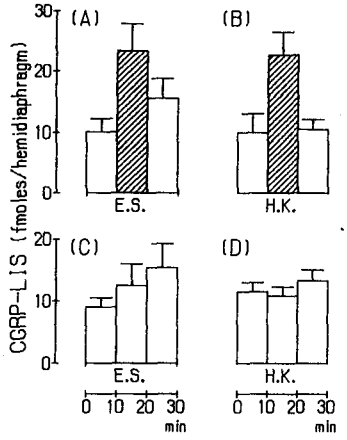

Fig.4 Release of CGRP-LIS from phrenic nerve-hemidiaphragm preparations induced by electrical stimulation of the phrenic nerve or high K^+ medium.

Tissues were incubated for 30 min after equilibration. The incubation media after the first 10 min and last 10 min were used as control samples. In the second 10 min, the phrenic nerve was stimulated electrically (A,C) or with high K^+ medium (B,D). The incubation media for (A) and (B) contained 1.0 mM $CaCl_2$ and those for (C) and (D) were Ca^{++}-free. Hatched columns indicate significant difference from values in the first 10 min (control) ($p<0.02$).

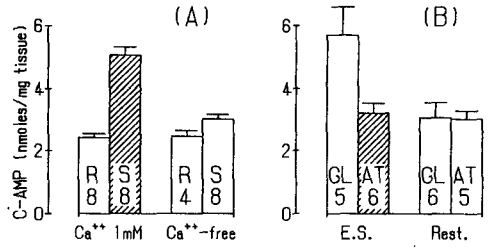

Fig.5 Elevation of the cyclic AMP content in phrenic nerve-hemidiaphragm preparations by electrical stimulation of the phrenic nerve and its inhibition by anti-CGRP serum.
(A) Preparations were incubated for 10 min with (S) or without (R) electrical stimulation in 1 mM $CaCl_2$ or Ca^{++}-free medium.
(B) Preparations were incubated for 10 min with anti-CGRP antiserum (AT) or with bovine gamma-globlin (GL) during electrical stimulation (E.S.) or in the resting condition (Rest.).
Data are means ± S.E.M. from the numbers of experiments indicated in columns. Hatched columns indicate a significant difference from the left adjacent (control) column (A:$p<0.002$, B:$p<0.02$).

These results show that excitation of the motor nerve caused Ca^{++}-dependent release of CGRP-LIS, which increased the content of cyclic AMP in skeletal muscle cells, suggesting that CGRP has a physiological role as a co-transmitter in this tissue.

III.CHANGES IN THE CONTRACTION AND ADENYLATE CYCLASE SYSTEM OF SKELETAL MUSCLE AFTER DENERVATION

We demonstrated that CGRP activated adenylate cyclase via CGRP receptors. Therefore, we studied the effect of denervation on adenylate cyclase and contraction in skeletal muscle with the idea that denervation may induce supersensitivity of CGRP-activated adenylate cyclase and CGRP-induced enhancement of twitch contraction.

A) Adenylate Cyclase System in Rat Gastrocnemius Muscle

Rat gastrocnemius muscle was denervated by unilateral removal of the sciatic nerve. The weight of the denervated muscle decreased gradually and reached 28% of that of the control side 30-40 days after denervation (Hashimoto et al.,1989).

The stimulations by CGRP and forskolin of the adenylate cyclase activity of muscle membranes 30 days after denervation were compared with those of membranes from the contralateral normal muscle. Although the denervation caused increase in reactivity to CGRP, the reactivity to forskolin and the basal activity also increased (Fig.6). These results indicate that denervation caused supersensitivity of adenylate cyclase itself, but not that of CGRP-activation.

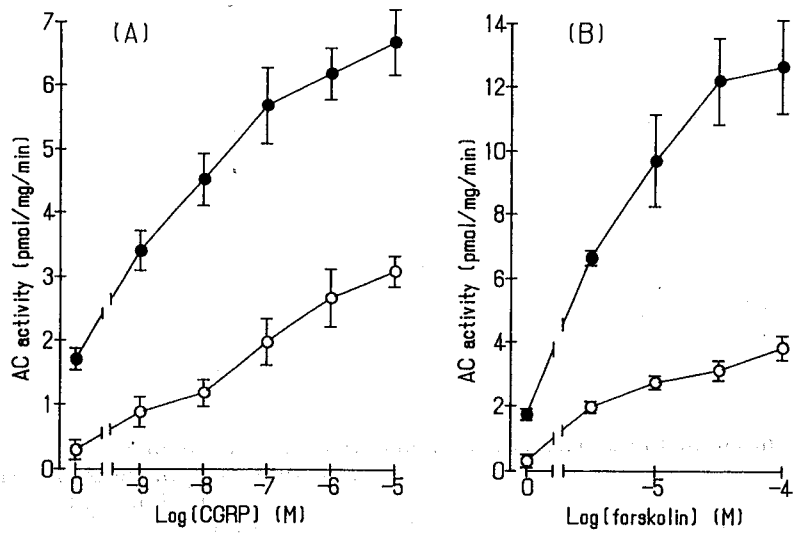

Fig.6 Effects of CGRP (A) and forskolin (B) on adenylate cyclase activity in denervated (●) and nondenervated (○) gastrocnemius muscle 30 days after unilateral denervation.

Then we examined the basal activity of adenylate cyclase and ^{3}H-forskolin binding as an indicator of the amount of adenylate cyclase molecules. Fig.7 shows the change in the ratio of the basal adenylate cyclase activity on the denervated side to that on the control side with time after denervation. The activity is expressed as total adenylate cyclase activity in whole muscle to avoid the effect of muscle atrophy.

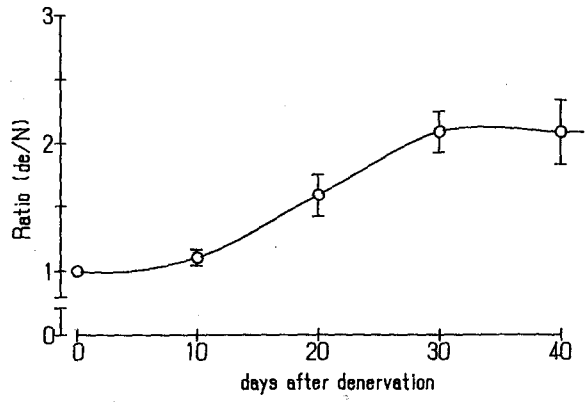

Fig.7 Change in ratio of total adenylate cyclase activities in denervated and control whole muscles with time after denervation. de; denervated muscle N; control muscle.

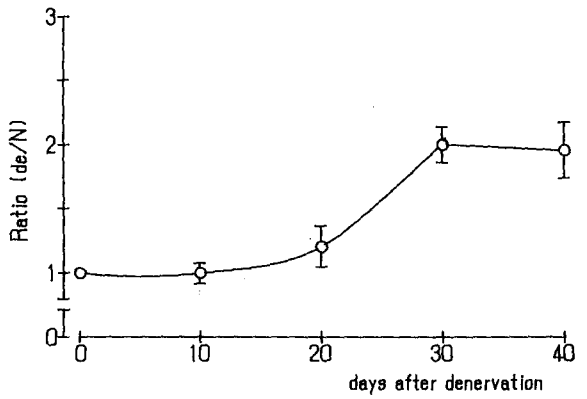

Fig.8 Change in ratio of specific ^{3}H-forskolin binding per cell of denervated and control muscle with time after denervation.

As shown in Fig.8, the ratio of specific ^{3}H-forskolin binding sites on denervated muscle to that on the control side also increased with time after denervation. This change was in good agreement with that of the basal adenylate cyclase activity. It is unknown whether forskolin binds to adenylate cyclase molecules directly. There are reports that forskolin acts on and bind to other molecules besides adenylate cyclase (Wadzinski et al.,1987; Hoshi et al.,1988; Wagoner and Pallotta,1988). But most,if not all, the the change in forskolin binding may reflect change in a component of adenylate cyclase system after the receptor.

These results indicate that the supersensitivity of the adenylate cyclase system after denervation is heterologous, resulting from increase in the amount of adenylate cyclase or a factor related to adenylate cyclase.

There are two possible mechanism for this heterologous supersensitivity. One is loss of continuous stimulation by CGRP, resulting in heterologous supersensitivity of the adenylate cyclase system. The other is that muscle disuse due to denervation may result in supersensitivity of adenylate cyclase for some unknown reason.

B) Changes in CGRP-Induced Enhancement of Twitch Contraction in Rat Diaphragm

Similar experiments were made on the left hemidiaphragm of rats by cutting the phrenic nerve. Two weeks after denervation, basal adenylate cyclase activity of the membrane was increased about 1.7 fold. But, activation ratios and ED_{50} values for CGRP and isoproterenol were not affected by denervation. These results were consistent with those in gastrocnemius muscles.

Twitch contraction by transmural stimulation was increased about 2 fold by denervation reflecting the increase of adenylate cyclase activity. However, CGRP-induced enhancement of twitch contraction was abolished by denervation, as shown in fig.9.

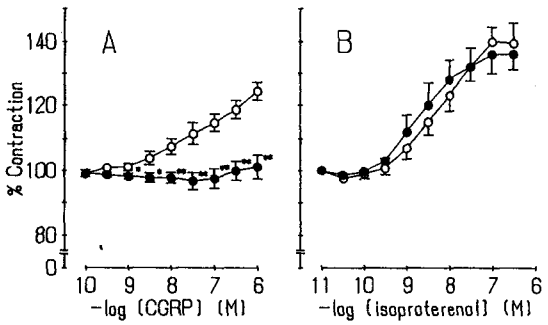

Fig.9 Enhancement of twitch contraction by CGRP(A) and isoproterenol(B) in normal and denervated diaphragms. Data are expressed as percentage increases in isometric tension induced by drugs over the steady level in normal (○) and denervated (●) muscles. Values are means ± SEM's.

CGRP at concentration of 3 x 10^{-8}M to 1 x 10^{-6}M caused dose-dependent potentiation of the contraction of normal diaphragm. In denervated muscle, no potentiation by CGRP was observed. On the other hand, isoproterenol potentiated the contractile responses of normal and denervated diaphragms in similar concentration-dependent manners and to similar extent.

In general, denervated tissues become hypersensitive to the neurotransmitters present in the nerves that are destroyed, as the result of increase in neurotransmitter receptors. After denervation, the adenylate cyclase system became hypersensitive to CGRP, although this hypersensitivity was heterologous resulting from an increase in adenylate cyclase molecules. Therefore, we expected that the muscle would become hypersensitive in CGRP-induced enhancement of contraction. But, on the contrary, the response to CGRP in twitch contraction was abolished by phrenic nerve destruction.

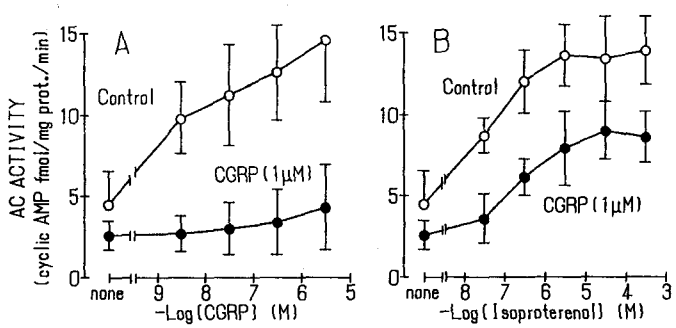

Fig.10 Effect of exposure of cultured cells to CGRP (1μM) for 24 hours on CGRP- (A) and isoproterenol- (B) stimulated adenylate cyclase activities.

To clarify this discrepancy, we measured cyclic AMP content in the muscle. The basal cyclic AMP content in the tissue was also elevated by denervation. This increase corresponds to the increase in the basal contractile force and suggests that the cyclic AMP level regulates the contractile force of skeletal muscle. But, the stimulation by CGRP and isoproterenol of the cyclic AMP content over basal level were decreased by denervation. This may be one reason of the decrease in CGRP-induced enhancement of twitch contraction.

Destruction of a motor nerve causes very unique heterologous supersensitization of the adenylate cyclase system in skeletal muscle, probably due to lack of CGRP release. The elevation of the basal twitch contraction by denervation may result from an increase in the basal cyclic AMP level. However, disappearance of CGRP-enhanced contraction cannot be explained entirely by change in the cyclic AMP system, and may have other underlying mechanisms.

IV. ADENYLATE CYCLASE SYSTEM IN CULTURED MUSCLE CELLS AND EFFECT OF CGRP

Isolated cells from gastrocnemius muscle of newborn rats were cultured in the presence of CGRP (Hashimoto et al.,1989B). The muscle cells in culture are free from control by the nerve, so that we thought they were a good model for denervated muscles. The adenylate cyclase activity of muscle cells stimulated by isoproterenol, CGRP, NaF and forskolin increased with time during culture until 4 days. These changes may reflect those by denervation in vivo although the time courses were different from each other.

Exposure of the cell cultures to CGRP (1μM) for 24 hr depressed their CGRP-stimulated adenylate cyclase activity to about one fourth of that of control (Fig.10,A). This treatment also depressed isoproterenol-stimulated adenylate cyclase activity as shown in Fig.10,B.

The effects of exposure of the cells to CGRP for 24 hr on their adenylate cyclase activities stimulated by drugs are summarized in Table 1. All drug-stimulated adenylate cyclase activities were depressed by exposure to CGRP, but the depression of CGRP-stimulated activity was the greatest.

Next, exposure to CGRP was prolonged to 3 days in the same conditions and the results are shown in Table 2. Exposure to CGRP for 3 days again depressed the stimulations by various drugs, but its effects on the adenylate cyclase activities stimulated by CGRP, NaF and forskolin were not significantly different.

Table 1

Comparison of adenylate cyclase activities stimulated by various drugs after exposure of cultured cells to CGRP (1μM) for 24 hr.

Stimulator	Control	CGRP-exposure	% Ratio
CGRP (5 μM)	10.1 ± 1.3	2.1 ± 1.0	20.8 ± 10.5
Isoproterenol (0.3 mM)	9.4 ± 0.9	6.3 ± 0.6	67.0 ± 11.7
NaF (10 mM)	11.2 ± 2.0	5.9 ± 1.0	52.7 ± 15.6
Forskolin (1 μM)	13.2 ± 1.9	9.7 ± 1.0	73.5 ± 15.9
None(Basal Activity)	4.5 ± 2.0	2.0 ± 0.9	57.7 ± 21.6

Adenylate cyclase activities in the presence of stimulators are shown as total minus basal activity (cyclic AMP fmol/mg prot./min). Values are means ± S.D. Percentage ratios mean CGRP-exposure/Control. * Significantly different from other values ($p<0.01$).

Table 2

Comparison of adenylate cyclase activities stimulated by various drugs after exposure of cultured cells to CGRP (1 μM) for 3 days.

Stimulator	Control	CGRP-exposure	% Ratio
CGRP (5 μM)	16.7 ± 3.6	9.4 ± 2.6	56.3 ± 22.8
Isoproterenol (0.3 mM)	16.4 ± 0.9	14.3 ± 3.8	87.2 ± 10.8 *
NaF (10 mM)	23.8 ± 3.1	8.6 ± 4.3	36.1 ± 20.1
Forskolin (1 μM)	27.2 ± 3.1	10.7 ± 3.6	39.3 ± 15.9
None(Basal Activity)	6.6 ± 2.1	2.9 ± 1.8	43.7 ± 31.3

* Significantly different from other values ($p<0.01$).
Explanations are as for Table 1.

These results suggest that exposure of cultured skeletal muscle cells to CGRP for 24 hr caused homologous desensitization mainly at the level of the CGRP receptor, whereas exposure to CGRP for a longer period caused heterologous desensitization mainly at some level after the receptor.

To determine whether these desensitization were mediated by an increased concentration of cyclic AMP, muscle cells were cultured in medium containing dibutyryl cyclic-AMP (dbc-AMP). Table 3 shows the CGRP-stimulated adenylate cyclase activity in muscle cells after exposure to dbc-AMP (1 mM) for 24 hr.

Table 3

Effect of 24 hr exposure of cultured cells to dbc-AMP (1 mM) on CGRP-stimulated adenylate cyclase activity.

Adenylate cyclase activity	Control	Exposure dbc-AMP (1mM)	CGRP(1μM)
CGRP-stimulated	12.1 ± 2.7	6.3 ± 3.4	4.3 ± 2.6
Basal	4.5 ± 2.0	1.8 ± 1.0	2.6 ± 0.9

Values are means ± S.D. (cyclic-AMP, fmol/mg prot./min).

We also examined the time courses of change in adenylate cyclase activity stimulated by CGRP and forskolin in cultures with 1 mM dbc-AMP for 3 days(data not shown). The results showed that the adenylate cyclase activities stimulated by CGRP and forskolin were inhibited by exposure to dbc-AMP and that the time course was very similar to that of the desensitization by CGRP-exposure.

The results for cultured muscle cells indicated that desensitization of the adenylate cyclase system in muscle cells by exposure to CGRP was at first mainly homologous but later became heterologous with time of culture. These desensitizations seem to be mediated by elevation of the intracellular cyclic-AMP level.

V. DISCUSSION

We demonstrated that CGRP, like other neurotransmitters, is released Ca^{++}-dependently from nerve terminal by nerve excitation. The released CGRP activated adenylate cyclase via CGRP receptors and enhanced twitch contraction mediated by elevation of the cyclic-AMP level.

Affinities of CGRP for activation of adenylate cyclase and binding to membranes in this tissue were much lower than those reported in other tissues. The reason for this difference is unknown. However, it is possible that the concentration of CGRP released in the synaptic cleft can reach more than 10^{-7} M and cause a physiological response because the synaptic cleft of the neuromuscular junction is larger and narrower than other synapses. Our findings that elevation of cyclic AMP by nerve stimulation was blocked by antiserum against CGRP supports this idea. The CGRP receptor in this tissue may be a different subtype with lower affinity for CGRP from those in other tissues.

CGRP inhibited adenylate cyclase via inhibitory GTP binding protein in breast cancer cells, in which the affinity was higher than that of activation of adenylate cyclase (Barsony and Marx,1988). However, we could not detect any inhibition of adenylate cyclase by CGRP in skeletal muscles.

CGRP may regulate acetylcholine release from nerve terminals by binding to presynaptic receptors. But, this possibility seems unlikely from our analysis of the effects of CGRP on twitch contraction by nerve stimulation. Further studies are necessary on this problem.

As the enhancement of twitch contraction by CGRP was at most 30 % in rat diaphragm, we thought that CGRP might have other physiological roles, such as a neuronal trophic factor regulating the homeostasis of muscle cells. In this report, we demonstrated that denervation caused heterologous supersensitivity of the adenylate cyclase system in the in-

nervated muscles and that CGRP induced the heterologous desensitization in cultured muscle cells. These findings suggest that CGRP regulate the adenylate cyclase system in skeletal muscle cells.

Some properties of muscle have been demonstrated to be regulated trophically by unknown molecular mechanisms (Fambrough,1970; Grampp et al.,1972). Lentz (1972) suggested that the actions of a presumed 'trophic hormone' might be mediated by cyclic-AMP. Additional evidence that the adenylate cyclase system in skeletal muscle is neurotrophically regulated is as follows : First, the changes in cyclic-AMP concentration resulting from muscle denervation and simple disuse are different. Second, the onset of increase in cyclic-AMP concentration after denervation depends on the length of the residual nerve stump. Third, reinnervation of a denervated muscle leads to reduction in the cyclic-AMP concentration (Carlson,1975).

Some long-term effects of CGRP on skeletal muscle have been also reported. Culture in the presence of CGRP increased the number of nicotinic acetylcholine receptors on skeletal muscle cells (Fontaine et al.,1986; New and Mudge,1986). Daily injection of CGRP prevented disuse-induced sprouting of motor nerve terminals in rat skeletal muscle (Tsujimoto and Kuno,1988).

Our results and these findings suggest that CGRP, which is located in motor nerve terminal, may regulate the adenylate cyclase system in skeletal muscle physiologically and may be one of the trophic factors derived from motor neurons. To establish that CGRP is a trophic factor, more work on the effect of continuous treatment with CGRP in the denervated state is necessary.

REFERENCES

Amara, S. G., Jones, V., Rosenfeld, M. G., Ong, E. S., and Ewans, R. M., 1982, Alternative RNA processing in calcitonin gene expression generate mRNA encoding different polypeptide products, Nature, 298:240-244.

Barsony, J., and Marx, S. J., 1988, Dual effects of calcitonin and calcitonin gene-related peptide on intracellular cyclic AMP in a human breast cancer cell line. Endocrinology, 122:1218-1223.

Carlsen, R. C., 1975, The possible role of cyclic AMP in the neurotrophic control of skeletal muscle. J.Physiol., 247:343-361.

Fambrough, G. H., 1970, Acetylcholine sensitivity of muscle fiber membrane: Mechanism of regulation by motoneurons. Science, 168:372.

Fontaine, B., Klarsfeld, A., Hökfelt, T., and Changeux, J. -P., 1986, Calcitonin gene-related peptide, a peptide present in spinal cord motoneurons, increases the number of acetylcholine receptors in primary cultures of chick embryo myotubes. Neurosci. Lett., 71:51-65.

Gibson, S. J., Polak, J. M., Bloom, S. R., Sabate, I. M., Mulderry, P. M., Chatei, M. A., McGregor, G. P., Morrison, J. F. B., Kelly, J. S., Evans, R. M., and Rosenfeld, M. G., 1984, Calcitonin gene-related peptide immunoreactivity in spinal cord of man and of eight other species. J. Neuroscience, 4:3101-3111.

Gibson, S. J., Polak, J. M., Giaid, A., Hamid, Q. A., Kar, S., Jones, P. M., Denny, P., Legon, S., Amara, S. G., Craig, R. K., Bloom, S. R., Penketh, R. J. A., Rodek, C., Ibrachim, N. B. N., and Dawson, A., 1988, Calcitonin gene-related peptide messenger RNA is expressed in sensory neurones of dorsal root ganglia and also in spinal motoneurons in man and rat. Neurosci. Lett., 91:283-288.

Grampp, W., Harrus, J. B., and Thesleff, S., 1972, Inhibition of denervation changes in skeletal muscle by blockers of protein synthesis. J. Physiol. 221:743-745.

Hashimoto, K., Watanabe, Y., Uchida S., and Yoshida, H., 1989A, Increase in the amount of adenylate cyclase in rat gastrocnemius muscle after denervation. Life Sci., 44:1887-1895.

Hashimoto, K., Uchida, S., and Yoshida, H., 1989B, Effects of calcitonin gene-related peptide on the adenylate cyclase system in cultured rat skeletal muscle cells. Life Sci. 45:2183-2193.

Hoshi, T., Garber, S. S., and Aldrich, R. W., 1988, Effect of forskolin on voltage-gated potassium channels is independent of adenylate cyclase activation. Science, 240:1652-1655.

Kawai, Y., Takami, K., Shiosaka, S., Emson, P. C., Hillyard, C. J., McIntyre, I., and Tohyama, M., 1985, Topographic localization of calcitonin gene-related peptide in rat brain : An immunohistochemical analysis. Neuroscience, 15:747-763.

Kobayashi, H., Hashimoto, K., Uchida, S., Sakuma, J., Takami, K., Tohyama, M., Izumi, F., and Yoshida, H., 1987, Calcitonin gene-related peptide stimulates adenylate cyclase activity in rat striated muscle. Experientia, 43:314-316.

Lentz, T. L., 1972, A role of cyclic AMP in a neurotropic process. Nature (New Biology), 238:154-155.

New, H. V., and Mudge, A.V., 1986, Calcitonin gene-related peptide regulates muscle acetylcholine receptor synthesis. Nature, 323:129-135.

Rosenfeld, M. G., Mermod, J. J., Amara, S. G., Swanson, L. W., Sawchenko, P. E., River, J., Vale, W. W., and Evans, R. M., 1983, Production of novel neuropeptide encoded by the calcitonin gene via tissue specific RNA processing. Nature, 304:129-135.

Takami, K., Kawai, Y., Shiosaka, S., Lee, Y., Girgis, S., Hillyard, C. J., MacIntyre, I., Emson P. C., and Tohyama, M., 1985A, Immunohistochemical evidence for coexistence of calcitonin gene-related peptide- and choline acetyltransferase-like immunoreactivity in neurons of the rat hypoglossal, facial and ambiguus nuclei. Brain Res., 328:386-389.

Takami, K., Kawai, Y., Uchida, S., Tohyama, M., Shiotani, Y., Yoshida, H., Emson, P. C., Girgis, S., Hillyard, C. J., and MacIntyre, I., 1985B, Effect of calcitonin gene-related peptide on contraction of striated muscle in the mouse. Neurosci. Lett., 60:227-230.

Takami, K., Hashimoto, K., Uchida, S., Tohyama M., and Yoshida, H., 1986, Effect of calcitonin gene-related peptide on the cyclic AMP level of isolated mouse diaphragm. Jpn. J. Pharmacol., 42:345-350.

Tsujimoto, T., and Kuno, M., 1988, Calcitonin gene-related peptide prevents disuse-induced sprouting of rat motor nerve terminals. J. Neurosci., 8:3951-3957.

Uchida, S., Yamamoto, H., Iio, S., Matsumoto, N., Wang, X. -B., Yonehara, N., Imai, Y., Inoki, R., and Yoshida, H., in press, Release of CGRP-like immunoreactive substance from neuromuscular junction by nerve excitation and its action on striated muscle. J. Neurochem.,

Wadzinski, B. E., Shanahan, M. F,, and Ruoho, A. E., 1987, Derivatization of the human erythrocyte glucose transporter using a novel forskolin photoaffinity label. J. Biol. Chem., 262:17683-17689.

Wagoner, P. K., and Pallotta, B. S., 1988, Modulation of acetylcholine receptor desensitization by forskolin is independent of cyclic AMP. Science 240:1656-1657.

Journal of Neurochemistry
Raven Press, Ltd., New York

参考論文

Release of Calcitonin Gene-Related Peptide-Like Immunoreactive Substance from Neuromuscular Junction by Nerve Excitation and Its Action on Striated Muscle

Shuji Uchida, Hiromasa Yamamoto, Sadaharu Iio, Naoko Matsumoto, Xiao-Bing Wang, *Norifumi Yonehara, *Yasuo Imai, *Reizo Inoki, and Hiroshi Yoshida

*Department of Pharmacology I, Medical School, and *Department of Pharmacology, Dental School, Osaka University, Kitaku, Osaka, Japan*

Abstract: In a rat phrenic nerve–hemidiaphragm preparation, calcitonin gene-related peptide (CGRP) increased the twitch contraction induced by nerve or transmural stimulation dose dependently. Either electrical or high K^+ stimulation of the phrenic nerve caused release of a CGRP-like immunoreactive substance (CGRP-LIS) in a Ca^{2+}-dependent manner. Electrical stimulation of the phrenic nerve also increased the cyclic AMP content in diaphragm. This increase was not observed in Ca^{2+}-free medium and was blocked by antiserum against CGRP. These results indicate that excitation of the motor nerve causes release of CGRP-LIS at nerve terminals and that the released CGRP-LIS increases the cyclic AMP content of skeletal muscles and potentiates twitch contraction. **Key Words:** Calcitonin gene-related peptide—Neuromuscular junction—Cyclic AMP. **Uchida S. et al.** Release of calcitonin gene-related peptide-like immunoreactive substance from neuromuscular junction by nerve excitation and its action on striated muscle. *J. Neurochem.* **54,** 1000–1003 (1990).

Calcitonin gene-related peptide (CGRP) is a neuronal peptide, whose mRNA is translated and processed from the same gene as calcitonin. CGRP is expressed specifically in neuronal tissues and distributes widely in central and peripheral nervous systems, where it coexists with other neurotransmitters (Rosenfeld et al., 1983; Kawai et al., 1985). Among them, motor neurons have been shown to contain CGRP together with acetylcholine (Takami et al., 1985; Fontaine et al., 1986; New and Mudge, 1986). Thus the neuromuscular junction of skeletal muscles is a good model for the study of a physiological role of so-called "co-transmitters."

In previous experiments on a mouse phrenic nerve–diaphragm preparation, we demonstrated that CGRP increased the cyclic AMP level through CGRP receptors and enhanced muscle contractions induced by nervous or direct stimulation (Takami et al., 1986). This elevation of cyclic AMP was due to activation of adenylate cyclase (Kobayashi et al., 1987).

In addition to those short-term effects, CGRP also has been reported to have long-term effects on skeletal muscles. Culture in the presence of CGRP increased the number of nicotinic acetylcholine receptors on skeletal muscle cells (Fontaine et al., 1986; New and Mudge, 1986). Daily injection of CGRP prevented disuse-induced sprouting of motor nerve terminals in rat skeletal muscle (Tsujimoto and Kuno, 1988). We observed that denervation of skeletal muscle increased the number of adenylate cyclase molecules measured by the binding of forskolin (Hashimoto et al., 1989) and that the adenylate cyclase activity in isolated muscle cells in culture was suppressed by CGRP (Hashimoto et al., 1989). These results indicate that CGRP may have important roles as a neuronal trophic factor in maintaining homeostasis of muscle activities.

For confirmation of the physiological significance of CGRP as a neurotransmitter or neuromodulator, the release on nerve excitation must be demonstrated. In this study, we showed that stimulation of the phrenic nerve caused the release of CGRP-like immunoreactive substance (CGRP-LIS) followed by elevation of the cyclic AMP level in a hemidiaphragm preparation in vitro.

Received March 29, 1989; accepted August 9, 1989.
Address correspondence and reprint requests to Dr. S. Uchida at Department of Pharmacology I, Osaka University Medical School, Nakanoshima, Kitaku, Osaka 530, Japan.

Abbreviations used: CGRP, calcitonin gene-related peptide; CGRP-LIS, CGRP-like immunoreactive substance.

MATERIALS AND METHODS

Animals

Male Sprague–Dawley rats (150–200 g) were used for all experiments.

Contraction of diaphragm muscles

A left phrenic nerve–hemidiaphragm preparation was mounted in an organ bath containing 5 ml of Krebs–Ringer solution (NaCl 124 m*M*, KCl 4.7 m*M*, $CaCl_2$ 1.0 m*M*, KH_2PO_4 1.25 m*M*, glucose 11 m*M*, and $NaHCO_3$ 25 m*M*) aerated with 95% O_2 and 5% CO_2 at 37°C. The phrenic nerve and diaphragm were stimulated alternately at a frequency of 1 Hz with rectangular pulses (10 ms duration, supramaximal amplitude). Twitch contractions were detected isometrically with a force displacement transducer (Nihon Koden). CGRP was added to the medium cumulatively after the effect of the previous addition of CGRP had reached a plateau.

Release of CGRP-LIS

The left hemidiaphragm of the phrenic nerve–hemidiaphragm preparation was cut into a 2–3 mm wide strip from end to end along the region of nerve ending and the strip was mounted in an organ bath containing 1 ml of Krebs–Ringer solution supplemented with 10 μg/ml aprotinin and 250 μM phenylmethylsulfonyl fluoride and aerated with 95% O_2 and 5% CO_2 at 37°C. After equilibration for 30 min with several washings, the tissue was incubated for 10 min and then the medium was collected as a control sample. Then, the phrenic nerve was stimulated with rectangular pulses (10 Hz, 10 ms duration, 5 V) or 50 m*M* KCl was added to the medium for 10 min. The medium was then used as the test sample. The tissue was finally incubated in Krebs–Ringer solution again for 10 min and a second control sample was taken. In some experiments, Ca-free Krebs–Ringer solution was added at the start of the control incubation.

The samples collected were lyophilized and the residues were dissolved in 0.5 ml of 50 m*M* sodium phosphate buffer (pH 7.4) containing 0.3% bovine serum albumin and 10 m*M* EDTA. Then, their CGRP content was measured by radioimmunoassay with rabbit antiserum for human CGRP, ^{125}I-human CGRP, and synthetic rat CGRP as a standard. Incubation was carried out for 5 days at 0°C as recommended by the supplier of the kit (Amersham).

Assay of cyclic AMP content in diaphragm

A square portion (5 × 5 mm) of the left hemidiaphragm preparation around the point of attachment of the nerve was cut out. The phrenic nerve was placed on a platinum electrode and the diaphragm was incubated in 1 ml of Krebs–Ringer solution containing 0.5 m*M* isobutylmethylxanthine, 10^{-5} *M d*-tubocurarine, and 10^{-5} *M* propranolol aerated with 95% O_2 and 5% CO_2 at 37°C. After 20 min of equilibration, the phrenic nerve was stimulated in the same way as in experiments on release of CGRP. Unstimulated tissue was used as a control.

A vial of rabbit antiserum against human CGRP (Amersham) was diluted with 4 ml of H_2O and dialyzed against Krebs–Ringer solution. A 0.5-ml aliquot of the dialyzed antiserum was mixed with 0.5 ml of Krebs–Ringer solution and used as the incubation medium for the experiments on cyclic AMP level. Bovine γ-globulin was used for the control experiments.

After stimulation for 10 min, tissues were rapidly frozen in liquid nitrogen and stored at −80°C until measurement of cyclic AMP. The frozen tissues were weighed and homogenized in 20 volumes of HCl (0.1 *M*) with a motor-driven microhomogenizer (Physcotron, Nichion Irika, Japan) at 0°C. The homogenate was centrifuged at 13,000 *g* for 15 min at 4°C and the supernatant was used for cyclic AMP assay. Cyclic AMP was measured with a kit from Yamasa Shoyu by a radioimmunoassay involving prior succinylation of samples.

Materials

Synthetic rat CGRP was obtained from the Peptide Institute, Osaka, Japan. Antiserum against human CGRP and ^{125}I-CGRP, human (~2,000 Ci/mmol) were purchased from Amersham. Other drugs were of the highest grade available.

RESULTS

Increase in twitch contraction by CGRP

Figure 1 shows the dose-dependent increase by CGRP in the twitch contraction induced by transmural stimulation. On the basis of this figure, the ED_{50} of CGRP was about 3×10^{-8} *M*. The increase in contraction at 10^{-6} *M* CGRP was about 30% more than the basal contraction, but for evaluation of results, this was taken as 100% for all preparations in Fig. 1, because there was a large variation in the responses of different preparations. Similar results were obtained when the contraction was induced by nerve stimulation (data not shown).

Release of CGRP-LIS by nerve stimulation

Electrical stimulation of the phrenic nerve or membrane depolarization by high K^+ medium increased the content of CGRP-LIS in the medium (Fig. 2A and B). The increased release of CGRP-LIS induced by the stimulation was about 12 fmol/hemidiaphragm. This increased release was not observed in Ca^{2+}-free medium (Fig. 2C and D), indicating that release of CGRP-LIS from phrenic nerve terminal on tetanic stimulation was Ca^{2+} dependent.

Release of CGRP-LIS cannot be expressed in moles per gram wet weight or moles per gram of protein because phrenic nerve endings have a one-dimensional disposition in the diaphragm. Therefore, we expressed the release in femtomoles per hemidiaphragm.

Increase of cyclic AMP content in the diaphragm by phrenic nerve stimulation

Figure 3A shows the increase in the cyclic AMP level after phrenic nerve stimulation in the presence of a

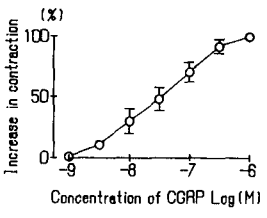

FIG. 1. Dose-dependent effect of CGRP on twitch contractions of rat diaphragm induced by direct stimulation. The phrenic nerve and diaphragm were stimulated alternately and results on direct stimulation are shown. CGRP was added to the medium cumulatively and increase of the contraction at 10^{-6} *M* CGRP was taken as 100% increase. Points and bars indicate means ± SEM for 11 preparations.

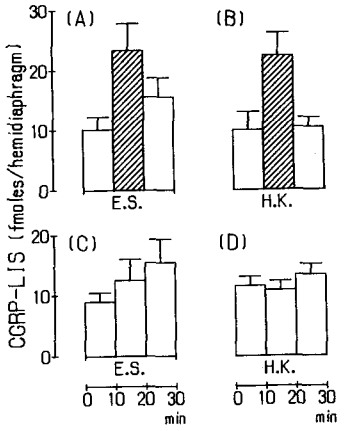

FIG. 2. Release of CGRP-LIS from phrenic nerve–hemidiaphragm preparations induced by electrical stimulation of the phrenic nerve or high K^+ medium. The tissues were incubated for 30 min after equilibration. The incubation media after the first 10 min and the last 10 min were used as control samples. In the second 10 min, the phrenic nerve was stimulated electrically (**A, C**) or in high K^+ medium (**B, D**). The incubation media for A and B contained 1.0 m*M* $CaCl_2$ and those for C and D were Ca^{2+} free. Vertical bars indicate standard errors of means. Hatched columns indicate significant difference from values in the first 10 min (control) by Student's *t* test ($p < 0.02$). Numbers of experiments: A, 10; B, 10; C, 8; and D 7.

phosphodiesterase inhibitor. This increase was not observed in Ca^{2+}-free medium. In contrast, addition of CGRP caused a dose-dependent increase in the cyclic AMP content and this increase was not affected by the presence or absence of Ca^{2+} in the Krebs–Ringer solution (data not shown). This finding suggests that elevation of the cyclic AMP level resulted from Ca^{2+}-dependent release of neurotransmitters.

Addition of antiserum against human CGRP to the medium prevented the increase in the cyclic AMP content without affecting the cyclic AMP content in the resting state (Fig. 3B).

DISCUSSION

The results in this study show that excitation of motor nerve caused a Ca^{2+}-dependent release of CGRP-LIS (Fig. 2), which increased the content of cyclic AMP of the muscles (Fig. 3), suggesting that CGRP has a physiological role as a cotransmitter in this tissue.

In a previous study, we could not demonstrate a dose-dependent increase by CGRP in twitch contraction of phrenic nerve–hemidiaphragm preparations from mice because the effect of CGRP was very small. In this work with preparations from rats, however, we observed about 30% increase in the twitch contraction at 10^{-6} *M* CGRP, although the increase varied greatly in different preparations. The dose–response curve shown in Fig. 1 is consistent with those for elevation of the cyclic AMP content in mouse diaphragm (Takami et al., 1986) and activation of adenylate cyclase in a rat diaphragm membrane fraction by CGRP (Kobayashi et al., 1987).

The radioimmunoassay used in this study was specific for human CGRP rather than rat CGRP. However, the antiserum used reacted with rat CGRP well enough for the radioimmunoassay. It did not react with calcitonin, substance P, substance K, enkephalin, or cholecystokinin-32. In addition to many reports of immunohistochemical demonstration of CGRP in motoneurons, the presence of mRNA for CGRP in motoneurons was also reported (Gibson et al., 1988). Thus, it seems very likely that the CGRP-LIS in neuromuscular junctions is actually CGRP itself.

Ca^{2+}-dependent release of CGRP-LIS by high K^+ stimulation in cultured cells of rat trigeminal ganglia was reported by Mason et al. (1984). Our results are consistent with theirs. But they reported that the increased release of CGRP-LIS from 5×10^6 cultured ganglion cells during 1 h of stimulation was about 200 fmol, which is 20 times higher than that in single hemidiaphragm during 10 min of stimulation in this work.

We demonstrated that elevation of cyclic AMP by nerve stimulation was mediated through the release of CGRP-LIS. In our experiment, activation of nicotinic acetylcholine receptors and subsequent contraction were blocked by *d*-tubocurarine, and the effect of β-adrenergic stimulation, which is known to activate adenylate cyclase in skeletal muscle, was blocked by propranolol. We also found that antiserum against CGRP abolished the effect of nerve stimulation in increasing the cyclic AMP content. The concentration of antiserum used in this experiment was high (about five times higher than that recommended for radioimmunoassay), but the same concentration of bovine γ-globulin was ineffective, indicating that this effect of the antiserum was specific.

High K^+ medium or 10 Hz pulses applied to the phrenic nerve, as in this study, is an extremely strong stimulation and far from physiological. It remains to be determined whether the release of CGRP is parallel with that of acetylcholine, or whether it occurs only when nerve excitations are frequent and their effects

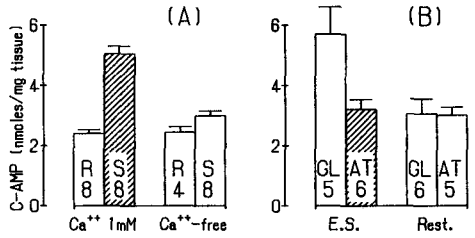

FIG. 3. Elevation of the cyclic AMP content in phrenic nerve–hemidiaphragm preparations by electrical stimulation of the phrenic nerve and its inhibition by anti-CGRP antiserum. **A:** Preparations were incubated for 10 min with (S) or without (R) electrical stimulation in 1 m*M* $CaCl_2$ or Ca^{2+}-free medium. **B:** Preparations were incubated for 10-min periods with anti-CGRP anti-serum (AT) or with bovine γ-globulin (GL) during electrical stimulation (E.S.) or in the resting condition (Rest.). Data are means ± SEM (bars) from the numbers of experiments indicated in columns. Hatched columns indicate a significant difference from the left adjacent (control) column by Student's *t* test (A, $p < 0.002$; B, $p < 0.02$).

are accumulated. However, our results suggest that posttetanic potentiation of the contraction of skeletal muscles (Guttman et al., 1937) may be caused in part by the release of CGRP because increase of the cyclic AMP level in muscles enhanced the contraction.

Acknowledgment: We thank Mrs. Mieko Nakamura for assistance in preparation of this article. This study was supported in part by a grant-in-aid for Scientific Research from the Ministry of Education, Science and Culture of Japan.

REFERENCES

Fontaine B., Klarsfeld A., Hökfelt T., and Changeux J.-P. (1986) Calcitonin gene-related peptide, a peptide present in spinal cord motoneurons, increases the number of acetylcholine receptors in primary cultures of chick embryo myotubes. *Neurosci. Lett.* **71,** 51–65.

Gibson S. J., Polak J. M., Giaid A., Hamid Q. A., Kar S., Jones P. M., Denny P., Legon S., Amara S. G., Craig R. K., Bloom S. R., Penketh R. J. A., Rodek C., Ibrachim N. B. N., and Dawson A. (1988) Calcitonin gene-related peptide messenger RNA is expressed in sensory neurones of dorsal root ganglia and also in spinal motoneurones in man and rat. *Neurosci. Lett.* **91,** 283–288.

Guttman S., Horton R. G., and Wilber D. T. (1937) Enhancement of muscle contraction after tetanus. *Am. J. Physiol.* **119,** 463–473.

Hashimoto K., Watanabe Y., Uchida S., and Yoshida H. (1989) Increase in the amount of adenylate cyclase in rat gastrocnemius muscle after denervation. *Life Sci.* **44,** 1887–1895.

Hashimoto K., Uchida S., and Yoshida H. (1989) Effects of calcitonin gene-related peptide on the adenylate cyclase system in cultured rat skeletal muscle cells. *Life Sci.* **45,** 2183–2192.

Kawai Y., Takami K., Shiosaka S., Emson P. C., Hillyard V. J., Girgis S., MacIntyre I., and Tohyama M. (1985) Topographic localization of calcitonin gene-related peptide in the rat brain; an immunohistochemical analysis. *Neuroscience* **15,** 747–763.

Kobayashi H., Hashimoto K., Uchida S., Sakuma J., Takami K., Tohyama M., Izumi F., and Yoshida H. (1987) Calcitonin gene related peptide stimulates adenylate cyclase activity in rat striated muscle. *Experientia* **43,** 314–316.

Mason R. T., Peterfreund R. A., Sawchenco P. E., Corrigan A. Z., River J. E., and Vale W. W. (1984) Release of the predicted calcitonin gene-related peptide from cultured rat trigeminal ganglion cells. *Nature* **308,** 653–655.

New H. V. and Mudge A. W. (1986) Calcitonin gene-related peptide regulates muscle acetylcholine receptor synthesis. *Nature* **323,** 129–135.

Rosenfeld M. G., Mermold J.-J., Amara S. G., Swanson L. W., Sawchenko P. E., River J., Vale W. W., and Evans R. M. (1983) Production of a novel neuropeptide encoded by the calcitonin gene via tissue specific RNA processing. *Nature* **304,** 129–135.

Takami K., Kawai Y., Shiosaka S., Lee Y., Girgis S., Hillyard C. J., MacIntyre I., Emson P. C., and Tohyama M. (1985) Immunohistochemical evidence for the coexistence of calcitonin gene-related peptide- and choline acetyltransferase-like immunoreactivity in neurons of the rat hypoglossal, facial and ambiguous nuclei. *Brain Res.* **328,** 386–389.

Takami K., Hashimoto K., Uchida S., Tohyama M., and Yoshida H. (1986) Effect of calcitonin gene-related peptide on the cyclic AMP level of isolated mouse diaphragm. *Jpn. J. Pharmacol.* **42,** 345–350.

Tsujimoto T. and Kuno M. (1988) Calcitonin gene-related peptide prevents disuse-induced sprouting of rat motor nerve terminal. *J. Neurosci.* **8,** 3951–3957.

Life Sciences, Vol. 47, pp. 547-555 Pergamon Press
Printed in the U.S.A.

EFFECT OF DENERVATION OF THE PHRENIC NERVE ON THE ACTION OF CALCITONIN GENE-RELATED PEPTIDE IN RAT DIAPHRAGM

Naoko Matsumoto, Shuji Uchida, Wang Xiao-Bing and Hiroshi Yoshida

Department of Pharmacology I, Osaka University Medical School, 4-3-57, Nakanoshima, Kitaku, Osaka, Japan

(Received in final form June 7, 1990)

Summary

The effect of denervation on Calcitonin gene-related peptide (CGRP)-induced enhancement of the twitch contraction of skeletal muscle was studied. In rat diaphragm denervated 2 weeks previously, the basal twitch contraction induced by transmural stimulation was about twice that in control muscle, and the basal adenylate cyclase activity and cyclic AMP (cAMP) contents of the tissue were increased. This denervation did not affect the dose-dependent β -adrenergic stimulation of twitch contraction, but abolished the CGRP-induced enhancement of twitch contraction. The latter phenomenon seems to be caused in part by decrease in CGRP-induced accumulation of cAMP over the basal level, because of increase in the basal cAMP level after denervation. The involvement of another inhibitory second messenger system coupled with CGRP receptors is discussed.

Calcitonin gene-related peptide (CGRP) is a peptide composed of 37 amino acids that has been found in the central (1-3) and peripheral (4-7) nervous systems. It coexists with acetylcholine (ACh) in motor neurons and in nerve terminals of neuromuscular junctions (8-9). We and others demonstrated that, in skeletal muscle, CGRP increased the cAMP level (10) as a result of activation of adenylate cyclase (AC) (11), and enhanced twitch contraction (9,12).

Cannon proposed the law of denervation stating: "When in a series of efferent neurones a unit is destroyed, an increased irritability to chemical agents developed in the isolated structure or structures, the effect being maximal in the part directly denervated"(13). Denervation is known to cause supersensitivity to ACh due to a dramatic increase in the number of nicotinic ACh receptors in skeletal muscles.

We demonstrated nonspecific supersensitivity of AC after denervation of the motor nerve in vivo, resulting from an increase in the amount of AC molecules measured by ^{3}H-forskolin binding (14). But no CGRP-specific supersensitivity of AC was observed. Therefore, we were interested in whether denervation caused supersensitivity to CGRP-induced enhancement of twitch contraction.

Unexpectedly, in this work we found that CGRP-induced en-

0024-3205/90 $3.00 +.00

hancement of twitch contraction was abolished by denervation. So, we also examined change in metabolism of cAMP as a possible reason for this phenomenon.

Materials and Methods

Denervation

Male Sprague-Dawley rats of 6 weeks old, weighing 150-200g were used. The left hemidiaphragm was denervated by section of the left phrenic nerve at the level of CVI under pentobarbital anesthesia. Control rats were subjected to a sham operation. After 2 weeks, the rats were sacrificed by decapitation and their diaphragms were used for experiments.

Measurement of twitch contraction

A phrenic nerve-left hemidiaphragm preparation was mounted in a 5ml organ bath containing Krebs-Ringer bicarbonate(KRB) solution at 37℃ and continuously aerated with 5% CO_2 in O_2. A tension of approximately 0.5g was applied and the strip stimulated transmurally with rectangular pulses (0.25Hz, 1 msec duration, supramaximal voltage). The twitch contraction was measured isometrically. When twitch responses became steady, the dose-dependence of the effects of rat CGRP (rCGRP) and isoproterenol were examined by adding these compounds cumulatively. The maximum isometric tension observed in experiments was expressed as the percentage increase in tension developed by electrical stimulation during the control period.

Preparation of membranes of striated muscle

Muscle of the left hemidiaphragm was excised, cut up with scissors and homogenized for 30 sec in a microhomogenizer in 10 volumes of cold 10 mM Tris/maleate buffer(pH 7.4) containing 5 mM EDTA (TME buffer). The homogenate was strained through nylon mesh and centrifuged twice for 10-min periods at 15,000g. The pellets were suspended in a suitable volume of TME buffer to obtain an appropriate concentration for AC assay.

Assay of membrane-bound adenylate cyclase

The AC activity in membranes of rat striated muscle was determined by measuring the synthesis of cAMP from ATP in incubation mixture containing 80 mM Tris/maleate (pH 7.4), 1 mM 3-isobutylmethylxanthine, 0.5μ M GTP, 6 mM $MgSO_4$, 0.5 mM EGTA, 1.5 mM ATP and 20μ g of membrane protein suspended in TME buffer, with the indicated concentration of rCGRP or isoproterenol in a total volume of 100μ l. The incubation mixture was preincubated for 2 min at 37℃ and then the reaction was started by addition of ATP with the indicated concentration of rCGRP or isoproterenol. After 10 min, the reaction was stopped by addition of 25μ l of 0.5N HCl and cooling. The mixture was centrifuged, and cAMP in the supernatant was measured by radioimmunoassay (15). Assays were performed in duplicate.

Measurement of cAMP accumulation in tissues

Strips of hemidiaphragmatic muscle of 3mm width from around the phrenic nerve were excised and cut into three parts. The tissues were preincubated for 5 min at 37℃ in 980μ l of KRB solution aerated continuously with 5% CO_2 in O_2. The reaction was started by addition of 20μ l of rCGRP or isoproterenol, or 20μ l of distilled water for measurement of basal activity. After 3 min, the tissues were removed from the incubation mixture and

promptly frozen in liquid nitrogen. The tissues were homogenized with a microhomogenizer in 20 volumes of cold 0.1N HCl and centrifuged for 10 min at 13,000g, and the supernatant was used for assay of cAMP as described above.

Measurement of cyclic nucleotide-phosphodiesterase (PDE) activity in tissues

Muscles of hemidiaphragms were homogenized for 1min in a microhomogenizer in 6 volumes of cold saline. The homogenate was strained through nylon mesh and disrupted by sonication for 30 sec per 1ml in an ice bath. The homogenate was centrifuged for 10 min at 1,000g at 4℃ , and the supernatant was used for PDE assay.

PDE activity was assayed by the method of Rutten et al. (16) with some modifications. The incubation mixture (final volume, 100μ l) contained 0.1M Tris-HCl(pH 8.1), 5mM $MgCl_2$, 4μ M [^{3}H]-cAMP (about 7.4kBq) and 20μ g of tissue homogenate. The reaction was initiated by addition of homogenate, incubated for 15 min at 37℃ , and stopped by boiling for 1 min. After addition of 50μ l of a solution of 5'-nucleotidase of Crotalus atrox (2mg/ml of 50mM $MgCl_2$), the mixture was incubated at 37℃ for 30 min and centrifuged. An aliquot of 100μ l of the supernatant was applied to a column of Dowex AG 1-X_2 resin, and material was eluted with 10ml of 0.1M $NaHCO_3$. Radioactivity in the total eluate was counted in a liquid scintillation spectrometer.

Treatment of rats with pertussis toxin

According to the procedure of X.-M.Zhou et al.(17), pertussis toxin (PT) was injected intravenously at a dose of 40 μ g/kg body weight 2 days before sacrifice.

Protein measurement

Protein was measured by the method of Bradford (18) with bovine serum albumin as a standard.

Statistical analysis

Values were expressed as means ± SEM's. Statistical analysis was carried out by Student's t-test.

Materials

Synthetic rat CGRP was purchased from the Peptide Institute (Osaka, Japan). Pertussis toxin was from Seikagaku Kogyo Co. Ltd.(Tokyo,Japan). A cyclic AMP assay kit was obtained from Yamasa Shouyu Co.(Chiba, Japan). [^{3}H]-cAMP (1.1TBq/mmol) was from New England Nuclear, and 5'-nucleotidase of Crotalus atrox from Sigma Chemical Co.

Results

Twitch contractions on transmural stimulation of normal and denervated diaphragm

On transmural stimulation in fixed conditions (1.0 msec pulse width and 0.25Hz frequency), the mean active tension was 40.4± 6.2 g/g tissue in normal muscle, but significantly ($P<0.01$) higher 76.7± 4.9 g/g in denervated muscle. In our conditions, the total wet weight of the diaphragm decreased only 11% after denervation, and so the effect of muscle atrophy on the twitch tension was negligible.

Effects of CGRP and isoproterenol on twitch contraction in normal and denervated diaphragm

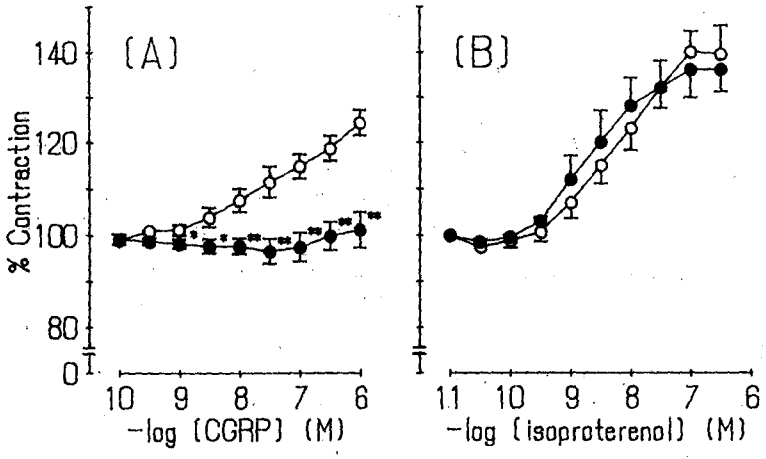

FIG.1
Enhancements of twitch contraction by CGRP (A) and isoproterenol (B) in normal and denervated muscles. Data are expressed as percentage increases in isometric tension induced by CGRP and isoproterenol, over the steady level, in normal (○) and denervated (●) muscles. Values are means ± SEM's. *P<0.05, **P<0.01 vs. corresponding values for normal muscle.

CGRP at concentrations of $3x10^{-8}$M to $1x10^{-6}$M caused dose-dependent potentiation of the contraction of normal diaphragm. The highest dose of CGRP used in this experiment ($1x10^{-6}$M) caused marked augmentation (24%) of the contraction, but not maximal contraction. In denervated diaphragms, CGRP tended to weaken twitch contractions (FIG.1A). On the other hand, isoproterenol potentiated the contractile responses of normal and denervated muscles in similar concentration-dependent manners and to similar extents. The threshold concentration of isoproterenol for these effects was $3x10^{-9}$M and the ED_{50} values for normal and denervated muscles were $4.5x10^{-9}$M and $3.1x10^{-9}$M, respectively (FIG.1B).

When rats treated with PT, the basal contractions of both the normal and denervated muscle were increased slightly, but CGRP-induced enhancement of twitch contraction in denervated muscle remained inhibited (data not shown).

To detect a possible inhibitory second messenger system, we also investigated whether isoproterenol-stimulated twitch contraction of denervated muscle was affected by preincubation with $1x10^{-4}$M N^2,2'-O-dibutyryl-guanosine 3',5'-cyclic monophosphate, $1x10^{-6}$M phorbol 12-myristate 13-acetate or $1x10^{-5}$M arachidonic acid. Enhancement of twitch contraction by isoproterenol was not affected by any of these treatments.

Effects of CGRP and isoproterenol on AC activity in membranes

Both CGRP and isoproterenol caused significant, dose-dependent stimulation of AC activity in rat diaphragmatic membrane, isoproterenol being more potent than CGRP. The basal AC activity of the membranes was increased about 1.6-fold from 2.8±

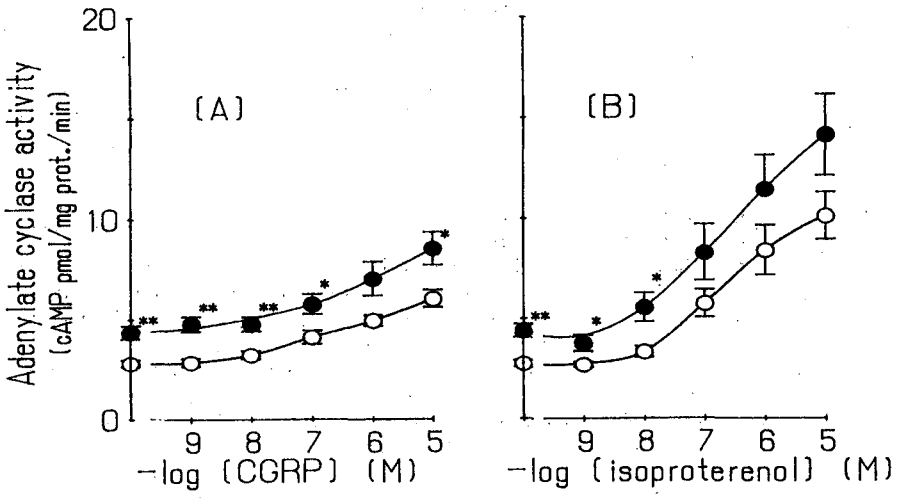

FIG.2
Effects of CGRP (A) and isoproterenol (B) on AC activity in normal and denervated muscles. The AC activities of membranes from normal (○) and denervated (●) muscles were measured. Values are means ± SEM's. (n=9 for normal muscle , n=8 for denervated muscle) *P<0.05, **P<0.01 vs. corresponding value for normal muscle.

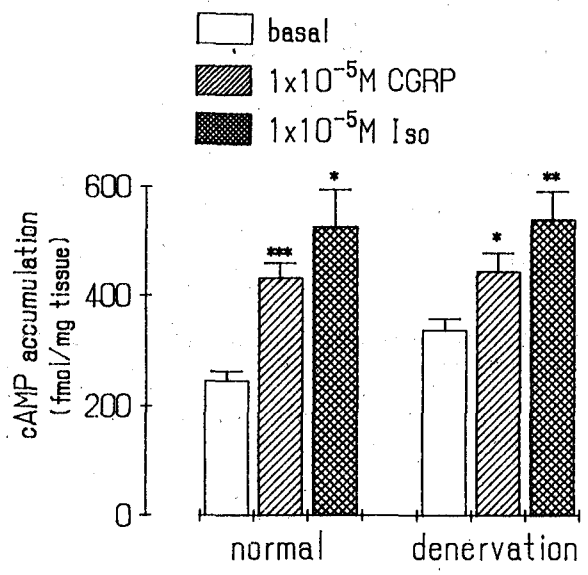

FIG.3
Effects of CGRP and isoproterenol on cAMP accumulation. The amount of cAMP in tissue segments of normal and denervated diaphragm after incubation with and without 1x10⁻⁵M of CGRP or isoproterenol for 3min was measured. The basal concentration of cAMP in denervated muscle was significantly higher than that in normal muscle (P<0.01). Values are means ± SEM's. (n=5) *P<0.05, **P<0.01, ***P<0.001 vs. basal value.

0.17 to 4.4± 0.33 pmol/mg prot. per min by denervation. The AC activities of normal and denervated membranes were 6.0± 0.43 and 8.5± 0.83 pmol/mg prot. per min respectively in the presence of $1x10^{-5}$M CGRP, and 10.1± 1.2 and 14.1± 2.0 pmol/mg prot. per min respectively in the presence of $1x10^{-5}$M isoproterenol. The ED_{50} values of CGRP and isoproterenol were not changed significantly by denervation (FIG.2 A,B). The stimulation ratio by both CGRP and isoproterenol versus the basal activity were suppressed to some degree, but not significantly.

Effects of CGRP and isoproterenol on cAMP accumulation in tissues

The amount of cAMP accumulation during incubation for 3min was 245± 17 fmol/mg tissue in normal tissue and 338± 28 fmol/mg tissue in denervated tissue, which was significantly more than that in normal tissue. In the presence of $1x10^{-5}$M of concentrations of CGRP and isoproterenol, the contents were 432± 28 and 527± 67 fmol/mg tissue, respectively, in normal tissue, and 444± 35 and 540± 51 fmol/mg tissue in denervated tissue (FIG.3). Thus the increases in cAMP levels over the basal level by these two drugs were both decreased by denervation.

Change of PDE activity in homogenates of diaphragm by denervation

The PDE activities in homogenates of normal and denervated diaphragm were 187± 11 and 207± 7 fmol /mg prot. per min, respectively. Thus denervation caused a slight, but not significant increase, in the activity.

Discussion

In general, denervated tissues become hypersensitive to the neurotransmitters present in the nerves that are destroyed, as the result of increase in neurotransmitter receptors. This phenomenon is called 'up-regulation'.

Previously, we demonstrated that after denervation in the rat sciatic nerve-gastrocnemius muscle system, the AC system became hypersensitive to CGRP, although this hypersensitivity was nonspecific and was due to increase in AC molecules (14). Therefore, we expected that after denervation, rat diaphragm would become hypersensitive to CGRP-induced enhancement of the contractile response. But, on the contrary, we found that the response of rat diaphragm was abolished by phrenic nerve destruction. On the other hand, after denervation, the muscle became hyperreactive on isoproterenol-induced enhancement of twitch contraction judging from absolute values of the contractile force (FIG.1B and the fact that the mean active tension was increased by denervation).

To clarify this discrepancy, we investigated the metabolism of cAMP in this tissue. The basal AC activity was increased by denervation and, as a result, the CGRP- and isoproterenol-activated AC activities were also increased. These results are consistent with those on gastrocnemius muscles reported previously and suggest that denervation also caused nonspecific hypersensitivity of diaphragmatic muscles to AC. The basal cAMP content in the tissue was also elevated by denervation. This increase corresponds to the increase in the basal contractile force and suggests that the cAMP level regulates the contractile force of skeletal muscle. The stimulations by CGRP and isoproterenol of the twitch response over the basal level were decreased by the denervation. This may be one reason for the decrease of CGRP-induced enhancement of twitch contraction.

The reason why the difference between the basal and CGRP-stimulated cAMP levels became smaller after denervation is unknown, but was probably due to acceleration of cAMP degradation. This possibility is consistent with a report by Pacifici et al. (19), that cAMP-PDE activity in rat gastrocnemius muscle increased significantly from the third day after denervation and remained high for at least for 60 days. In the present work, the activity of PDE was slightly increased in homogenates of rat diaphragm 2 weeks after denervation. This increase seems insufficient to explain the above data. However, we cannot deny the possibility that in intact cells, PDE is activated by CGRP via another second messenger system, although CGRP did not affect PDE in homogenate.

As discussed above, decrease in CGRP-induced elevation of cAMP may be one reason why CGRP-induced enhancement of twitch contraction disappeared after denervation. However, it is not enough to explain the marked difference between changes in the CGRP- and isoproterenol-induced enhancements.

There is some suggestive evidence that the actions of CGRP are mediated by some other second messenger system besides activation of AC. In a human breast cancer cell line, MCF7, CGRP at low doses of 10^{-11}M to 10^{-10}M inhibited cAMP accumulation mediated by a PT-sensitive inhibitory GTP binding protein, in addition to having a stimulatory effect at higher doses (20). So, it is possible that another subtype of CGRP receptor coupled with inhibition of AC was supersensitized by denervation in skeletal muscles. However, we could not detect any inhibitory phase in the CGRP-AC activity relationship in normal or denervated conditions. We also investigated the effect of pretreatment of animals with PT. The treatment caused about 1.6-fold increase in the basal activity of AC (data not shown). It is consistent with the observation previously reported that PT treatment resulted in a 2-fold increase in the basal activity in C6 glioma cells (21). But PT treatment did not restore the enhancement of the twitch contraction by CGRP in denervated muscle.

Leighton and Cooper showed that CGRP acted on insulin-dependent metabolism of glucose in skeletal muscles in a different way from a β-agonist, isoprenaline (22). Their results strongly suggest the presence of another second messenger system coupled with CGRP receptors. As it seems reasonable that denervation would cause hypersensitivity in a system that is coupled with inhibition of twitch contraction, we tested for the involvement of some inhibitory second messenger system in this phenomenon. However, the addition of dibutyryl-cGMP, phorbol ester and arachidonic acid to the medium had no inhibitory effect on isoproterenol-induced enhancement of the twitch contraction in the denervated diaphragm. So the existence of an inhibitory second messenger system is still uncertain.

There are some reports concerning the effects of CGRP on the ACh receptor level. It was shown that addition of CGRP to chick muscle cells in primary cultures significantly increased the level of surface ACh receptors (23,24). And it was suggested that CGRP might regulate the synaptic ACh receptor-channel conductance (25), or might have both a pre- and a post-junctional action which is able to enhance both twitch contractions produced by the nerve excitation and the membrane depolarization (12). However, in our experimental conditions, involvement of ACh receptor system is un-

likely because effects of CGRP on twitch contraction by direct stimulation were not changed with presence or absence of d-tubocurarine (data not shown). So, in our conditions, the reaction through the ACh receptor is negligible.

Destruction of a motor nerve causes very unique heterologous supersensitization of the AC system in skeletal muscles, probably due to lack of CGRP release (14,26). The elevation of the basal twitch contraction by denervation may reflect increase in the basal cAMP level. However, disappearance of CGRP-enhanced twitch contraction cannot be explained entirely by change in the cAMP system, and may have some underlying mechanism.

References

1. M.G.ROSENFELD, J.-J.MERMOD, S.G.AMARA, L.W.SWANSON, P.E.SAWCHENKO, J.RIVIER, W.W.VALE and R.M.EVANS, Nature 304 129-135 (1983)
2. G.SKOFITSCH and D.M.JACOBOWITZ, Peptides 6 721-745 (1985)
3. Y.KAWAI, K.TAKAMI, S.SHIOSAKA, P.C.EMSON, C.J.HILLYARD, S.GIRGIS, I.MACINTYRE and M.TOHYAMA, Neuroscience 15 747-763 (1985).
4. S.J.GIBSON, J.M.POLAK, S.R.BLOOM, I.M.SABATE, P.M.MULDARY, M.A.GHATEL, G.P.MCGREGOR, J.F.B.MORRISON, J.S.KELLY, R.M.EVANS and M.G.ROSENFELD, J. Neurosci. 4 3101-3111 (1984)
5. WIESENFELD-HALLIN, T.HOKFELT, J.M.LUNDBERG, W.G.FORSSMANN, M.REINECKE, F.A.TSCHOPP and J.A.FISCHER, Neurosci. Lett. 52 199-204 (1984)
6. Y.LEE, Y.KAWAI, S.SHIOSAKA, K.TAKAMI, H.KIYAMA, C.J.HILLYARD, S.GIRGIS, I.MACINTYRE, P.C.EMSON and M.TOHYAMA, Brain Res. 330 194-196 (1985)
7. Y.LEE, K.TAKAMI, Y.KAWAI, S.GIRGIS, C.J.HILLYARD, I.MACINTYRE, P.C.EMSON and M.TOHYAMA, Neuroscience 15 1227-1237 (1985)
8. K.TAKAMI, Y.KAWAI, S.SHIOSAKA, Y.LEE, S.GIRGIS, C.J.HILLYARD, I.MACINTYRE, P.C.EMSON and M.TOHYAMA, Brain Res. 328 386-389 (1985)
9. K.TAKAMI, Y.KAWAI, S.UCHIDA, M.TOHYAMA, Y.SHIOTANI, H.YOSHIDA, P.C.EMSON, S.GIRGIS, C.J.HILLYARD, and I.MACINTYRE, Neurosci. Lett. 60 227-230 (1985)
10. K.TAKAMI, K.HASHIMOTO, S.UCHIDA, M.TOHYAMA and H.YOSHIDA, Japan. J. Pharmacol. 42 345-350 (1986)
11. H.KOBAYASHI, K.HASHIMOTO, S.UCHIDA, J.SAKUMA, K.TAKAMI, M.TOHYAMA, F.IZUMI and H.YOSHIDA, Experientia 43 314-316 (1987)
12. T.OHHASHI and S.M.JACOBOWITZ, Peptides 9 613-617 (1988)
13. W.B.CANNON, Am. J. Med. Sci. 198 737-750 (1939)
14. K.HASHIMOTO, Y.WATANABE, S.UCHIDA and H.YOSHIDA, Life Sci. 44 1887-1895 (1989)
15. M.HONMA, T.SATOH, J.TAKEZAWA and M.UI, Biochem. Med. 18 257-273 (1977)
16. W.J.RUTTEN, B.M.SCHOOT and J.J.H.H.M.DE PONT, Biochim. Biophys. Acta 315 378-383 (1973)
17. X.-M.ZHOU, A.MIZUSHIMA, S.UCHIDA, Y.WATANABE and H.YOSHIDA, Eur. J. Pharmacol. 154 229-236 (1988)
18. M.M.BRADFORD, Analyt. Biochem. 72 248-254 (1976)
19. G.M.PACIFICI, C.PELLEGRINO, C.MAFFEI and D.BECONCINI, Ital. J. Biochem. 30 20-29 (1981)
20. J.BARSONY and S.J.MARX, Endocrinology 122 1218-1223 (1988)

21. T.KATADA, T.AMANO and M.UI, J. Biol. Chem. 257 3739-3746 (1982)
22. B.LEIGHTON and G.J.S.COOPER, Nature 353 632-635 (1988)
23. B.FONTAINE, A.KLARSFELD, T.HOKFELT and J.P.CHANGEUX, Neurosci. Lett. 71 59-65 (1986)
24. H.V.NEW and A.W.MUDGE, Nature 323 809-811 (1986)
25. F.EUSEBI, D.FARINI, F.GRASSI, L.MONACO and F.RUZZIER, Proc. R. Soc. Lond. B234 333-342 (1988)
26. K.HASHIMOTO, S.UCHIDA and H.YOSHIDA, Life Sci. 45 2183-2192 (1989)